PEOPLE'S DEMOCRATIC AND REPUBLIC OF ALGERIA
Ministry of Higher Education and Scientific Research

N° Series: /2023

University of Kasdi Merbah Ouargla

Faculty of Hydrocarbons, Renewable Energies, and Science of Earth & Universe

**Department of Hydrocarbon's Production**

# THESIS

Submitted in Candidacy for the Degree of

**MASTER OF SCIENCE**

**IN**

**Petroleum Production Engineering**

Submitted By:

**Salah Bouattia – Mohamed Anis Khelas – Abderazzak Khelili**

- THEME -

# Evaluation of Hydraulic Fracture Propagation in Naturally Fractured Reservoirs

Publicly Defended on: 06 /10/ 2023 in front of the examination board

**Jury:**

| | | | |
|---|---|---|---|
| President: | Mr. Nabil Brahmia | MCB | Univ.Ouargla |
| Rapporter: | Ms. Fadila Hafsi | MAA | Univ.Ouargla |
| Examiner: | Mr. Ammar Mahsoul | MCA | Univ.Ouargla |

**Scholar Season: 2022 – 2023**

# Acknowledgements


## TO ALLAH BE THE GLORY

### ALL THANKS TO ALLAH FOR ENABLING US TO COMPLETE THIS WORK

Our sincere gratitude and appreciation go to our great families for their great love, encouragement and support during our university years.

A special thanks to our advisor **Ms. Fadila Hafsi** for her professional guidance, patience, and her valuable advice to achieve this work.

We would like to extend our gratitude to all the staff in the faculty of hydrocarbons for the knowledge they have transferred to us, especially the professors of production department, each one in his name and position.

A warm thanks to our colleagues and friends for cordial relationship and assistance during this academic journey.

Thanks to our second family: Petroleum Club Ouargla – Université Kasdi Merbah Ouargla Society of Petroleum Engineers Student chapter members.

# Dedication

*To my beloved Grandma, who has always been my guiding light and a source of unconditional love and wisdom. Your unlimited support and presence in my life have shaped me into the person I am today.*

*To my dear parents, for their endless sacrifices, unwavering belief in me, and the love they have showered upon me. Your constant encouragement has fueled my ambitions and given me the strength to overcome any obstacles.*

*To my two older sisters, Your guidance, friendship, and unwavering belief in my abilities have been a constant source of inspiration.*

*To my brother, a source of constant laughter and companionship. Your presence has brought joy to my life and taught me the importance of loyalty and resilience.*

*To my incredible colleagues and friends, who have stood by my side through thick and thin. Your unwavering support, camaraderie, and shared experiences have made this journey more meaningful and enjoyable.*

*To my second family PCO-SPE Student Chapter members thanks for always being there for me, for the guidance, for the help during this academic journey.*

*To my biggest support A.L.R.*

*This thesis is dedicated to all of you, as a token of gratitude for your love, support, and unwavering belief in me. Without you, this achievement would not have been possible.*

*Salah Bouattia*

# Dedication

*This thesis is proudly dedicated to all my precious family and friends.*

*To the memory of my grandma "MAMITA" ZOHRA Khelas allah yarhamha .*

*To my great support my grandma MESSOUADA Bousetla.*

*To my parents, NOUREDDINE and FARIDA Khelas, the most helpful parents ever who gave me love, trust, patience, support, and encouragements.*

*To my caring brothers SEIF and IHEB and my sister SARAH who have been a great source of motivation.*

*To my uncle MOHAMED Khelas.*

*To my aunt ABLA Hamlaoui.*

*My cousins IYAD, RAOUF, MOSSAB and TANOU.*

*To my dear friends ALI Ramoul, ABDERRAHMAN Thabet and ACHREF Benchehla.*

*To my colleagues who supported me and believed in me.*

*Mohamed Anis Khelas*

# Dedication

***I dedicate this modest work to my beloved parents for their love, patience, care, and continuous support during the five years of my Study.***

***To my wonderful parents who have raised me to be the person, I am Today.***
***Thank you for everything.***

***To my brothers and sister for their encouragement and love.***

***To all my family.***
***To KHELILI family.***
***To FERCHANE family.***

***To my colleagues for their encouragement and support during five yeras.***

***To all my friends and colleagues without exception.***
***I would like to say '' Thank you So much ''***

***Abderazzak Khelili***

## Abstract

This study aims to evaluate the hydraulic fracture propagation in naturally fractured reservoirs, to interpret its propagation models and to identify the behaviors associated with its propagation utilizing Nolte & Smith analysis and G-Function plots. A large portion of global oil and gas resources trapped in naturally fractured formations with low permeability. The low conductivity of the natural fracture networks requires a stimulation with hydraulic fracturing to make the economic production possible. Hydraulic fracturing in naturally fractured reservoirs is a complex process that presents numerous challenges and uncertainties. In most cases the hydraulic fracturing ends to failure due to the complex behavior of hydraulic fracture propagation in anisotropic milieu, and the miss understanding of the interaction between hydraulic fracture and natural fractures. In Algeria, there are several reservoirs considered as naturally fractured reservoirs such as in Gassi El Agreb and Hassi R'mel fields. These reservoirs have undergone operations of hydraulic fracturing in order to enhance their productivity and bypass wellbore damage. The common observations during hydraulic fracturing in naturally fractured reservoirs include high leak-off rate, low fluid efficiency, small fracture geometry, and unintended propagation beyond the target zone, even after stress calculations and data calibration.

**Key Words:** naturally fractured reservoirs, hydraulic fracturing, hydraulic fracture, natural fractures, propagation models, propagation behaviors.

## Résumé

Cette étude vise à évaluer la propagation de la fracture hydraulique dans les réservoirs naturellement fracturés, à interpréter ses modèles de propagation et à identifier les comportements associés à sa propagation en utilisant l'analyse de Nolte & Smith et les graphiques de fonction G. Une grande partie des ressources mondiales en pétrole et en gaz est piégée dans des formations naturellement fracturées à faible perméabilité. La faible conductivité des réseaux de fractures naturelles nécessite une stimulation par fracturation hydraulique pour rendre possible une production économiquement viable. La fracturation hydraulique dans les réservoirs naturellement fracturés est un processus complexe qui présente de nombreux défis et incertitudes. Dans la plupart des cas, la fracturation hydraulique échoue en raison du comportement complexe de la propagation de la fracture hydraulique dans un milieu anisotrope et de la mécompréhension de l'interaction entre la fracture hydraulique et les fractures naturelles. En Algérie, plusieurs réservoirs sont considérés comme des réservoirs naturellement fracturés, tels que les champs de Gassi El Agreb et de Hassi R'mel. Ces réservoirs ont fait l'objet d'opérations de fracturation hydraulique afin d'améliorer leur productivité et de contourner les dommages causés au puits. Les observations courantes lors de la fracturation hydraulique dans les réservoirs naturellement fracturés comprennent un taux de fuite élevé, une faible efficacité du fluide, une petite géométrie de fracture et une propagation non intentionnelle au-delà de la zone cible, même après les calculs de contrainte et l'étalonnage des données.

**Mots-clés:** réservoirs naturellement fracturés, fracturation hydraulique, fracture hydraulique, fractures naturelles, modèles de propagation, comportements de propagation.

**الملخص:**

تهدف هذه الدراسة إلى تقييم انتشار الكسر الهيدروليكي في خزانات الصخور المتشققة بشكل طبيعي، وتفسير نماذج انتشارها وتحديد السلوكيات المرتبطة بانتشارها باستخدام Nolte & Smith analysis و G-Function plot. جزء كبير من موارد النفط والغاز العالمية محصور في تكوينات الصخور المتشققة بشكل طبيعي ذات النفاذية المنخفضة. تتطلب التشققات الطبيعية ذات القدرة المنخفضة على التوصيل تحفيزًا بالكسر الهيدروليكي لجعل الإنتاج الاقتصادي ممكنًا. إن عملية الكسر الهيدروليكي في خزانات الصخور المتشققة بشكل طبيعي هي عملية معقدة تواجه العديد من التحديات والشكوك. في معظم الحالات، ينتهي الكسر الهيدروليكي بالفشل نتيجة السلوك المعقد لانتشار الكسر الهيدروليكي في بيئة غير متماثلة وفهم غير صحيح للتفاعل بين الكسر الهيدروليكي والشقوق الطبيعية. في الجزائر، هناك العديد من خزانات الصخور التي تعتبر خزانات متشققة بشكل طبيعي مثل حقلي قاسي العقرب وحاسي رمل. خضعت هذه الخزانات لعمليات الكسر الهيدروليكي من أجل تعزيز إنتاجيتها وتجاوز تلف الآبار. الملاحظات الشائعة أثناء التكسير الهيدروليكي في مخازن متصدعة بشكل طبيعي تشمل معدل تسرب عالٍ، كفاءة سائل منخفضة، هندسة تشقق صغيرة، وانتشار غير مقصود خارج منطقة الهدف، حتى بعد حسابات التوتر ومعايرة البيانات.

**الكلمات الرئيسية:** خزانات الصخور المتشققة بشكل طبيعي، الكسر الهيدروليكي، الكسور الطبيعية، نماذج الانتشار، سلوك الانتشار.

# Table of Contents

**CHAPTER II: Hydraulic Fracturing Concepts and Fundamentals**

**CHAPTER III: Hydraulic Fracture Propagation Models and Analysis in NFRs**



**CHAPTER IV: Study Cases On Hydraulic Fracture Propagation In Naturally Fractured Reservoirs**

# List of Figures

## CHAPTER I: Naturally Fractured Reservoirs (NFRs)



## CHAPTER II: Hydraulic Fracturing Concepts and Fundamentals



## CHAPTER III: Hydraulic Fracture Propagation Models and Analysis in NFRs

**CHAPTER IV: Study Cases On Hydraulic Fracture Propagation In Naturally Fractured Reservoirs**

# List of Tables

## CHAPTER II: Hydraulic Fracturing Concepts and Fundamentals



## CHAPTER III: Hydraulic Fracture Propagation Models and Analysis in NFRs



## CHAPTER IV: Study Cases On Hydraulic Fracture Propagation In Naturally Fractured Reservoirs

## List of symbols and Abbreviations

$\sigma$ : the porosity partitioning coefficient, porosity, overburden pressure,
$\phi_{core}$ : core porosity
$\phi_f$ : Fracture porosity
$\phi_m$ : Matrix porosity
$(\phi_t)$ : Total porosity
A : surface area of the matrix block $ft^2$, cross-sectional area
$c_t$ : otal compressibility, $psi^{-1}$
D : fracture spacing
dh/dl : head gradient
e : distance
F : the total formation resistivity factor
FMI : formation micro imager, Formation Micro imager
h : thickness
HMD : Hassi Messaoud
K : hydraulic conductivity
$k_f$ : fracture permeability, permeability of a fracture, permeability of the fracture plus intact-rock system
$k_m$ : matrix permeability, matrix permeability
$k_r$ : permeability of the intact-rock
mf : the fracture porosity exponent
$m_m$ : the matrix porosity exponent
NFRs : naturally fractured reservoirs
$p_f$ : fracture pressure
$P_i$ : the initial pore pressure
$p_m$ : matrix pressure
Q : the flow rate
$R_0$ : the resistivity of porous
$r_w$ : wellbore radius
$R_w$ : the formation water resistivity
UBI : ultrasonic borehole imager
V : volume of the matrix block, matrix rock volume
x : characteristic length of the matrix block, ft
$\alpha$ : angle between the axis of the pressure gradient and the fracture planes
$\Gamma$ : the matrix fracture transfer function
$\tau$ : the tortuosity factor
$\lambda$ : interporosity flow coefficient, interporosity flow coefficient
$\mu$ : fluid viscosity
$\sigma$ : block-shape factor, The shape factor
$\omega$ : storativity ratio

$\nu$ : Poisson's ratio
$\sigma_1$ : the vertical stress (Overburden stress)
$\sigma_2$ : the minimum horizontal stress
$\sigma_3$ : the maximum horizontal stress
C : Bulk Compressibility
CFA : Closed Fracture Acidizing
CT : coiled tubing
E : Young's Modulus
G : Shear modulus
HF :hydraulic fracturing
ISIP : the instantaneous shut-in pressure
$p_p$ : reservoir fluid pressure or pore pressure
RCS : resin-coated sand
$\alpha$ : Biot's constant
$\varepsilon$ : tensile strain
$\sigma$ : tensile stress
$\sigma_{ext}$ : tectonic stress
$\Delta P_{net}$ : Net fracture pressure
$C_L$ : Leak-off Coefficient
dp/dG : Plateau value of first derivative
FE : Fluid Efficiency
$G_c$ : G-function time
$G_f$ : Fracture propagation gradient
HF : Hydraulic Fracture
NF Natural Fracture
P3D : pseudo-three-dimensional
$P_c$ : Closure pressure
PKN : Perkins and Kern
$t_p$ : Pumping time
$\Delta P$ :Differntial Pressure
BH :Bottom Hole
CFA : Closed Fracture Acidizing
CSA : Carbonate Stimulation Acid
DST :Drill Stem Test
FPP :Fracture Propagation Pressure, Voir
GCR : Gas Compression & Reinjection
GEA : Gassi EL-AGREB Area
NWB : Neer Well Bore
OOS : Oil Optimization System)
$P_B$ : Breakdown Pressure
PDL : Pressure-Dependent Leak-off
WOC :Water Oil Cut

# General Introduction

# General Introduction

Naturally fractured reservoirs are geological formations characterized by pre-existing fractures that have formed over time due to natural processes like tectonic forces and sedimentation. These fractures serve as pathways for fluid movement but can pose challenges in terms of fluid flow patterns and production efficiency. The use of hydraulic fracturing techniques in naturally fractured reservoirs aims to enhance reservoir performance by improving connectivity between fractures and the wellbore, leading to increased production rates and hydrocarbon recovery.

Hydraulic fracturing, also known as fracking, is a well stimulation technique employed in the oil and gas industry to improve the productivity of reservoirs. It involves injecting high-pressure fluids into a wellbore, creating fractures in the underground rock formations. While hydraulic fracturing is commonly used in conventional reservoirs, it is also applied in naturally fractured reservoirs to optimize hydrocarbon extraction.

The successful implementation of hydraulic fracturing in naturally fractured reservoirs requires a comprehensive understanding of the existing fracture network. Advanced techniques such as well log analysis, core sampling, and microseismic monitoring are employed to identify the distribution, orientation, and connectivity of fractures within the reservoir. This information guides the design of effective fracture treatments that target the most productive pathways.

Designing hydraulic fracturing treatments in naturally fractured reservoirs involves a customized approach that considers the unique characteristics of the reservoir. Parameters like injection rate, fluid viscosity, proppant selection, and fracturing fluid composition are optimized to achieve the desired fracture geometry and connectivity. Precise planning and execution are crucial to ensure that the created fractures intersect the natural fractures, thereby maximizing reservoir productivity.

While hydraulic fracturing in naturally fractured reservoirs offers significant benefits, it also presents challenges and risks. Fracture interference, where newly created fractures intersect with existing ones, can lead to uneven fluid flow distribution and reduced overall productivity. Managing the extent and direction of fractures is essential to mitigate these issues. Additionally, monitoring induced seismicity and preventing fluid migration into adjacent formations are important considerations in well design and operation.

Despite the challenges, hydraulic fracturing in naturally fractured reservoirs has proven to be a valuable technique for unlocking the potential of these complex reservoirs. By optimizing fluid flow connectivity and combining existing fractures with artificially created ones, this method significantly enhances production rates and hydrocarbon recovery. Ongoing advancements in technology and improved understanding of reservoir characteristics continue to enhance the effectiveness of hydraulic fracturing in naturally fractured reservoirs, contributing to the sustainable development of energy resources.

**Thesis Outline:**

This thesis is divided into 4 chapters:

**The first chapter:** gives an overview of naturally fractured reservoirs, some of petrophysics parameters of NFRs, as well as the indicators of natural fractures.

**The second chapter:** key hydraulic fracturing terminology from the oil and gas industry is discussed in order to familiarize the reader with the fundamentals of hydraulic fracturing process.

**The third chapter:** highlights the interaction between hydraulic fracture and natural fractures, introduces and compares the different propagation models of hydraulic fracture and gives the analysis methods utilizing in hydraulic fracturing process.

**The fourth chapter:** presents analysis of field data taken from wells in in Gassi El Agreb and Hassi R'mel reservoirs, and evaluation of hydraulic fracture propagation and its associated behaviors.

# Chapter I:

## Naturally Fractured Reservoirs (NFRs)

# CHAPTER I: Naturally Fractured Reservoirs (NFRs)

## Introduction

Large amounts of oil reserves are contained in naturally fractured reservoirs. Most of these hydrocarbon volumes have been left behind because of the inadequate knowledge and/or description methodology of those reservoirs. This lack of knowledge has led to the nonexistence of good quantitative models for this complicated type of reservoirs. The complexity of naturally fractured reservoirs causes the need for integration of all existing information at all scales (drilling, well logging, seismic, well testing, etc.) to provide a reservoir description for such reservoirs.

## I.1 Definition

Naturally fractured reservoirs represent more than 50% of reservoirs and contribute in a large extent to the worldwide production of oil and gas. These highly heterogeneous reservoirs possess a complex network of several fracture families with different spatial distribution and conductivity. Performing a reservoir characterization work on these naturally fractured systems is a challenging task because they present an extreme property contrast between the two domains and it comprises: rock matrix and fractures.

Naturally fractured reservoirs are found in many depositional environments, including [1]:

- Carbonates
- Shales
- Sandstones

A **reservoir's fracture** is a naturally occurring macroscopic planar discontinuity in rocks due to deformation or physical diagenesis. If it is related to brittle failure, it was probably initially open, but may have been subsequently altered or mineralized. If it is linked to more ductile failure, it may exist as a band of highly deformed country rock. As a result, natural reservoir fractures may have either a positive or negative effect on fluid flow within the rock.[2]

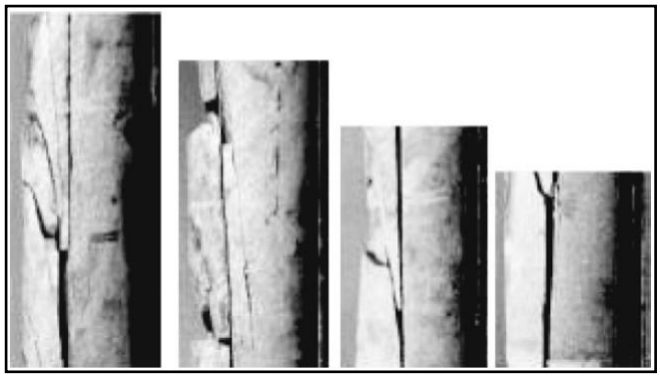

**Figure I.1: Naturally fractured rock cores taken from wells. [3]**

## I.2 Geological Classifications of Natural Fractures

Natural fracture patterns are frequently interpreted on the basis of laboratory derived fracture at the time of fracture.[3]

### I.2.1 Classification Based on Stress/Strain Conditions

- **Shear fractures** that exhibit a sense of displacement parallel to the fracture plane. They are formed when the stresses in the three principal directions are all compressive. They form at an acute angle to the maximum principal stress and at an obtuse angle to the direction of minimum compressive stress.[3]
- **Extension fractures** that exhibit a sense of perpendicular displacement away from the fracture plane. They are formed perpendicular to the minimum stress direction. They result when the stresses in the three principal directions are compressive, and can occur in conjunction with shear fracture.[3]
- **Tension fractures** that also display a sense of displacement similar to Extension fractures. However, in order to form this type of fracture, at least one of the principal stresses has to be tensile. Since rocks exhibit significantly reduced strength in tension tests, this results in increased fracture frequency.[3]

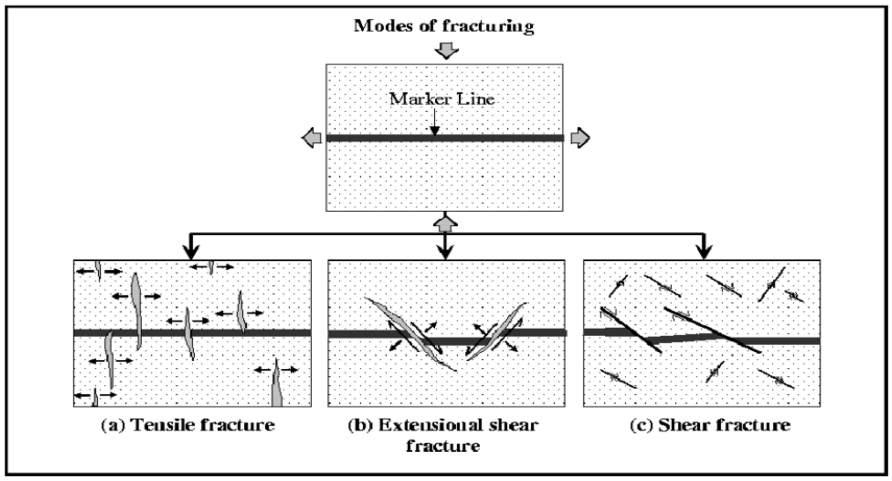


**Figure I.2: Three Principal Modes of Fracturing.[4]**

### I.2.2 Classification Based on Paleostress Conditions

- **Tectonic Fractures:** The orientation, distribution, and morphology of these fracture systems are associated with local tectonic events. Tectonic fractures form in networks with specific spatial relationships to faults and folds. Fault-related fracture systems could be shear fractures that they are formed either parallel to the fault or at an acute angle to it. The intensity of fractures associated with faulting is a function of lithology, distance from the fault plane, magnitude of the fault displacement, total strain in the rock mass, and depth of burial. Fold-

related fracture systems exhibit complex patterns that are consistent with the complex strain and stress history associated with the initiation and growth of a fold. Fracture types in fold-related systems are defined in terms of the dip and strike of the beds.[3]

- **Regional Fractures:** These fracture systems are characterized by long fractures indicating little change in orientation over their length. They also show no evidence of offset across the fracture plane and are always perpendicular to the bedding surfaces.

  Regional fracture systems can be distinguished from tectonic fractures in which they generally exhibit simpler and more consistent geometry and have relatively large spacing.[3]
- **Contractional Fractures:** These types of fractures result from bulk volume reduction of the rock. Desiccation fractures may result from shrinkage upon loss of fluid in subaerial drying. Mud cracks are the most common fractures of this type. Syneresis fractures result from bulk volume reduction within the sediments by subaqueous or surface dewatering. Dewatering and volume reduction of clays or of a gel or a colloidal suspension can lead to syneresis fractures. Desiccation and syneresis fractures can be either tensile or extension fractures and are initiated by internal body forces.[3]

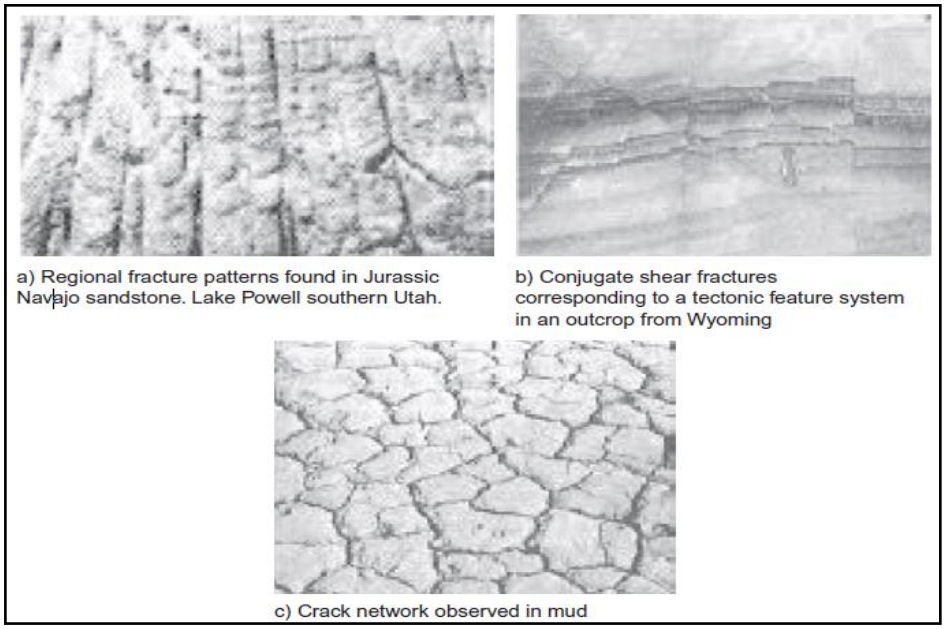


**Figure I.3: Different Fracture Systems in Rocks and Mud.[3]**

## I.3 Engineering Classification of Naturally Fractured Reservoirs (NFRs)

Nelson identified four types of naturally fractured reservoirs (NFRs), based on the positive effects that fracture system provides to overall reservoir quality:

**Type 1:** Fractures represent the essential reservoir porosity and permeability (such as the Amal field in Libya).

**Type 2:** They represent the essential reservoir permeability (such as the Monterey fields of California).

**Type 3:** They assist permeability in an already producible reservoir (such as Dukhan field of Qatar). Nelson includes the Hassi Messaoud (HMD) field of Algeria in this list. Indeed, although, there are several low-permeability zones in HMD that are fissured; in most zones, the evidence of fissures is not clear or unproved.

**Type 4:** They provide no additional porosity or permeability but create significant reservoir anisotropy (barriers).[2]

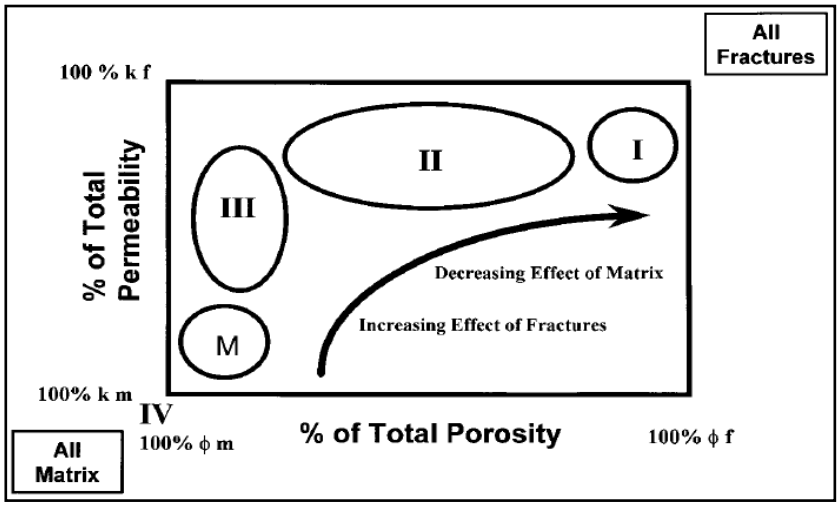


**Figure I.4: Nelson Classification of NFRs.[2]**

## I.4 Parameters of Fractures

### I.4.1 Fracture Opening and Width

Fracture opening or fracture width is represented by the distance between the fracture walls. The width of the opening may depend (in reservoir conditions) on depth, pore pressure and type of rock. Its width varies between 10-200 microns. The fracture opening depends on the lithological-petrographic characteristics of the rock, nature of stresses and reservoir's environment. In reservoir conditions where the confined pressure $\sigma$ (overburden pressure) remains constant, but the initial pore pressure $P_i$ is reduced (during reservoir depletion) to $P_1$, the width will become smaller (**Figure I.5**), due to the effect of rock expansion.[5]

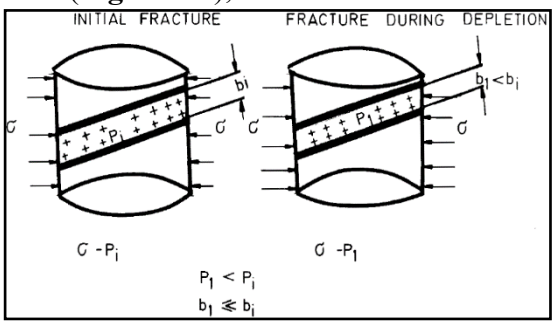


**Figure I.5: Reduction of Fracture Width as an Effect of Reservoir Pressure Depletion.[5]**

### I.4.2 Fracture Size

Fracture size refers to the relationship between fracture length and layer's thickness, especially if a qualitative evaluation is being formulated. In this case fractures can be evaluated as minor, average and major:

a. minor fractures have a length less than the single layer pay

b. average fractures traverse more layers

c. major fractures have a very large extension, often tens or even hundreds of meters.[5]

### I.4.3 Fracture Nature

The nature of fractures mainly is concerned with the state of fractures under observation with reference to opening, filling and wall characteristics, and is generally discussed in the following terms:

a. opening - open, joint, closed

b. filling - mineral, various minerals

c. closed by - homogeneous or diffused filling material

d. fracture walls - rugose, smooth, polished, creeping.[5]

### I.4.4 Fracture Dip and Azimuth

Each fracture in a discrete fracture model is defined by its properties which include fracture azimuth angle, dip angle, center point (x, y and z) and radius. Fracture azimuth is represented by the angle formed between the fractures plan and the geographic north. These angles are inferred from core and Fullbore Formation Micro imager (FMI) data. Fracture dip is the angle between the fracture plane and horizontal plane (see **Figure I.6**) and it is inferred from the geological interpretations (e.g. dip of the geological formation).[6]

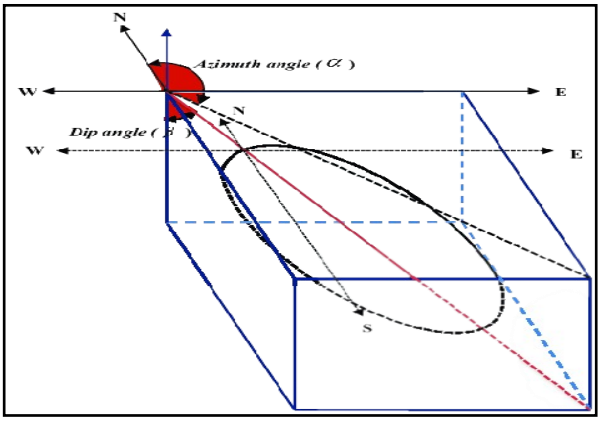


**Figure I.6: Description of the plane in which the fracture lies. The ellipse represents a fracture with (α is the fracture azimuth angle and β is the dip angle).[6]**

# I.5 Petrophysical Properties of Naturally Fractured Reservoirs (NFRs)

## I.5.1 Porosity

NFRs are often called dual-porosity reservoirs because of the different fluid storage and conductivity characteristics of the matrix and fractures, and described by the following dual porosity systems:

• Matrix porosity that is categorized as primary porosity $\phi_m$.

• Fracture porosity that is categorized as secondary porosity $\phi_f$.[1]

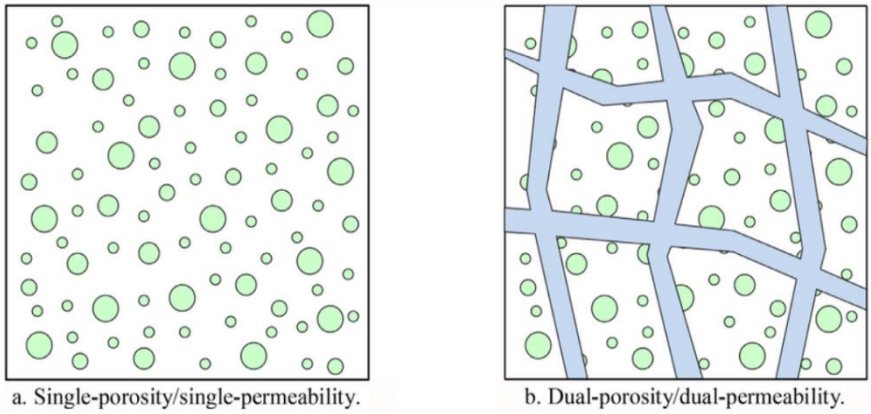


**Figure I.7: Schematic Illustration of Reservoir and Naturally Fractured Reservoir.[7]**

- **Primary porosity $\phi_m$:** is established when the sediment is first deposited.
- **Secondary porosity $\phi_f$:** also known as induced porosity, is the result of geological processes after the deposition of sedimentary rock.

Fracture porosity is defined as fracture volume divided by total volume [1]:

$$\phi_f = \frac{\text{fracture volume}}{\text{total volume}} = \frac{V_f}{V_t} \quad \text{(I.1)}$$

where:

$\phi_f$: fracture porosity (%)

$V_f$: fracture volume ($m^3$)

$V_t$: total volume of rock ($m^3$)

The sonic log only measures the matrix porosity. However, neutron porosity is the combination of both the matrix and fracture porosity. Thus, fracture porosity can be estimated from well logs as [3]:

$$\phi_f = \phi_{Neu} - \phi_{Son} \quad \text{(I.2)}$$

where:

$\phi_f$: fracture porosity (%)

$\phi_{Neu}$: neutron log porosity (%)

$\phi_{Son}$: sonic log porosity (%)

Matrix porosity is also defined with respect to total volume. Therefore, matrix porosity is not the same as unfractured core porosity $\phi_{core}$ measured in the laboratory, that is [1]:

$$\phi_m = \phi_{core}(1 - \phi_f) \quad \text{(I.3)}$$

where:

$\phi_m$: matrix porosity (%)

$\phi_{core}$: fracture porosity (%)

$\phi_f$: fracture porosity (%)

In a fractured reservoir the Total porosity ($\phi_t$) is the sum of fracture porosity and matrix porosity:

$$\phi_t = \phi_f + \phi_m \quad \text{(I.4)}$$

where:

$\phi_t$: total porosity (%)

$\phi_f$: fracture porosity (%)

$\phi_m$: matrix porosity (%)

**I.5.2 Permeability**

The first quantitative description of fluid flow through porous media was by Darcy. In his general equation, derived for laminar, incompressible, single-phase, Newtonian flow in a continuous, homogeneous, porous material, the flow rate (Q) is [2]:

$$Q = KA\frac{dh}{dl} \quad \text{(I.5)}$$

where K = hydraulic conductivity
A = cross-sectional are
dh/dl = head gradient

In an attempt to model fractures, the parallel-plate theory of flow was developed. Flow in this theory is assumed to occur between two smooth parallel plates separated by a distance (e). The basic equation used is [2]:

$$Q = \frac{e^3}{12D}\frac{dh}{dl}\cdot\frac{\rho g}{\mu} \quad \text{(I.6)}$$

where D = fracture spacing, the average distance between parallel regularly spaced fractures. This equation is valid for single-phase, Newtonian, laminar flow in planar fractures with small overall changes in width (e).[2]

Each of these two quantitative relations (Equations I.5 and I.6) describes only a portion of the total flow through a fractured, porous rock; Darcy's equation for the intact-rock portion of the system, and the parallel-plate theory for the fractures. The next logical approach to determine the total flow was to combine these equations [2]:

$$K_{fr} = K_r + \frac{e^2 \cos^2 \alpha}{12D} \tag{I.7}$$

and

$$K_f = \frac{e^2}{12} \cdot \frac{\rho g}{\mu} \tag{I.8}$$

where $k_{fr}$= permeability of the fracture plus intact-rock system
$k_f$ = permeability of a fracture
$k_r$ = permeability of the intact-rock
α = angle between the axis of the pressure gradient and the fracture planes

### I.5.3 Important Parameters Related to Matrix-Fractures System

#### I.5.3.1 The Matrix-Fracture Transfer Function (Γ)

The formation fluid flows from the matrix system into the fractures under pseudo-steady state conditions with the fractures acting like conduits to the wellbore. Mathematically the matrix fracture transfer function Γ is defined by the following relationship [1]:

$$\Gamma = \sigma \left(\frac{K_m}{\mu}\right) V(p_m - p_f) \tag{I.9}$$

where $k_m$ = matrix permeability
σ = block-shape factor
μ = fluid viscosity
V = matrix rock volume
$p_m$ = matrix pressure
$p_f$ = fracture pressure

The shape factor σ is a geometric factor that depends on the geometry and the characteristic shape of the matrix–fissures system:

$$\sigma = \frac{A}{Vx} \tag{I.10}$$

where A = surface area of the matrix block, $ft^2$
V = volume of the matrix block
x = characteristic length of the matrix block, ft

In addition to permeability and skin, which control the behavior of double-porosity systems, there are two other characteristic parameters fully describe the fluid exchange between the

matrix and fractures. These two parameters are called storativity ratio (ω) and interporosity flow coefficient (λ) [1].

### I.5.3.2 Storativity Ratio (ω)

The dimensionless parameter (ω) defines the storativity of the fractures as a ratio to that of the total reservoir. Mathematically, it is given by [1]:

$$\omega = \frac{(\phi hc_t)_f}{(\phi hc_t)_{f+m}} = \frac{(\phi hc_t)_f}{(\phi hc_t)_f + (\phi hc_t)_m} \quad \text{(I.11)}$$

where ω = storativity ratio
h = thickness
$c_t$ = total compressibility, $psi^{-1}$
ϕ = porosity

The subscripts **f** and **m** refer to the fissure and matrix, respectively.

A typical range of **ω** is 0.1 to 0.001.

### I.5.3.3 Interporosity Flow Coefficient (λ)

The interporosity flow coefficient describes the ability of the fluid to flow from the matrix into the fissures, and is defined by the following mathematical relationship [1]:

$$\lambda = \sigma \left(\frac{K_m}{K_f}\right) r_w^2 \quad \text{(I.12)}$$

where λ =interporosity flow coefficient
$k_m$ = matrix permeability
$k_f$ = fracture permeability
$r_w$ = wellbore radius
σ =block-shape factor

### I.5.4 Formation Resistivity

Aguilera developed the following equation that relates the total formation resistivity factor (F), for dual porosity systems, to the total porosity:

$$F = \frac{R_0}{\nu\phi_t R_0 + (1-\nu)R_w} \quad \text{(I.13)}$$

where $R_0$ is the resistivity of porous invaded and $R_w$ is the formation water resistivity, both expressed in ohm-m.

If only the matrix porosity is present in the system, the porosity partitioning coefficient (ν), is equal to zero, thus:

$$F = \frac{R_0}{R_w} \quad \text{(I. 14)}$$

and is the same as for a consolidated matrix.

If only fracture porosity is present in the system, such as in type 1 naturally fractured reservoirs, the porosity partitioning coefficient is equal to unity. In this case, the formation resistivity factor can be expressed as:

$$F = \frac{1}{\phi_f^{m_f}} \quad \text{(I.15)}$$

Laboratory tests indicate that the tortuosity factor (r), and the fracture porosity exponent (mf), are approximately unity in systems with open and well-connected fractures. In type 2 and type 3 naturally fractured reservoirs, the formation resistivity factor can be more generally expressed as:

$$F = \frac{r}{(1-\phi_f^{m_f})\phi_f^{m_m} + \phi_f^{m_f}} \quad \text{(I.16)}$$

where $m_m$ is the matrix porosity exponent. [3]

## I.6 Indicators of Natural Fractures

All rock formations contain some fractures, and their presence in sufficient quantity to influence the reservoir is a matter of degree. The degree of fracturing present in a wellbore can be determined by either direct or indirect methods [2]:

### I.6.1 Direct Detection

There are three basic techniques:

- ✓ Direct observation and analysis of core
- ✓ Downhole cameras
- ✓ Inflatable packers

#### I.6.1.1 Direct Observation and Analysis of Core

Unquestionably, the best method for detecting reservoir fractures is by the observation of core material from the zone of interest, provided fracturing is not so intense as to impede core recovery. A whole-core material (including rotary side-wall cores) can provide fracture dip and intensity data as well as data on rock strength, rock fabric, and the interactive flow capabilities of the fractures and matrix. Oriented core material can, additionally, provide data on fracture azimuth. Such data facilitates in-depth quantitative analysis of fracture distribution and generation. Percussion sidewall cores are not recommended because the percussive event often generates numerous induced fractures into the sample.[2]

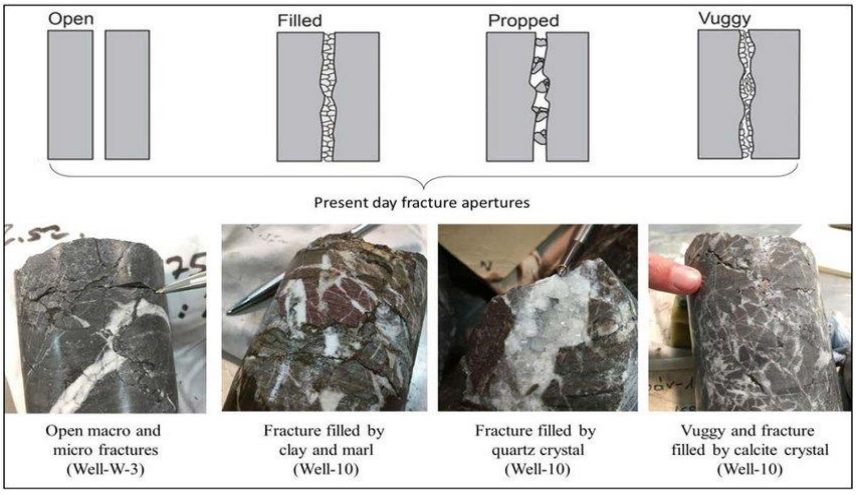


**Figure I.8: Fractured Core Samples with Various Types of Textures and Apertures.[8]**

### I.6.1.2 Downhole Cameras

Small downhole photographic and television cameras can be used to take pictures of the wellbore. These give direct information on such physical features as hole size, bedding planes, fractures, and faults. With the addition of an orientation device, downhole pictures can provide the same gross directional data on fractures as oriented cores. The latter, however, will provide rock composition, fabric, and strength data. Such data are often essential to a complete understanding of fractured reservoirs.

The photographic cameras are capable of taking up to 1,000 pictures per trip at downhole conditions of up to 200 ºF and pressures to 4,000 psi. Besides of to normal photographic problems, the greatest drawback of this method is that this tool can only be used in dry, gas filled, or clear water-filled wells. In addition, any drilling mud cake on the well wall may impede, or even eliminate, direct photography of the wellbore.[2]

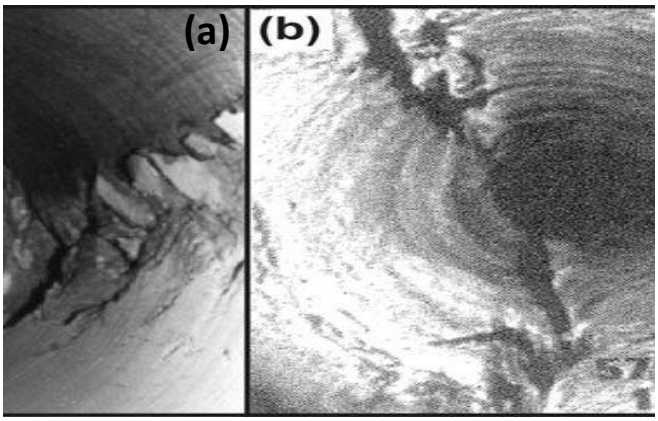


**Figure I.9: (a) Example of borehole breakout taken by a downhole camera. (b) Example of a borehole fracture observed on a downhole camera.[9]**

### I.6.1.3 Impression Packers

Impression packers are bladders coated with a soft pliable material. The unpressurized packer is lowered to the zone of interest in the well and then pressurized. As the soft coating is pressed against the wellbore, it conforms to the topography of the hole, including fractures. The pressure in the packer is then released, and the tool is removed from the hole. Subsequent observation of the packer coating gives an idea of the physical character of the wellbore, hopefully including the fracture system. Impression packers have been used almost exclusively in the detection of hydraulic fractures. This method works well for hydraulic fracture detection in uncased holes, because the hydraulic fractures are wide and cut the drilling mud cake. Natural fracture systems, however, may not cut the mud cake or may not be of sufficient width to be seen in the rubber skin. Therefore, this tool is often limited for detecting natural reservoir fractures. In addition, very large or irregular wellbores characteristic of many fractured formations often cause overextension and blowouts in the packers, making the technique somewhat unreliable.[2]

### I.6.2 Indirect Detection

Indirect techniques include:

- ✓ Primary well log evaluation
- ✓ Flow or well test evaluation
- ✓ Manipulation of reservoir rock property data.[2]

### I.6.2.1 Primary Well Log Evaluation

Nine logging tools used to detect reservoir fractures. Generally, these tools have been used to detect (with varying degrees of success) high-intensity fractured zones and not to determine fracture spacing. Because responses that are used to detect fractures on well logs are non-unique, a thorough knowledge of the tool and the various rock property effects, which could cause fracture-like responses, is necessary for fracture detection by well logs.[2]

#### I.6.2.1.1 Sonic Amplitude Log

This tool has probably been used more than any other to detect fractures. Compressional waves are attenuated more by vertical or high-angle fractures, while shear waves are more attenuated by horizontal and low-angle fractures. When a compressional wave encounters a fluid-filled fracture, its amplitude is reduced due to reflection at the interface. When a shear wave strikes a fluid-filled fracture, its amplitude essentially. Furthermore, one service company describes constructive/destructive interference as an indication of fractures that parallel the wellbore but do not intersect it.[2]

#### I.6.2.1.2 Variable Intensity of 3-D Log

Variable intensity logs record depth and amplitude versus time after an acoustic transmitter pulse. A large portion of the sonic wave train is recorded and plotted out in a seismic like trace on the log. Amplitude changes are evidenced by variations in shading on the log; dark shades show the largest positive amplitudes, and light shades show the largest negative amplitudes. This tool is used for fracture detection by looking for jumbled or chaotic zones (fractured rock) on the log between zones of distinct banding of parallel wave lines (unfractured rock). Other analysts do not look only for jumbled zones on the record, but also for specific W-shaped patterns. In both cases, however, unless the stratigraphic section is well known to the analyst, variations in lithology could be misinterpreted as fractured zones.[2]

#### I.6.2.1.3 Caliper Log

With a good knowledge of the stratigraphic section, the caliper log can be an appropriate tool for finding fractured zones in a well. In brief, it is assumed that highly fractured zones cave into the hole, thus enlarging the wellbore. Because normal hole enlargement can occur due to compositional differences, this tool works best in detecting relative fracture intensity differences in continuous, competent rock units such as carbonates. Any one of the different caliper tools (2, 3, 4-, or 6-arm) can be used to detect fractures. However, each one will give slightly different data about borehole configuration.[2]

#### I.6.2.1.4 Electrical and Acoustic Borehole Imaging Logs

The dominant fracture detection tools in today's industry are the fracture imaging logs. These include acoustic and electrical resistivity tools. The acoustic tools image the topography of the wellbore, while the resistivity tools image fluids within open fractures. A comparison of the two tools is shown in Figure I.10. This is a Schlumberger example of an ultrasonic borehole imager (UBI) and formation micro imager (FMI) log of a fractured reservoirs. The acoustic tool is often used when the well was drilled with oil-based muds because the resistivity imaging logs do not work well in these systems (improvements have been made allowing the resistivity imaging logs to be used in wells with these muds, but at the time of writing are not fully available). Also, the acoustic log is the best imaging log to define borehole breakouts for in situ stress direction determinations. But on the other hand, the resistivity imaging logs have finer resolution and can calculate a relative width or aperture of the fractures.[2]

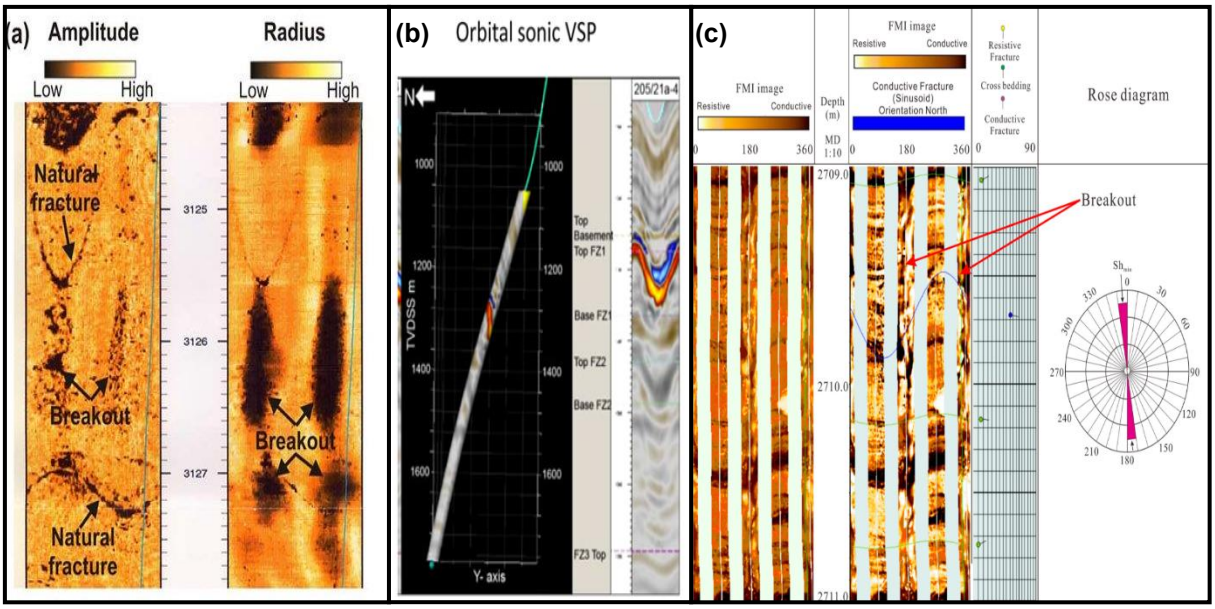


**Figure I.10: (a) Borehole breakouts observed on Ultrasonic Borehole Imager log. (b) Orbital Sonic VSP. (c) Breakouts Observed on FMI Imager Log.[9]**

### I.6.2.1.5 Dipole Sonic Log

The dipole sonic log utilizes both normal and shear wave acoustic data in the wellbore. The concept in the analysis of the data is that fractures in the rock mass do not affect the P wave travel, while they retard the S wave travel. Analysis of the sonic anisotropy derived from this oriented tool allows the interpreter to determine the dominant fracture direction within the wellbore and perhaps an estimation of fracture porosity as well. This tool seems to work best in carbonate sections.[2]

### I.6.2.1.6 Induction Log

The induction log has been used to determine the presence of fractures using the assumption that the presence of fractures provides resistivity anomalies. This process depends on the invasion of vertical fractures with a nonconductive fluid.

### I.6.2.1.7 Microlaterolog

This tool, like the induction log, uses resistivity anomalies to locate fracture zones. The laterolog is affected by vertical resistivity changes while the induction log is affected by horizontal resistivity changes. The difference between amplitudes on the microlaterolog and induction log has been used as an indication of the presence of vertical versus horizontal fractures depending on which tool reads higher resistivity.[2]

### I.6.2.1.8 Dipmeter Log

The continuous four-pad dipmeter has been used to detect fractures in two different ways. On one hand, the dipmeter is used as a two-directional caliper measuring hole

enlargement in one direction relative to another (maximum and 90 degrees from maximum enlargement). As in the caliper log, it is assumed that fractured zones cave into the hole parallel to the in-situ fracture system. On the other hand, the second method assumes resistivity changes due to fluid-filled fracture planes to be evidenced by each of the four pads of the four-pad dipmeter. Vertical displacement in response to the four pads can be used to calculate fracture dip and strike.[2]

**I.6.2.1.9 Density Log Compensation Curve**

This approach assumes that in a constant lithology (dense formation, such as clean carbonates), borehole roughness corresponds to the presence of fractures. The compensation curve acts as a very sensitive caliper to detect the roughness and, therefore, fractures. Of course, the detector is only about 2 in. in diameter. Therefore, it sees only a very small portion of the borehole circumference (≅ 8%). But since the detector is usually pushed into the major diameter of the wellbore, it may be looking at the most likely-to-be-fractured area, assuming the washout direction corresponds to fracture orientation.[2]

**I.6.2.1.10 Borehole Gravity Meter:**

While it is difficult to obtain and very difficult to interpret correctly, borehole gravity meter data can be used to detect large fractured zones in a well. The gravity meter determines the bulk density of a very large rock volume surrounding the wellbore. If there is very good data on the porosity and grain, and fluid density distribution in the rock, fracture porosity can be found. Providing the matrix data is very good and relatively consistent, and structure or terrain corrections can be handled. This tool has potential in not only finding fractures but in quantifying fracture porosity.[2]

**I.6.2.2 Flow or Well Test Evaluation**

Several models have been proposed to represent the pressure behavior in a naturally fractured reservoir. These models differ conceptually only in the assumptions made to describe fluid flow in the matrix. Most dual-porosity models assume that production from the naturally fractured system comes from the matrix, to the fracture, and then to the wellbore. Two common models, pseudosteady-state and transient flow, that describe flow in the less-permeable matrix are presented here. Pseudosteady-state flow was assumed transient flow in the matrix.

The more probable flow regime in the matrix is unsteady-state or transient flow; that is, flow in which an increasing pressure drawdown starts at the matrix/fracture interface and moves further into the matrix with increasing time. Only at late times pseudosteady-state flow should be achieved, although a matrix with a thin, low-permeability damaged zone at the fracture face

may behave as predicted by the pseudosteady-state matrix flow model even though the flow in the matrix is actually unsteady-state.

A semilog graph of test data for a formation with transient matrix flow has a particular shape different from that for pseudosteady-state flow in the matrix. Three distinct flow regimes have been identified that are characteristic of dual-porosity reservoir behavior with transient matrix flow. **Figure I.11** illustrates these flow regimes on a semilog graph as regimes 1, 2, and 3.[1]

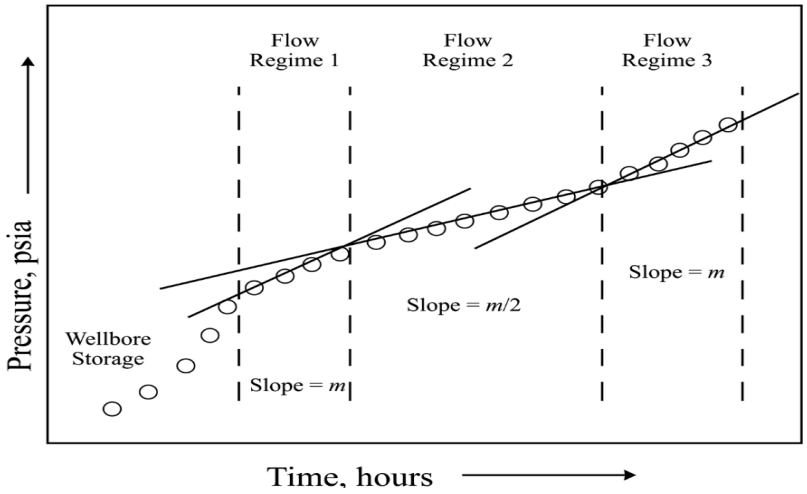


**Figure I.11: Flow Regimes in a Dual-Porosity Reservoir with Transient Matrix Flow.[10]**

Flow regime 1 occurs at early times during which all production comes from the fractures. Flow regime 2 occurs when production from the matrix into the fracture begins and continues until the matrix-to-fracture transfer reaches equilibrium. This equilibrium point marks the beginning of flow regime 3, during which total system flow, from matrix to fracture to wellbore, is dominant. The same three flow regimes appear when there is pseudosteady-state matrix flow. However, the duration and shape of the transition flow regimes is considerably different for the two matrix flow models.[10]

### I.6.2.3 Manipulation of Reservoir Rock Property Data

There are several indirect techniques used to detect fractures, or the effect of fractures, in the reservoir from reservoir rock property data. Each of these deals with cross-plotting various core- or log-derived data. All of these techniques can only give an indication of fracturing, and should, therefore, be followed up with additional direct or indirect detection techniques to prove the existence of fractures in the reservoir:

- Core Porosity Vs Core Permeability.
- Vertical Vs Horizontal Whole-Core Permeability.
- Core Permeability Vs Flow Test Permeability.
- Core Porosity Vs Porosity Determination from Neutron Log.
- Resistivity Vs Log Porosity.

- Sonic and Neutron or Density Log Curve Separation.[2]

### I.6.3 Remote Sensing

One method of very indirect detection of natural fractures in the subsurface is remote sensing. These approaches are basically extrapolations of surface data derived from remotely sensed images to subsurface formations. The basic data types used are radar imagery, and various types and scales of black and white or color photographs from low altitude to satellite-based scales.[2]

## Conclusion

In conclusion, naturally fractured reservoirs present both opportunities and challenges in hydrocarbon extraction. Their pre-existing fractures offer increased permeability, but complex fluid flow patterns can impact productivity. Hydraulic fracturing techniques provide a means to optimize connectivity between fractures and the wellbore, resulting in improved production rates and hydrocarbon recovery. However, careful reservoir characterization, customized fracture treatments, and effective monitoring are crucial to overcome challenges such as fracture interference and induced seismicity. Continued advancements in technology and understanding will further enhance the success of extracting hydrocarbons from naturally fractured reservoirs, contributing to the sustainable development of energy resources.

# Chapter II:

## Hydraulic Fracturing Concepts and Fundamentals

# CHAPTER II: Hydraulic Fracturing Concepts and Fundamentals

## Introduction

Hydraulic fracturing has become an essential part of petroleum and natural gas production, especially petroleum and natural gas that are otherwise trapped in low-permeability (shale) formations. The procedure significantly improves the recovery from the reservoir by stimulating the movement of petroleum and natural gas. Since the late 1940s, over 1 million wells have been hydraulically fractured in the United States, and more than 2 million have been fractured on a worldwide basis. When used in conjunction with horizontal drilling, an advanced drilling technology, hydraulic fracturing, has made it possible to develop vast unconventional resources.

## II.1 Definition of Hydraulic Fracturing

Hydraulic fracturing is the process of pumping a fluid into a wellbore at an injection rate that is too great for the formation to accept in a radial flow pattern. As the resistance to flow in the formation increases, the pressure in the wellbore rises to a value that exceeds the breakdown pressure of the formation open to the wellbore. Once the formation "breaks down" a fracture is formed, and the injected fluid begins moving down the fracture. In most formations, a single, vertical fracture is created that propagates in two directions from the wellbore. These fracture "wings" are 180° apart and normally are assumed to be identical in shape and size at any point in time; however, in actual cases, the fracture wing dimensions may not be identical. In naturally fractured or cleated formations, it is possible that multiple fractures can be created and propagated during a hydraulic fracture treatment.[11]

### II.1.1 The Objective of Hydraulic Fracturing

In general, hydraulic fracture treatments are used to increase the productivity index of a producing well or the injectivity index of an injection well. The productivity index defines the rate at which oil or gas can be produced at a given pressure differential between the reservoir and the wellbore, while the injectivity index refers to the rate at which fluid can be injected into a well at a given pressure differential. Hydraulic fracturing can:

- Increase the flow rate of oil and/or gas from low-permeability reservoirs
- Increase the flow rate of oil and/or gas from wells that have been damaged
- Connect the natural fractures and/or cleats in a formation to the wellbore
- Decrease the pressure drop around the well to minimize sand production
- Enhance gravel-packing sand placement
- Increase the area of drainage or the amount of formation in contact with the wellbore

- Decrease the pressure drop around the well to minimize problems with asphaltene and/or paraffin deposition
- Connect the full vertical extent of a reservoir to a slanted or horizontal well.[11]

## II.2 Development of Hydraulic Fracturing

Hydraulic fracturing is not a new technology, and the use of this technology can be traced to the early 1900s. Fracturing was first developed in the United States in the 1950's. In Canada much of the fracture treatments were applied to conventional reservoirs. In the mid of 1990, over the past 50 years, there have been significant advances in hydraulic fracturing technology.[12]

**Table II.1: Highlights in the Development of Hydraulic Fracturing.[12]**

| Date | Comment |
|---|---|
| Early 1950s | Fracturing with cement pumpers Vertical wells fractured with foam |
| 1947 | Klepper gas unit no.1: first well to be fractured to increase productivity |
| 1949 | Stephens County, Oklahoma: first commercial fracturing treatment |
| 1950 | Fracturing with cement pumpers |
| 1950s | Evolution of fracture geometry, Increasing well productivity |
| 1960s | Fracturing pumpers and blenders |
| 1970s | Massive hydraulic fracturing, Increase recoverable reserves, Hydraulic fracturing in Europe |
| 1983 | First gas well drilled in Barnett shale in Texas |
| 1980s | Evolution of proppant transport, Fracture conductivity testing, Cross-linked gel fracturing fluids developed; used in vertical wells |
| 1990s | First horizontal well drilled in Barnett shale Orientation of induced fractures identified Foam fracturing |
| 1996 | Slickwater fracturing fluids introduced |
| 1996 | Microseismic postfracturing mapping developed |
| 1997 | Hydraulic fracturing in Barnett shale, Slickwater fracturing developed |
| 1992 | Slickwater refracturing of originally gel-fractured wells |
| 2002 | Multistage slickwater fracturing of horizontal wells |
| 2003 | First hydraulic fracturing of Marcellus shale |
| 2004 | Horizontal wells become dominant |
| 2005 | Increased emphasis on improving the recovery factor |
| 2007 | Use of multi well pads and cluster drilling |

### II.2.1 New Developments of Hydraulic Fracturing

#### II.2.1.1 Fracturing Through Coiled Tubing

Recently, as a field-driven, cost-effective application, a hydraulic fracturing technique was introduced by Schlumberger, mainly in western Canada so far. It consists of a coiled tubing (CT) with a bottomhole assembly to isolate sets of perforations (straddle packers). The primary candidates are wellbores that produce gas commingled from multiple low-permeability zones after the fracturing operation. The primary objective is to place proppant effectively within all the producing intervals throughout the wellbore.

This service is called CoilFRAC and can be used both in old wells (which may have a weakened casing that might not withstand fracturing pressures) and new wells with perforated completions. Multiple hydraulic fracture stimulation treatments can be carried out in one single trip. It has been applied in temperatures up to 170°C, in deviated wells up to 75° deviation. CT diameters of 1.75" to 2.375" have been used, with flow rates of 8 to 25 bpm, proppant loadings of 5 to 12 ppg, in well depths up to 10,000 ft. When frictional pressure losses with standard polymer gel fluids become prohibitively high to use CT fracturing technology, a newly developed viscoelastic surfactant base fluid can be used (see below).

Halliburton recently also introduced a similar coiled tubing fracturing service, called Cobra Frac.[13]

#### II.2.1.2 Waterfracs

An unconventional hydraulic fracturing technique has been discussed in the literature, comprising fracturing treatments using treated water and very low proppant concentrations, or no propping agents at all, in microdarcy formations.

These treatments, referred to as waterfracs, were observed to be very successful, but for reasons not well understood as yet.

A waterfrac typically uses as fluid "treated water" (either 10 lbs/Mgal gel, or water with a friction reducer only), 50% pad, a constant 0.5 lbs/gal sand concentration and a tail-in with 0.5 - 2 lbs/gal ramp for the last 1 - 5% of the job. Treatment costs were lower by more than 50%, when compared to conventional hydraulic fracturing treatments.

While the success of waterfracs is not fully understood, it is thought to be due to one of the following hypotheses:

1- Hydraulic fractures do not fully close after pumping. Residual width, caused by asperities (i.e. a protrusion or irregularity above the surface of a fracture face, which inhibits slip) in all three dimensions can create a highly conductive path. Here, the stress regime plays a role on fracture roughness, and the more anisotropy in different directions, the more fracture

roughness. When pumping small amounts of proppant, this could assemble near obstructions. The proppant then acts as an extended asperity, keeping the fracture open. The conductivity is then given by channels in between asperities and proppant, rather than by a proppant pack (similar to partial monolayers).

2- Conventional treatments do not clean up efficiently.

In sum, it was concluded that long fractures have been achieved with low viscosity fracturing fluids (water), with easier cleanup than with more conventional fluids.[13]

**II.2.1.3 Acid Fracturing**

This technique applied in carbonates only, involves the use of a non-reactive "conventional"- low or high viscosity preflush to initiate and propagate a fracture, followed by the injection of low-viscous acid, usually HCl. As the acid flows along the fracture, portions of the fracture face are dissolved. Since flowing acid tends to etch the fracture walls in a nonuniform manner, conductive channels are created which usually remain open when the fracture closes.

The basic principles and objectives of acid fracturing are the same as for propped hydraulic fracturing treatments in sandstones. In both cases the goal is to produce a conductive fracture with sufficient length, to allow more effective drainage of the reservoir. The major difference is how fracture conductivity is achieved. In propped fracturing treatments, sand or other propping agent is placed in the fracture to prevent closure when pressure is released. Acid fracturing in carbonates, relies on nonuniform etching of fracture faces to provide the required conductivities. For homogeneous carbonates, a highly viscous preflush is required. This will cause the low viscous acid to displace the high viscous preflush in a finger-type pattern, thus creating high conductivity flow channels. To prevent these fingers from merging, special perforation schemes should be applied, e.g., 2 ft of high-density perforations (4 spf or more) every 5 ft, and a viscosity ratio between the preflush and acid of around 300 should be maintained.[13]

**II.2.1.3.1 Propped Acid Fracturing**

In very soft carbonates, the walls of the etched channel may be too weak to withstand the closing pressure of the fracture under producing conditions. The channel may lose its conductivity, which will render the stimulation totally ineffective. To prevent this, proppant may be used to keep the channels open. Such a treatment then comprises an acid fracturing treatment, followed by a proppant stage. The advantage of this approach over conventional propped fracturing, is that a relatively high fracture conductivity can be obtained with relatively low proppant concentrations. However, practical results (offshore Denmark and Norway) show a

rapid decline of production after the initial increase in production. With the introduction of more sophisticated fluids and equipment for conventional fracturing, allowing more aggressive designs with higher sand concentrations, the application of propped acid fracturing has virtually been abandoned, being replaced by "conventional" propped hydraulic fracturing in such soft carbonates.[13]

#### II.2.1.3.2 Closed Fracture Acidizing (CFA)

The injection of a low viscosity acid at a pressure just below the fracture closure pressure of a previously, or naturally fractured (soft) carbonate formation, is a possible solution for the above described problem of fracture closure. Although the fracture is closed, it still forms a preferential flow path for the acid. This causes a wormhole type penetration of the acid along the original fracture plane, when acid is injected in the closed fracture. Since only a small portion of the overall fracture face will be dissolved into relatively deep channels or grooves, the remaining unetched fracture face can hold these channels open under very severe formation closure conditions, without completely collapsing the etched channels. This is especially beneficial in chalk formations.[13]

## II.3 Hydraulic Fracturing Fluid

A hydraulic fracturing fluid for geothermal applications needs to combine a number of, sometimes conflicting, properties. While traveling down the well the viscosity should be relatively low to avoid an excess of friction. During the time it creates the fracture the viscosity should be high to increase the efficiency and to carry the proppant into the fracture. Upon terminating the treatment, the fluid should lose its viscosity to allow easy flow back (in a producer) or easy (re-) start of injection. Furthermore, a fluid should be compatible with the formation rock and should not pose a threat to the environment.[14]

### II.3.1 Types of Fracturing Fluid

To combine all these requirements in a single fluid formulation is not easy but the oil and gas industry has succeeded in formulating fluids that come very close. following fluid types are the mostly used:

**Table II.2: Fracturing Fluids and Conditions for Their Use.[15]**

| Base Fluid | Fluid type | Main composition | Used for |
|---|---|---|---|
| **Water** | Linear | Guar, HPG, HEC, CMHPG | Short fractures, low temperature |
| | Crosslinked | Crosslinker + Guar, HPG, CMHPG or CMHEC | Long fractures, High temperature |
| | Micellar | Electrolite + Surfactant | Moderate length fractures, Moderate temperature |
| **Foam** | Water based | Foamer +$N_2$ or $CO_2$ | Low pressure formations |
| | Acid based | Foamer + $N_2$ | Low pressure, carbonate formations |
| **Oil** | Alcohol based | Methanol + Foamer + $N_2$ | Low pressure, Water-sensitive formations |
| | Linear | Gelling agent | Short fractures, Water-sensitive formations |
| | Crosslinked | Gelling agent + Crosslinker | Long fractures, Water-sensitive formations |
| | Water emulsion | Water + Oil + Emulsifier | Moderate length fractures, good fluid loss control |
| **Acid** | Linear | Guar + HPG | Short fractures, carbonate formations |
| | Crosslinked | Crosslinker + Guar or HPG | Longer, Wider fractures, carbonate formations |
| | Oil emulsion | Acid + Oil +Emulsifier | Moderate length fractures, carbonate formations |

**Table II.3: Acceptable Levels for Mix Water.[15]**

| Item | Value |
|---|---|
| PH | 6 to 8 |
| IRON | < 10 ppm |
| Oxidizing agents | None |
| Reducing agents | None |
| Carbonate* | < 300 ppm |
| Bicarbonate* | < 300 ppm |
| Bacteria | None |
| Cleanliness | Reasonable |

*Higher Carbonate/ Bicarbonate content requires further pilot testing on gel break and crosslinking.

### II.3.2 Fracturing Fluid Additives

Fracturing fluids are complex mixtures containing as many as six or seven different components. Many low concentrations of various additives are used to control specific behavioral characteristics of the frac-fluids at several distinct phases of the fracture treatment.

The relative compatibility of the mixed additives must be determined for each formulation to avoid reactions that will lead to loss of the reacting additives through precipitation and/or deactivation. Gelling agents and crosslinkers define the specific fluid type, and they are not considered to be additives.[16]

Fluid additives are materials used to produce a specific effect, independent of fluid type. When using additives, however, their relative compatibility needs to be carefully verified. And in general, the question should be asked whether the additive, mostly advocated by the service companies, is really required. The basic principle of using additives in fracturing fluids should be to keep it as simple as possible.[17]

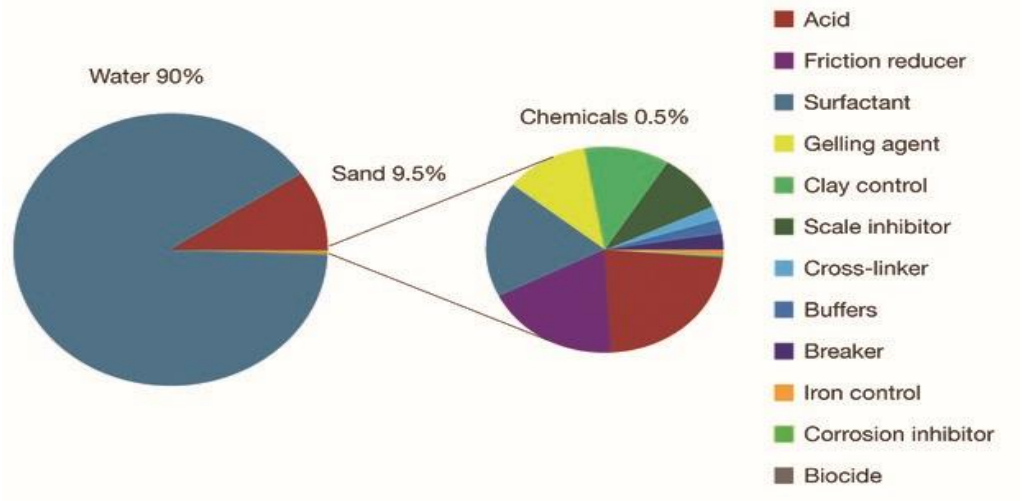


**Figure II.1: Typical Fracture Fluid Composition.[18]**

**Table II.4: Summary of Chemical Additives.[15]**

| Type of additive | Function Performed | Typical Products |
|---|---|---|
| Biocide | Kills Bacteria | Gluteraldehyde carbonate |
| Breaker | Reduces Fluid Viscosity | Acid, Oxidizer, Enzyme breaker |
| Buffer | Controls the PH | Sodium bicarbonate, Fumaric Acid |
| Clay Stabilizer | Prevents Clay Swelling | KCI, NHCI, KCI substitules |
| Diverting agent | Diverts Flow of Fluid | Ball sealers, rock salt, flake boric acid |
| Fluid Loss Additive | Improves Fluid Efficiently | Diesel, Particulates, Fine Sand |
| Friction Reducer | Reduces The Friction | Anionic Copolymer |
| Iron Controller | Keeps Iron In Solution | Acetic and Citric Acid |
| Surfuctant | Lowers surface tension | Fluorocarbon, Nonionic |
| Gel Stabilizer | Reduces thermal Degradation | MEOH, Sodium Thiosulphate |

## II.4 Hydraulic Fracturing Proppants

### II.4.1 Definition of Proppants

Proppants are small particles made of a solid material, the purpose of proppant is to keep the walls of a hydraulically created fracture apart, to maintain a conductive path to the wellbore after pumping has stopped. The propped fracture must have a conductivity at least high enough to eliminate most of the radial flow path, that exists around an unfractured well, and to allow linear flow from the reservoir into the fracture. For the design of a hydraulic fracturing treatment, it is important to select the right proppant. For instance, if sand is used and it crushes in the fracture, well productivity may be lost. However, if in such a case a proppant other than sand is used, there is an increase in cost, which should be balanced against the expected economics of the treatment.[19]

### II.4.2 Proppants Selection

The primary requirement for an ideal proppant for hydraulic fracturing is a sustained high permeability under reservoir conditions. This requires:

- Sufficient strength to withstand proppant particle crushing under the increased rock stresses arising from production and depletion.
- A uniform, preferably spherical shape. Well rounded particles are less likely to bridge in the perforations or in the fracture. At high closing pressure, they are less likely to crush under load.
- A narrow proppant size distribution, which helps to reduce point loading and crushing of the proppant in the fracture.
- A minimum of over- and undersized particles (including dirt).
- Resistance to fracturing fluid, formation fluids and acid.
- Availability in a range of suitable sizes. Size not only influences permeability, but also placement, since larger grains settle faster and bridge more easily.
- Low density, preferably equal to that of the fracturing fluid to avoid proppant settling during transport in the fracture.
- Availability in large quantities, at an acceptable cost.[13]

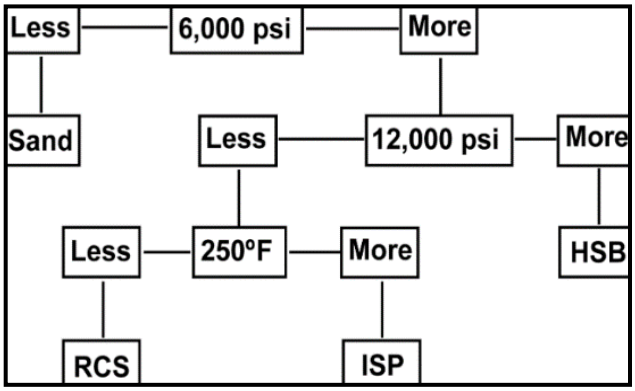


**Figure II.2: Proppant Selection Based on Closure Pressure.[20]**

### II.4.3 Proppant Pack Conductivity

The efficiency of a hydraulic fracturing stimulation is critically dependent on the conductivity of the propped fracture. The main factors that affect fracture conductivity are briefly discussed below.[13]

#### II.4.3.1 Fracture Closure Stress

The conductivity of a proppant pack is a function of the fracture closure stress. As a result of compaction, elastic deformation and grain crushing, the conductivity of a proppant pack decreases with increasing closure stress (deeper reservoirs). Increased closure stress can also be the result of reservoir depletion. Cycling of stress, as would occur with periodic shut-ins of a well, also reduces fracture conductivity irreversibly.[13]

**Figure II.3** shows the proppant pack permeability as a function of load for various types of 20-40 mesh proppant. Ottawa sand loses most of its permeability as a result of grain crushing above a stress of 6,000 psi. Between 6,000 and 8,000 psi, the conductivity of precured resin-coated sand is better than that of Ottawa sand. Intermediate strength proppant, has a much better conductivity up to 10,000 psi. At higher closure stress, sintered bauxite performs better.[13]

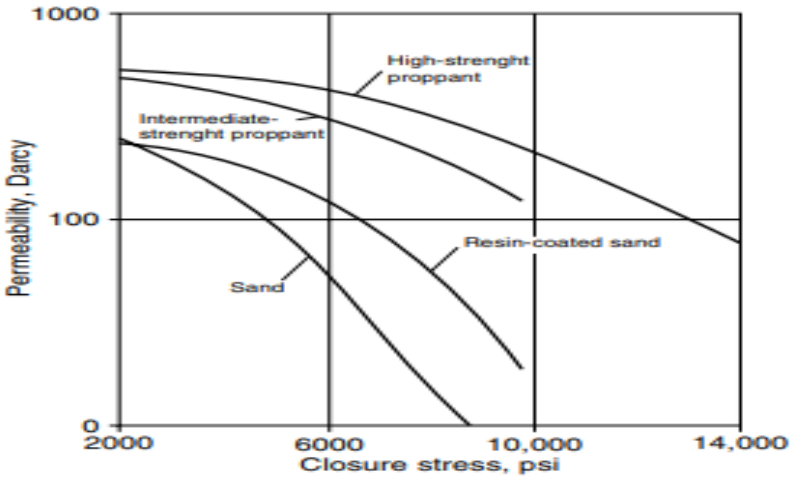


**Figure II.3: Strength Comparison of Various Types of Proppants.[16]**

### II.4.3.2 Particle Size, Shape, and Sorting

Proppant particle size has a significant effect on packed fracture permeability, and, in principle, the larger the size, the higher the permeability of the proppant pack. However, as stress levels increase, larger sand grains will crush earlier than smaller sand grains, which will result in a poorer sorting and thus in a lower conductivity.

Particle shape (roundness and sphericity) also plays a role in the proppant pack conductivity with increasing stress. When compared with other sands, the better roundness, the more uniform size and the higher percentage of the monocrystalline grains of Ottawa sand play an important role in reducing the number of fines generated under increasing closure stress. As a result, Ottawa sand performs better than any other sand at closure stresses above 4000 psi.

Another important consideration of proppant size in the design of fracturing treatments is that the perforation diameter must be large enough to prevent proppant bridging during the treatment, and a minimum fracture width is needed to allow the proppant to enter the fracture. Additionally, proppant transport should also be considered in the selection of the size of propping agent. Even though a 12-20 mesh proppant may be much more conductive than a 20-40 mesh proppant, the smaller proppant is much easier to transport deeply into a fracture than the larger proppant.

Generally, the use of two sizes of proppant in one job is not recommended. It may result in a zone of poorer sorting of the proppant since mixing of the proppants cannot be excluded.[13]

### II.4.3.3 Proppant Embedment

If proppant particles penetrate the walls of the fracture under closing stress, the effective permeability can reduce significantly, since the width of the fracture is reduced. This is not likely to be a problem in deep, tight reservoirs where the formation is hard, but it may be a problem, particularly in soft chalk reservoirs. With the introduction of more sophisticated fluids, allowing more aggressive designs with higher sand concentrations (e.g. 10 to 40 particles thick pack), this problem has been virtually resolved.[13]

### II.4.3.4 Proppant Concentration

Proppant concentration refers to the amount of proppant per unit area of fracture wall (measured on one side only). Fracture conductivity increases with increasing concentration of proppant in the fracture. This relationship does not hold for low concentrations (<2.44 $kg/m^2$), because of wall effects. This is caused by the greater void volume between the outside layer of the proppant and the fracture wall, than between the proppant layers. As a result, the

permeability of a proppant pack is greatly influenced by the outside layers when there are only a few layers of proppant. This effect becomes negligible above about five layers of proppant. During the early days of fracturing, much attention was given to creating high fracture conductivities by the use of monolayers of proppant. The very high conductivity obtained from a (partial) monolayer, however, is unrealistic, since it is very sensitive to filter cake effects, partial embedment, fluid residue, etc. This idea has now been abandoned, except for very low formation permeability. The application of high to ultra-high proppant concentrations, resulting in multiple layers of proppant, the conductivity of which is less sensitive to differences in hardness, proppant pack damage, etc., is currently the preferred approach to create highly conductive fractures.[13]

### II.4.3.5 Fracturing Fluid Residue

Actual fracturing fluids will always leave some residue in the proppant pack in the form of polymer residue, unbroken gel particles, fluid-loss material, filter cake etc., thus reducing the conductivity of the propped fracture. The problem is most pronounced when the volume of residue from the polymer is high, when polymer concentration is high, when the concentration of proppant in the closed fracture is low and when the stress on the fracture is high, causing lower porosity. In laboratory testing of several fluids, the reduction in fracture flow capacity was found to be greatest for crosslinked HPG fluids and least for emulsion fluids, as shown below in **Table II.5 [13]**

**Table II.5: Proppant Pack Damage from Fracturing Fluids.[13]**

| Fluid Type | Damage (%) |
|---|---|
| Polymer Emulsion | 15 - 35 |
| Gelled Oil | 30 - 55 |
| Linear Gel | 45 - 55 |
| Crosslinked HPG - Borate | 25 – 50 |
| - Ti/Zr | 50 - 80 |
| Liquid $CO_2$ | Less than 10 |
| VES fluids | Less than 10 |

### II.4.4 Proppant Types

Fracture conductivity in many hydraulic fracturing treatments can be inadequate and is subject to the concentration of the packed proppant in the fracture. Higher concentrations yield higher conductivity by virtue of a wider fracture. However, there are practical limitations to the amount of proppant that can be placed into any particular reservoir, and therefore production is often conductivity limited. Since propping agents are required to maintain the fracture in the

open configuration once the pumps are shut down and the fracture begins to close, the ideal prop ping agent must be strong, resistant to crushing, resistant to corrosion, has a low density, and is readily available at low cost. The products that best meet these desired traits are frac sand, RCS (resin-coated sand), and ceramic proppants.[21]

The first of these types is known as frac sand, and is simply a high-purity quartz sand with durable, round grains. As a result of its strength, it is crush-resistant, and thus is effective as propping open cracks made in the ground during the hydraulic fracturing process. Most of this sand is made from high purity sandstone. Although it is natural, this frac sand is not used directly out of the ground, rather it requires processing. The processing process involves washing to remove particles that are too small, and then a screening process to ensure the remaining grains are the correct size.[22]

Other types of proppant materials include resin-coated sand and ceramic proppants. Resin-coated sand is simply sand that is coated in a resin material to smooth the surface of the sand and make the shape more uniform. Along with this, coating the sand in resin increases its strength, making it more desirable as a proppant. Finally, ceramic proppants are the most uniform in shape and the strongest of the proppants as their manufacturing is entirely controlled. The uniform shape of this type of proppant ensures that there is more space for the oil and gas to flow through the proppant material and out of the well.[22]


**Figure II.4: Proppant Types Pyramid.[21]**

## II.5 Hydraulic Fracturing Process

### II.5.1 Equipments

Once the well has been drilled and the wellbore has been tested for integrity, the site is prepared for well stimulation through hydraulic fracturing. Various surface facilities and mobile equipment including fracture fluid storage tanks, sand storage units, chemical trucks, blending

equipment and pumping equipment surround the wellhead on the lease. The hydraulic fracturing process is monitored from a single truck often referred to as the Data Monitoring Van. The Data Monitoring Van will monitor and record the rate and pressure at which the fracturing fluid is pumped down the wellbore, the rates of the necessary additives present in the fracturing fluid and proppant concentration. Prior to and during the hydraulic fracturing job, you can expect to see an increase in heavy traffic on the roads surrounding the lease, as required equipment and services, such as graders, water trucks, the service rig and other heavy equipment is transported to and from the site. Once the hydraulic fracturing program and related operations are completed the traffic should decrease substantially.[23]

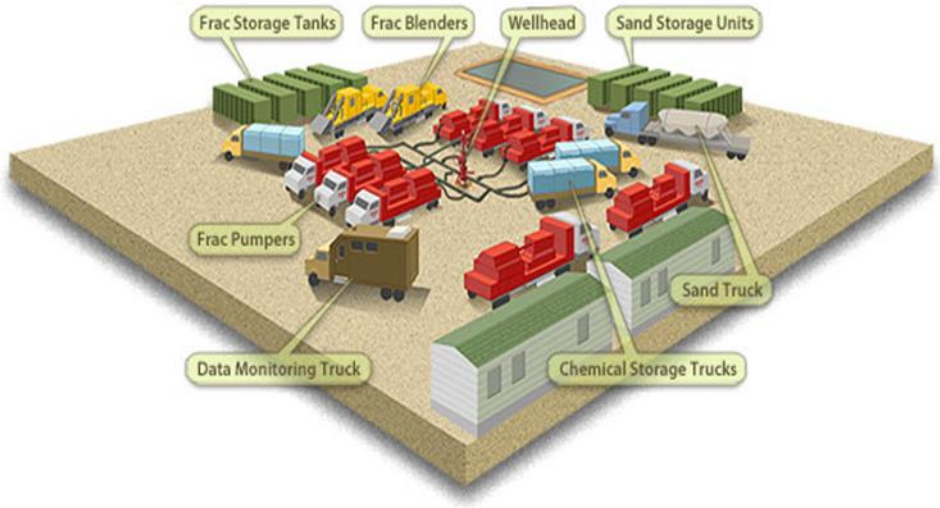


**Figure II.5: Hydraulic Fracturing Equipments.[23]**

### II.5.2 Chronological Sequence of Hydraulic Fracturing Process

1- Well Data Analysis: Well Location, Existing Well Diagram, Log / Petrophysics (Sw, Por), MDT (K, Pr), and Geomechanically modelling (Stress Distribution).

2- Fracturing Design: Optimum half length, Design pump Schedule, Treatment pressure, Flow capacity, and Fracture geometry.

3- Injection Tests.

4- Treatment Evaluation: Injection tests analysis, and Calibration injection Test / DATA Frac (Data Frac Analysis & Pressure Match analysis).

5- Treatment Redesign.

6- Main Frac Execution.

7- Main Frac Evaluation & Result: Pressure Match, and Frac Simulation [24]

### II.5.3 Injection Tests

The only reliable technique for measuring in-situ stress is by pumping fluid into a reservoir, creating a fracture, and measuring the pressure at which the fracture closes. The well tests used to measure the minimum principal stress are:

- In-situ stress tests
- Step-rate/flowback tests
- Minifracture tests
- Step-down tests

For most fracture treatments, minifracture tests and step-down tests are pumped ahead of the main fracture treatment. As such, accurate data are normally available to calibrate and interpret the pressures measured during a fracture treatment. In-situ stress tests and step-rate/flow-back tests are not run on every well; however, it is common to run such tests in new fields or new reservoirs to help develop the correlations required to optimize fracture treatments for subsequent wells.[25]

#### II.5.3.1 In-situ stress tests

An in-situ stress test can be either an injection-falloff test or an injection-flowback test. The in-situ stress test is conducted with small volumes of fluid (a few barrels) and injected at a low injection rate (tens of gal/min), normally with straddle packers to minimize wellbore storage effects, into a small number of perforations (1 to 2 ft). The objective is to pump a thin fluid (water or nitrogen) at a rate just sufficient to create a small fracture. Once the fracture is open, the pumps are shut down, and the pressure is recorded and analyzed to determine when the fracture closes. Thus, the term "fracture-closure pressure" is synonymous with minimum in-situ stress and minimum horizontal stress. When the pressure in the fracture is greater than the fracture-closure pressure, the fracture is open. When the pressure in the fracture is less than the fracture-closure pressure, the fracture is closed. Figure II.6 illustrates a typical wellbore configuration for conducting an in-situ stress test. Figure II.7 shows typical data that are measured. Multiple tests are conducted to ensure repeatability. The data from any one of the injection-falloff tests can be analyzed to determine when the fracture closes.[25]

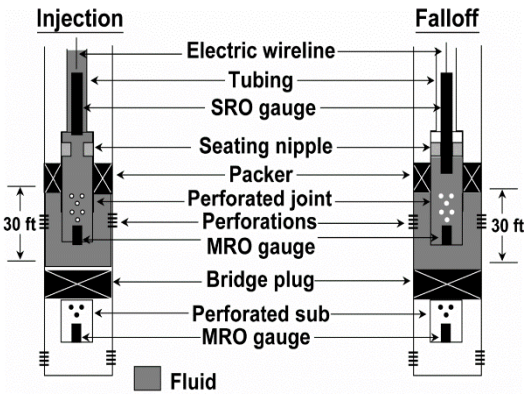


**Figure II.6: Wellbore hardware required for an in-situ stress test.[25]**

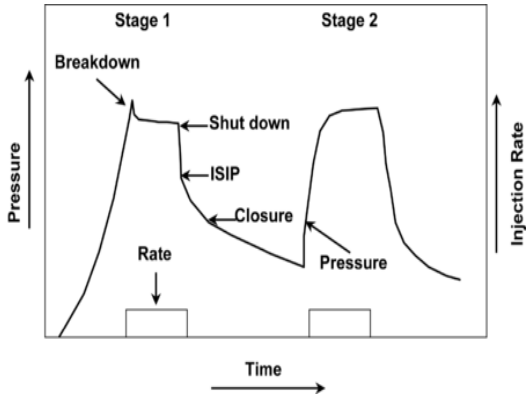


**Figure II.7: Typical data from an in-situ stress test.[25]**

### II.5.3.2 Minifracture tests

Minifracture tests are run to reconfirm the value of in-situ stress in the pay zone and to estimate the fluid-loss properties of the fracture fluid. A minifracture test is run with fluid similar to the fracture fluid that will be used in the main treatment. Several hundred barrels of fracturing fluid are pumped at fracturing rates. The purpose of the injection is to create a fracture that will be of similar height to the one created during the main fracture treatment. After the minifracture has been created, the pumps are shut down, and the pressure decline is monitored. The pressure decline can be used to estimate the fracture-closure pressure and the total fluid leakoff coefficient. Data from minifracture treatments can be used to alter the design of the main fracture treatment, if required.[25]

### II.5.3.3 Step-down tests

For any injection-falloff test to be conducted successfully, a clean connection between the wellbore and the created fracture is needed. The main objective of an in-situ stress test and the minifracture test is to determine the pressure in the fracture when the fracture is open and the pressure when the fracture is closed. If there is excess pressure drop near the wellbore because of poor connectivity between the wellbore and the fracture, the interpretation of in-situ stress test data can be difficult. In naturally fractured or highly cleated formations, multiple fractures that follow tortuous paths are often created during injection tests. When these tortuous paths are created, the pressure drop in the "near-wellbore" region can be very high, which complicates the analyses of the pressure falloff data. To determine the cause of near-wellbore pressure drop, step-down tests are run.

A step-down test is pumped just before the minifracture treatment. A step-down test is pumped at fracturing rates with linear fluids, the friction pressures of which are well known. The pressure at the bottom of the hole during the injection is a function of the net pressure in

the fracture and the near-wellbore pressure drop. To measure the near-wellbore pressure drop, the net pressure in the fracture needs to be relatively constant during the step-down portion of the test. To do this, the step-down test is started by injecting into the well for 10 to 15 minutes. Experience has shown that, in most cases, the net pressure is relatively stable after approximately 10 to 15 minutes of injection. The injection rate is then "reduced in steps" to a rate of zero. The injection rate at each step should be held constant for approximately 1 minute so the stabilized injection pressure can be measured. The injection rate should be stepped from the maximum value to zero, in three to five steps, in less than 5 minutes. The objective of the step-down test is to measure the near-wellbore pressure drop as a function of injection rate. If the net pressure in the fracture is relatively stable, then the change in bottomhole injection pressure as the injection rate is reduced will be a function of the near-wellbore pressure drop.[25]

### II.5.4 Main Frac Execution

The process of hydraulic fracturing treatment may be described very briefly, and generally, as a set of stages:

#### II.5.4.1 Stage 1

Fracture initiation is accomplished by pumping fluid at a rate faster than the leak-off rate into the formation in an open hole at the bottom of the well, or through perforations in the casing. Fluid pressure is increased in the rock to overcome the compressive stress of the rock. The rock then breaks (fractures) along a plane perpendicular to the minimum compressive stress in the matrix. After parting, the fracture is extended in width and length as fluid pressure in the fracture works against the elasticity of the rock.

The rock then breaks (fractures) along a plane perpendicular to the minimum compressive stress in the matrix. After parting, the fracture is extended in width and length as fluid pressure in the fracture works against the elasticity of the rock.

#### II.5.4.2 Stage 2

Proppant placement After the fracture is widened sufficiently to accept proppant material, sand or other granular matter is added to the frac-fluid and pumped into the fracture. Then, the fracture grows upward, downward, and outward.

#### II.5.4.3 Stage 3

Ending of fracture growth when the rate of frac-fluid leak-off equals the rate of fluid injection. When enough proppant has been added, pumping is stopped and the pressure in the fracture decreases. Growth of the fracture may also end due to “sand-out” As sand deposits in

the fracture, greater pressure is required to increase the fracture length. If the limit of pressure application has been reached, fluid injection slows, and may stop, causing sand to drop out of suspension and thus ending the fracture treatment prematurely.

### II.5.4.4 Stage 4

Removal of frac-fluid after a rest period to allow time for the viscosity breakers to decrease the viscosity of the frac-fluid in the fracture, the well is pumped to remove the frac fluid and fluid loss additives and to place the well back into production at a considerably enhanced flow rate.[26]

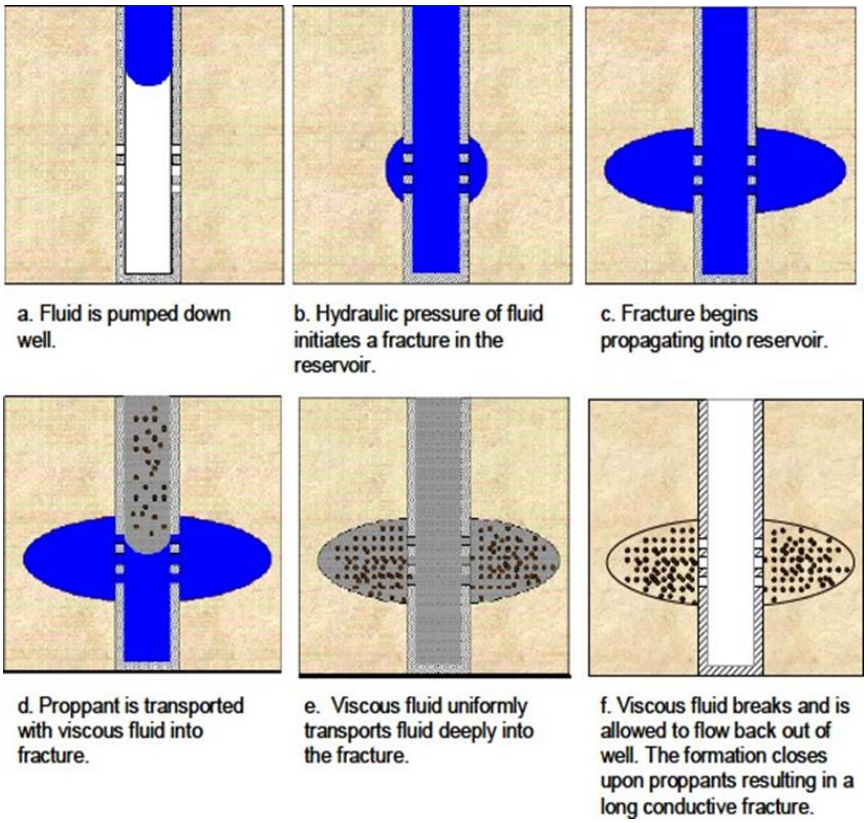


**Figure II.8: Hydraulic Fracture Stimulation Process.[26]**

## II.6 Rock Mechanics Applied in Hydraulic Fracturing

### II.6.1 In-situ stresses

Underground formations are confined and under stress. Figure II.7 illustrates the local stress state at depth for an element of formation. The stresses can be divided into three principal stresses. In Figure II.7:

- $\sigma_1$ is the vertical stress (Overburden stress).
- $\sigma_2$ is the minimum horizontal stress.
- $\sigma_3$ is the maximum horizontal stress.

These stresses are normally compressive, anisotropic, and nonhomogeneous, which means that the compressive stresses on the rock are not equal and vary in magnitude on the basis of direction. The magnitude and direction of the principal stresses are important because they control the pressure required to create and propagate a fracture, the shape and vertical extent of the fracture, the direction of the fracture, and the stresses trying to crush and/or embed the propping agent during production.[25]

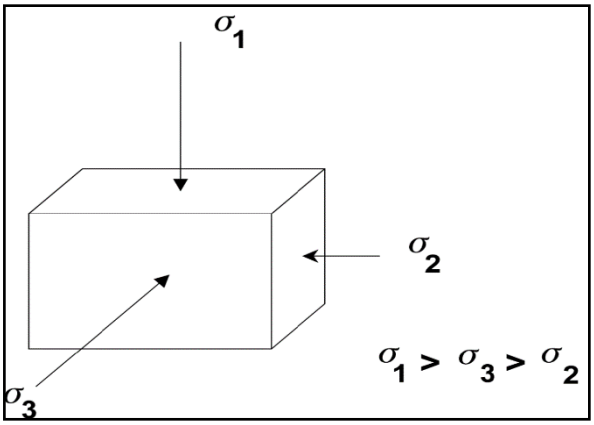


**Figure II.9: The Three Principal Compressive Stresses.[25]**

- **Vertical Stress (Overburden stress):**

Stress due to the weight of the reservoir rock overlaying above the formation, Overburden stress gradient (1.0 - 1.1) psi/ft.

- **Horizontal Stresses:**

Primarily result of overburden stress, reservoir pressure and tectonic forces, minimum horizontal stress gradient (0.3 - 0.9) psi/ft.

**In-situ stresses control ⟶ Fracture Orientation**

A hydraulic fracture will propagate perpendicular to the minimum principal stress. For a vertical fracture, the minimum horizontal stress can be estimated with:

$$\sigma_{min} = \frac{\nu}{1-\nu}\left(\sigma_1 - \alpha p_p\right) + \alpha p_p + \sigma_{ext} \qquad \text{(II.1)}$$

where:

$\sigma_{min}$: The minimum horizontal stress.
$\nu$ : Poisson's ratio.
$\sigma_1$ : Overburden stress.
$\alpha$ : Biot's constant.
$p_p$ : Reservoir fluid pressure or pore pressure.
$\sigma_{ext}$: Tectonic stress.

### II.6.2 Rock Properties

Different rock properties will affect the propagation of HF differently. The major rock properties of importance to HF are Young's modulus, Poisson's ratio, Bulk compressibility, and toughness.

#### II.6.2.1 Young's Modulus (E)

Young's modulus is the ratio of tensile stress (σ) to tensile strain (ε). Where stress is the amount of force applied per unit area (σ = F/A) and strain is extension per unit length (ε = dl/l). This value is an indication of rock stiffness.

The larger Young's modulus, the more brittle the rock and better for HF operation.

$$E = \frac{\sigma}{\varepsilon} \tag{II.2}$$

E : Young's Modulus, pressure units.

σ : Uniaxial stress, or uniaxial force per unit surface, pressure units.

ε : Strain, or proportional deformation (change in length divided by original length), dimensionless.[27]

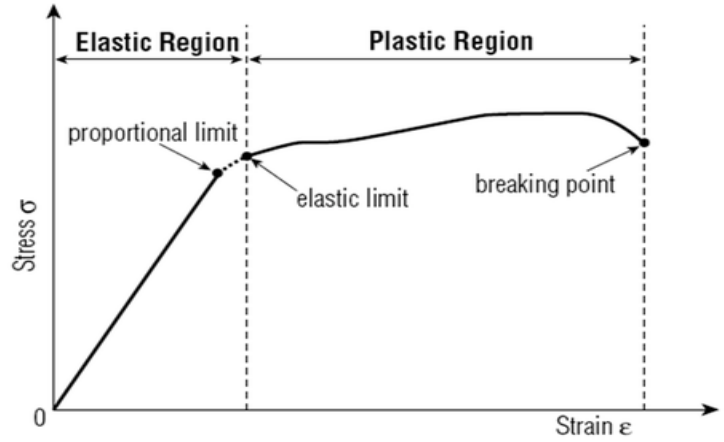


**Figure II.10: Young's Modulus.[27]**

#### II.6.2.2 Poisson's Ratio (ν)

which is the ratio of lateral to axial displacement of a rock under compressional load, responds in an opposite way. As the Poisson's ratio or rock deformability is increased, the brittleness reduces, which is less favorable for hydraulic fracturing operation.[28]

$$\nu = -\frac{d\varepsilon_{trans}}{d\varepsilon_{axial}} = \frac{\text{lateral strain}}{\text{longitudinal strain}} \tag{II.3}$$

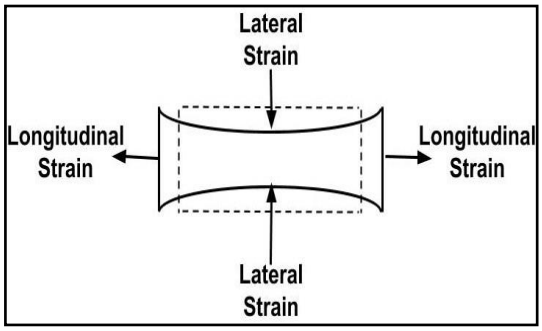


**Figure II.11: Poisson's Ratio.[28]**

**Table II.6: Typical Range of Values for Young's Modulus and Poisson's Ratio.[25]**

| Lithology | Young's Modulus (psi) | Poisson's Ratio |
|---|---|---|
| Soft sandstone | $0.1\text{-}1\times10^6$ | 0.2 to 0.35 |
| Meduim sandstone | $2\text{-}5\times10^6$ | 0.15 to 0.25 |
| Hard sandstone | $6\text{-}10\times10^6$ | 0.1 to 0.15 |
| Limestone | $8\text{-}10\times10^6$ | 0.30 to 0.35 |
| Coal | $0.1\text{-}1\times10^6$ | 0.35 to 0.45 |
| Shale | $1\text{-}10\times10^6$ | 0.28 to 0.43 |

### II.6.2.3 Shear Modulus (G)

Shear modulus is the ratio of shear stress (force per unit area) to shear strain (displacement at the edge). It is an indication of a material's rigidity and its resistance to deformation due to shear stress.[28]

$$G = \frac{E}{2(1+\nu)} \tag{II.4}$$

G : Shear modulus, pressure units
E : Young's Modulus, pressure units
ν : Poisson's ratio

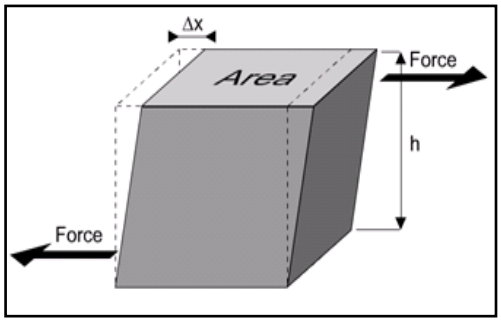


**Figure II.12: Shear Modulus.[28]**

### II.6.2.4 Bulk Compressibility (C)

Bulk modulus is numerical constant that describes the elastic properties of a solid or fluid when it is under pressure on all surfaces. The applied pressure reduces the volume of a material, which returns to its original volume when the pressure is removed. Sometimes referred to as the incompressibility, the bulk modulus is a measure of the ability of a substance to withstand changes in volume when under compression on all sides. It is equal to the quotient of the applied pressure divided by the relative deformation.[29]

$$C = \frac{\text{Stress}}{\text{Volumetric strain}} \quad \text{(II.5)}$$

C : Bulk Compressibility, pressure units

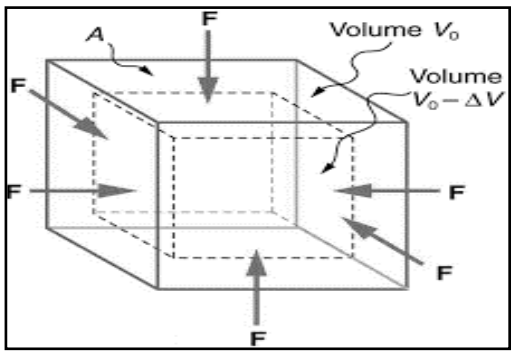


**Figure II.13: Bulk Modulus.[29]**

## II.7 Hydraulic Fracturing Pressure Evolution

Hydraulic fracturing is the prime technology to stimulate reservoirs. In general, in a hydraulic fracturing job, a viscous fluid is injected in order to initiate and propagate a fracture plane of a few hundred feet into the reservoir to create a flow path from the reservoir to the wellbore. Figure II.12 shows schematically the plot of the pressure-time curve obtained during the job. As the fluid injection is done at a constant flow rate, any change in the slope of this curve is related to the change of the rock volume, assuming there is not much leak into the formation. After the injection of the fluid some initial fractures are developed around the wellbore with fluid leakage and invasion into the formation near the wellbore. This point, known as the leak-off point, is usually associated with a small reduction of the pressure. Continuation the fluid injection, a fracture will open at the wellbore wall, and a noticeable drop in pressure is observed.

This is the breakdown pressure, after which under constant flow rate, the fracture propagates perpendicular to the minimum stress direction. Once the designed length for the fracture is reached the pump is stopped and a sudden reduction in pressure is happening due to removal of all existing frictions along the flow path. This pressure is known as the instantaneous shut-in pressure (ISIP). Then the fracture will start to close due to the force of the minimum stress component unless proppant has been injected to keep it open. The pressure ultimately reaches the fracture closure pressure, which is equivalent to the minimum stress.[30]

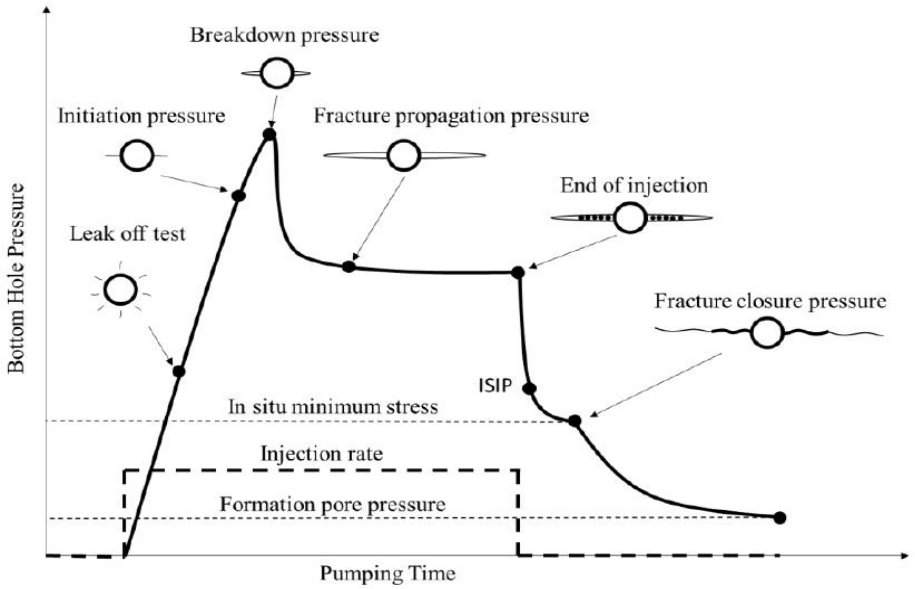


**Figure II.14: A typical Hydraulic Fracturing Pressure-Time Curve.[30]**

## Conclusion

Hydraulic fracturing is a significant technique in the oil and gas industry, offering improved productivity in reservoirs. By creating fractures in rock formations through the injection of high-pressure fluids, this method enhances fluid flow and increases hydrocarbon recovery. Despite challenges such as fracture interference and induced seismicity, advancements in technology and reservoir understanding continue to enhance the effectiveness of hydraulic fracturing. With careful planning and execution, this technique contributes to the sustainable development of energy resources and meets the growing global demand for oil and gas.

# Chapter III:

## Hydraulic Fracture Propagation Models and Analysis in NFRs

# CHAPTER III: Hydraulic Fracture Propagation Models and Analysis in NFRs

## Introduction

Hydraulic fracture growth in naturally fractured reservoirs presents numerous challenges in terms of theory, design, and application. The interaction between hydraulic fractures and natural fractures can have a significant impact on the propagation of hydraulic fracturing. However, a comprehensive understanding of this interaction is still lacking, particularly in unconventional reservoirs where natural fractures are crucial for hydrocarbon recovery.

Although natural fractures in these reservoirs are often partially or completely sealed, they cannot be ignored. During hydraulic fracturing treatments, these fractures can act as planes of weakness that are reactivated, thereby enhancing the efficiency of stimulation. Many experimental and field studies have shown that when a propagating hydraulic fracture encounters natural fractures, it can lead to fracture arrest, fluid flow into the natural fractures, creation of multiple fractures, and fracture offsets. As a result, the hydraulic fracture width is reduced, which can cause proppant bridging and premature blocking of proppant transport, leading to treatment failure (also known as screenout).

Various authors have proposed fracture interaction criteria to determine the path of induced fracture growth due to interaction with pre-existing fractures. However, there is still a lack of consensus regarding the decisive factors influencing hydraulic fracturing propagation in naturally fractured reservoirs. Experimental studies have suggested that horizontal differential stress, angle of approach, and treatment pressure are parameters that affect hydraulic and natural fracture interaction. However, a comprehensive analysis of how different parameters influence fracture behavior has not been fully investigated to date.

## III.1 Hydraulic Fracture and Natural Fractures Interaction

As briefly discussed above, HF is a complex problem with several parameters involved in the design of a fracking job. The problem becomes more complex when fracture propagation is studied in discontinuous media, such as naturally fractured reservoirs, laminated formations including shales or multi layered reservoirs. In any reservoir, some type of natural interfaces exists, so it is important to understand the effect of them on the propagation of the induced hydraulic fracture. Natural interface is a weak plane with generally negligible cohesion and toughness and the potential to be the fluid channel by activation. There are four interaction types when a hydraulic fracture encounters a natural fracture:

- **First type:** a hydraulic fracture can directly cross a natural fracture without changing its original propagation direction **(Figure III.1).**[31]

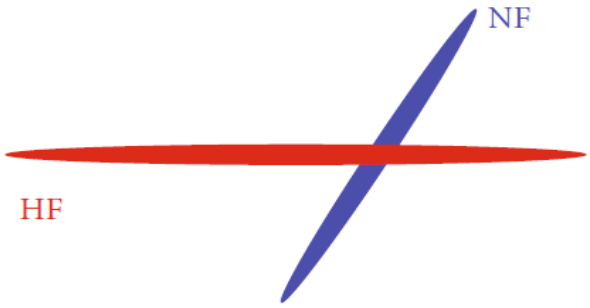


**Figure III.1: HF directly cross NF.[31]**

- **Second type:** a hydraulic fracture can join a natural fracture and create a new fracturing path at the tip of the natural fracture **(Figure III.2).**

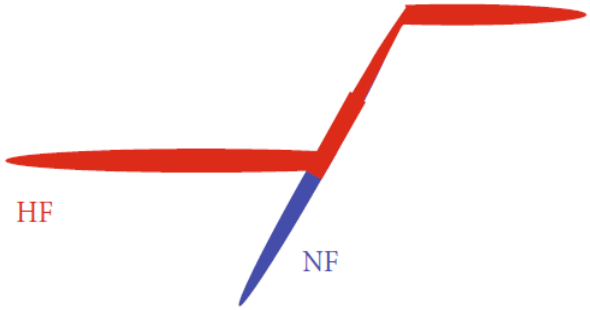


**Figure III.2: HF Cross NF at the tip.[31]**

- **Third type:** a hydraulic fracture can be diverted along a natural fracture and kink out at a weak point of the natural fracture **(Figure III.3).**

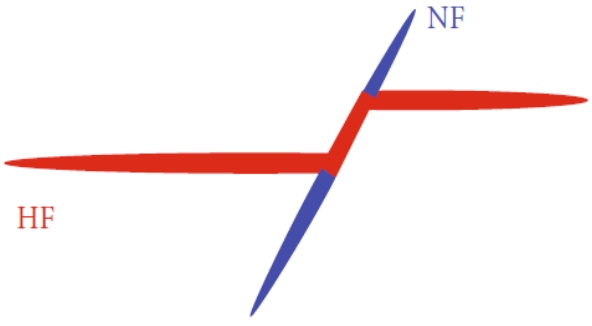


**Figure III.3: HF Cross NF at a weak point.[31]**

• **Last type:** a hydraulic fracture can be arrested within a natural fracture **(Figure III.4).**


**Figure III.4: HF arrested by NF.[31]**

For a hydraulic fracture to cross a natural fracture, two conditions must be satisfied. When the maximum principal stress reaches the tensile strength of porous media, a new fracture is initiated on the opposite side of the natural fracture interface. Also, there should be no shear slippage in the face of the natural fracture. Properties of a material interface, such as frictional resistance and cohesion, control the material's critical point to prevent slipping or allow fracture crossing.[31]

## III.2 Parameters Affecting the Interactions mode of HF and NF

### III.2.1 State of Stress:

Figure III.5 illustrates the impact of stress anisotropy on the induced fracture geometry. Large stress anisotropy will result in a single planar fracture, whereas low stress anisotropy can lead to a wide and complex fracture system.[30]

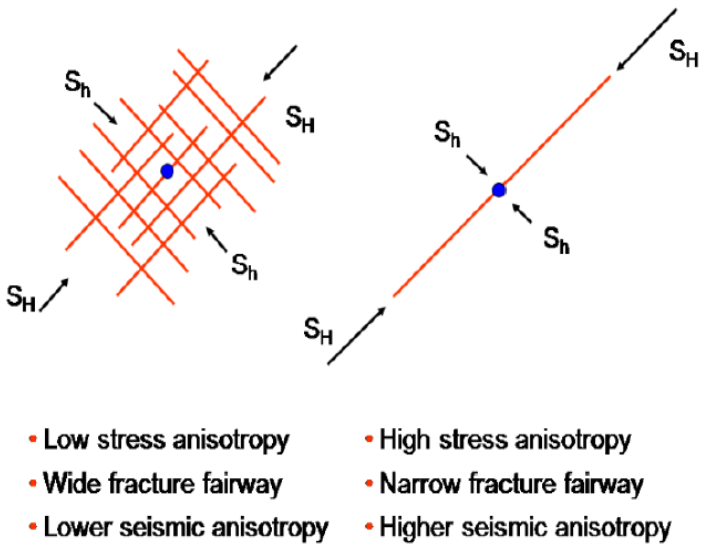


**Figure III.5: Fracture Fairway Affected by Stress Anisotropy.[30]**

### III.2.2 Natural Interface Properties

The frictional properties of the natural interface may have a substantial impact on the type of interaction modes occurring. Slippage of an interface is attributed to the interface shear strength, which is determined by interface friction angle and cohesion. Once the interface experiences slippage, the fluid has more chance to enter the fracture plane and open it.[30]

### III.2.3 Injecting Fluid Properties

The injection rate and fluid viscosity of the fracking fluid will affect the fracture pressures. These parameters can influence the type of interaction modes. The results of both numerical simulations and lab experiments indicate that higher injection rates may increase the tendency of the crossing mode.[30]

### III.2.4 Angle of Approach

The relative angle between HF and natural interface, also referred to as the angle of approach, has a dominant effect on the interaction mode. This is because the change of this angle will result in different magnitude of normal and shear stresses to the natural fracture plane. Therefore, one can understand that the potential for crossing mode is increasing as the angle of approach get closer to 90°, as in this case the shear component of the stress on the natural interface becomes less.[30]

## III.3 Positive and Negative Effects of Natural Fractures on Hydraulic Fracturing

Some of the positive effects of natural fractures on well stimulation include:

- Improved inflow characteristics due to more connection of the reservoir to the wellbore.
- Improved inflow characteristics if the natural fractures themselves are properly stimulated.
- Natural fractures may improve connection to the reservoir units.
- Natural fractures may need minimal stimulation if not damaged during drilling operations.

Negative effects of natural fractures on well stimulation include:

- In some cases, it is not possible to stimulate (acid or propped) the naturally fractured reservoirs. This results in higher expense and lower productivity.
- If the permeability is low this will reduce the fracture length resulting in lower productivity.
- Increased near wellbore fracture width leading to higher expenses.
- Higher bottom-hole propagation pressures leading to higher expenses.
- Increased risk of tip screenout in propped fractures leading to higher expenses and lower productivity.
- Greater fracturing fluid leakoff leading higher expenses and lower productivity.
- Rapid acid leakoff in calcite filled natural fractures leading to higher expenses and lower productivity.

- Few intersections of natural fractures if the stress is unfavorably oriented leading to lower productivity.[32]

## III.4 Hydraulic Fracture Initiation and Propagation

### III.4.1 Fracture Initiation and Orientation

The orientation of hydraulic fractures is important because it affects the productivity of the well. In general, hydraulic fractures are oriented perpendicular to the direction of the minimum horizontal stress. This is because the minimum horizontal stress is the least stress in the rock, and it is the stress that is most likely to cause the rock to fail. To initiate a fracture the injection pressure must exceed the minimum horizontal stress.

There are a number of factors that can affect the orientation of hydraulic fractures, including the following:

- The orientation of the wellbore
- The orientation of the in-situ stresses
- The permeability of the rock
- The viscosity of the fracturing fluid
- The amount of fluid that is pumped

The orientation of hydraulic fractures can be controlled by a number of factors, including the following:

- The use of directional drilling
- The use of packers
- The use of different fracturing fluids
- The use of different pumping rates

The orientation of hydraulic fractures is an important factor in the design and completion of hydraulic fracturing operations. By controlling the orientation of the fractures, operators can improve the productivity of their wells and increase the amount of oil and gas that they can produce.[33]

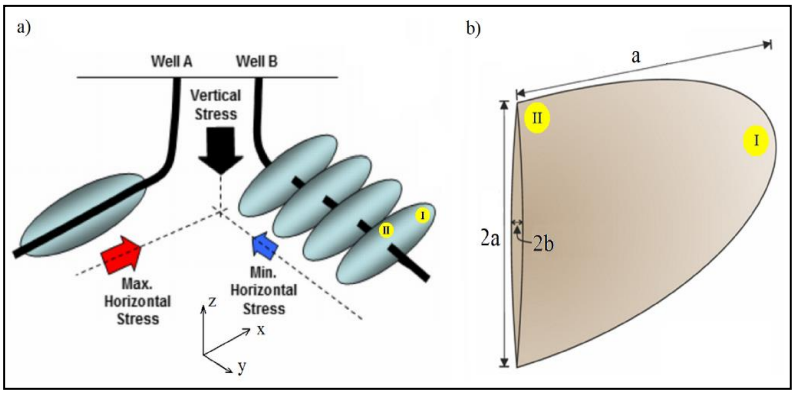


**Figure III.6: Orientation of hydraulic fractures in the initial stress field: (a) Longitudinal and transverse fractures. (b) An individual fracture as an ellipse with half-axes.[34]**

### III.4.2 Fracture Propagation Models

Hydraulic fracture propagation models are used to predict the behavior of hydraulic fractures in rocks. There are many different types of hydraulic fracture propagation models, that have different particular strengths and weaknesses such as two-dimensional fracture model and three-dimensional models. Some of the most common types of models include:

- Analytical models (KGD model).
- Numerical models (PKN model).
- Experimental models

#### III.4.2.1 PKN Model

Perkins and Kern developed equations to compute fracture length and width with a fixed height. Later Nordgren improved this model by adding fluid loss to the solution, hence, this model is commonly called PKN model. The PKN model assumes that fracture toughness could be neglected, because the energy required for fracture to propagate was significantly less than that required for fluid to flow along fracture length, and the plane strain behavior in the vertical direction, and the fracture has a constant height, and propagates along the horizontal direction (**Figure III.7**).[35]

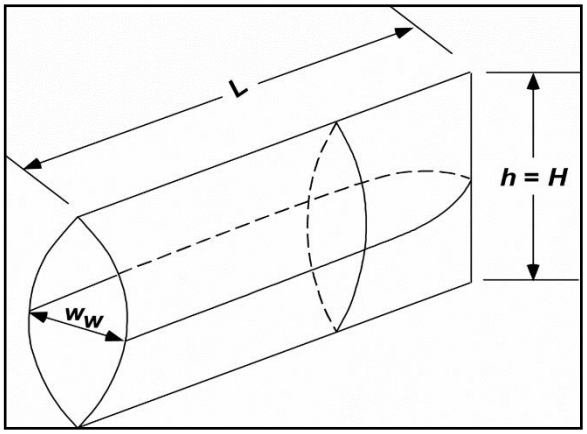


**Figure II.7: PKN Fracture Schematic Diagram.[35]**

#### III.4.2.2 KGD Model

KGD model was developed by Khristianovitch and Zheltov (Khristianovitch and Zheltov 1955) and Geertsma and de Klerk (Geertsma and Klerk 1969). It considers fracture mechanics effects on the fracture tip, and simplifies the solution by assuming that the flow rate in the fracture is constant and the pressure is also constant along the majority of the fracture length, except for a small region close to the tips. In this model, plane strain is assumed to be in horizontal direction, all horizontal cross sections act independently. This holds true only if fracture height is much greater than fracture length. Also, since it assumes that the fracture

width does not change along the fracture face all section are identical. The model also assumes that fluid flow and fracture propagation are in one dimension (**Figure III.8**).[35]

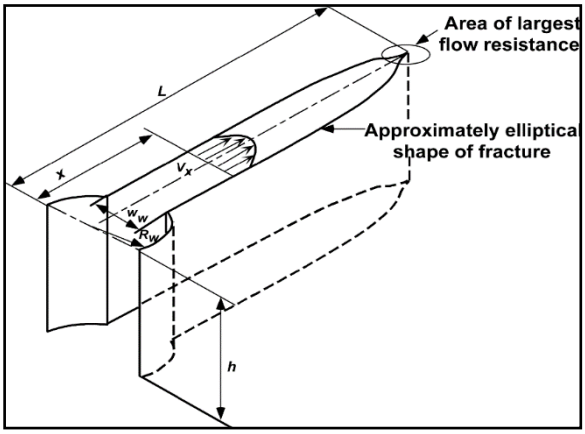


**Figure III.8: KGD Fracture Schematic Diagram.[35]**

### III.4.2.3 Penny-Shaped or Radial Model

In this model, the fracture is assumed to propagate within a given plane and the geometry of the fracture is symmetrical with respect to the point at which fluids are injected (Figure III.9).

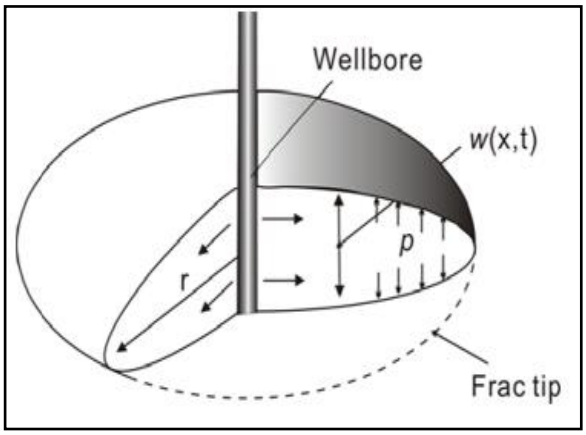


**Figure III.9: Geometry of a Penny-Shaped or Radial Model.[35]**

### III.4.2.4 Comparison Between 2D Models

The following **Table III.1** makes comparison of the three types of 2D hydraulic fracture models.

**Table III.1: Comparison Between Traditional 2D Hydraulic Fracture Models.[35]**

| Model | Assumptions | Shape | Application |
|---|---|---|---|
| PKN | Fixed Height,<br>Plain Strain in vertical direction | Elliptical Cross Section | Length>>Height |
| KGD | Fixed Height,<br>Plain Strain in horizontal direction | Rectangle Cross Section | Length<<Height |
| Radial | Propagate in a given plane<br>Symmetrical to the wellbore | Circular Cross Section | Radial |

### III.4.2.5 Three-dimensional and Pseudo Three-dimensional Models

2D models have been used for decades with reasonable success. Today, with high-powered computers available to most engineers, pseudo-three-dimensional (P3D) models are used by most fracture design engineers. P3D models are better than 2D models for most situations because the P3D model computes the fracture height, width, and length distribution with the data for the pay zone and all the rock layers above and below the perforated interval.

**Figure III.10 and III.11** illustrate typical results from a P3D model. P3D models give more realistic estimates of fracture geometry and dimensions, which can lead to better designs and better wells. P3D models are used to compute the shape of the hydraulic fracture as well as the dimensions. The key to any model, including 3D or P3D models, is to have a complete and accurate data set that describes the layers of the formation to be fracture treated, plus the layers of rock above and below the zone of interest. In most cases, the data set should contain information on 5 to 25 layers of rock that will or possibly could affect fracture growth. It is best to enter data on as many layers as feasible and let the model determine the fracture height growth as a function of where the fracture is started in the model. If the user only enters data on three to five layers, it is likely that the user is deciding the fracture shape rather than the model.

More complex fully 3D models are introduced to handle fractures of arbitrary shape and orientation by removing the assumptions in Pseudo-3D models.[36]

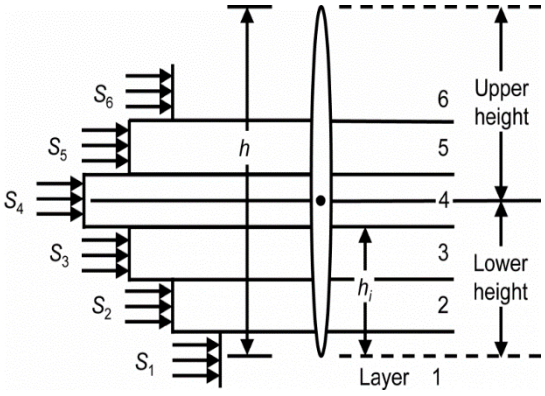


**Figure III.10: Width and height from a P3D model.[36]**

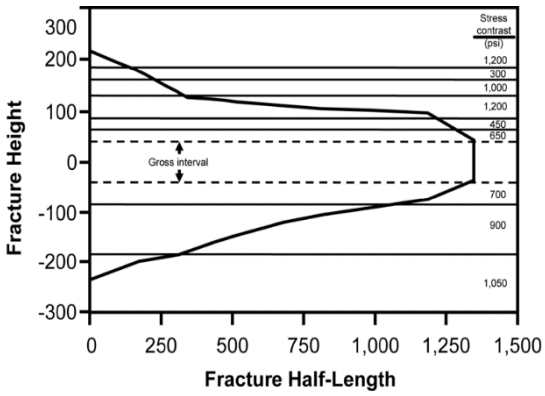


**Figure III.11: Length and height distribution from a P3D model.[36]**

## III.5 Hydraulic Fracturing Pressure Analysis

Hydraulic fracturing pressure analysis is the process of evaluating the pressure data collected during a minifrac test to determine the efficiency of the treatment design and to identify any potential problems. This information can be used to optimize the design of future

hydraulic fracturing treatments to obtain the optimum fracture shape. Furthermore, Hydraulic fracturing pressure analysis is a valuable tool to determine the effectiveness and success of the mainfrac treatment. There are a number of different methods that can be used to analyze hydraulic fracturing pressure data. The most common methods include:

### III.5.1 Pressure Curve Analysis

By analyzing the pressure curves recorded during the minifrac and mainfrac treatments, we obtain the following parameters:

- **Breakdown pressure:** it is characterized by a peak in the curve after that a decrease in the pressure because of the formation breakdown.
- **Instantaneous shut-in pressure (ISIP):**

  ISIP = Final injection pressure – Pressure drop due to friction (III.1)
- **Fracture propagation gradient ($G_f$):**

$$G_F\left(\frac{psi}{ft}\right)=\frac{\text{BHP ISIP (psi)}}{\text{TVD (ft)}} \quad \text{(III.1)}$$

- **Net fracture pressure ($\Delta P_{net}$):** Fracture net pressure is the difference between the pressure inside a fracture and the closure pressure of the rock. It is a measure of the driving force for fracture growth. The higher the net pressure, the more likely is that the fracture will grow.

  $\Delta P_{net}$ = ISIP – Closure pressure
- **Closure pressure ($P_c$):** Fracture closure pressure is the pressure at which a fracture closes after the fracturing fluid is removed. It is equal to the minimum horizontal stress.[37]

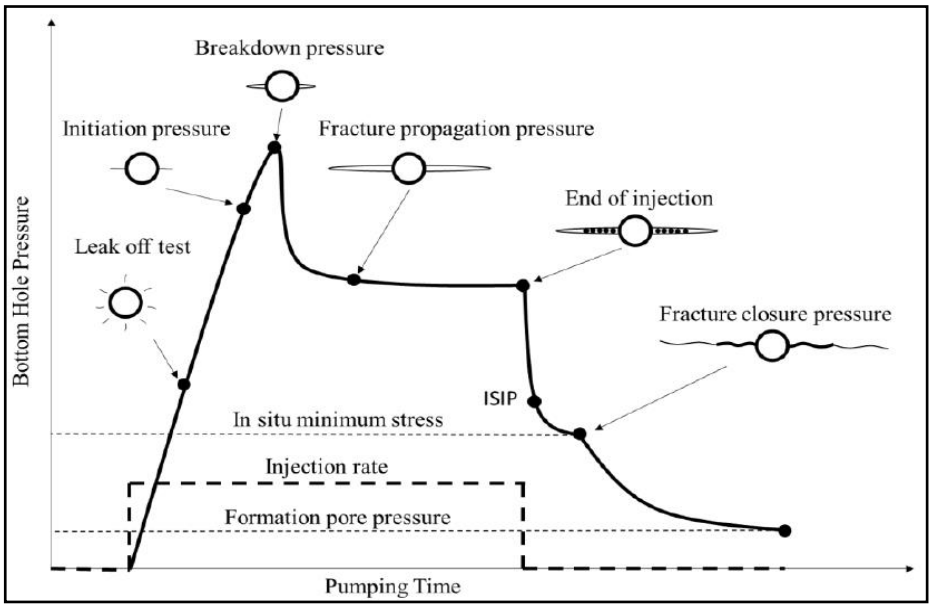


**Figure III.12: A typical pressure response during fracturing.[30]**

### III.5.2 G-Function Analysis Method

G-function analysis is a method used to characterize the properties of hydraulic fractures. It is based on the measurement of pressure decline after the injection of fluid into a wellbore. The G-function is a dimensionless time function that is proportional to the cumulative volume of fluid that has leaked off from the fracture. The slope of the G-function plot can be used to calculate the leak off rate, and the intercept can be used to calculate the fracture closure pressure.[37]

$$\Delta t_D = \frac{t_s - t_p}{t_p} \quad \text{(III.3)}$$

$$g(\Delta t_D) = \frac{4}{3}((1 + \Delta t_D)^{1.5} - \Delta t_D^{1.5}) \quad \text{(III.4)}$$

$$G(\Delta t_D) = \frac{4}{3}(g(\Delta t_D) - g_0), \quad g_0 = \frac{4}{3} \quad \text{(III.5)}$$

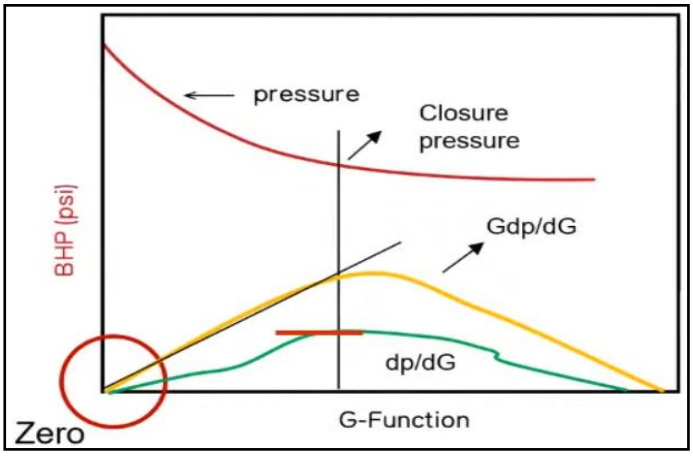


**Figure III.13: A Typical G-Function Plot.[37]**

1- G-function analysis can be used to identify fracture propagation behaviors, including:

- Normal Leak-off.
- Pressure Dependent Leak-off.
- Delayed Leak-off (Transverse Storage / Fracture Height Recession).
- Fracture Tip Extension.

2- G-function analysis can be used to calculate:

- **Fluid Efficiency (FE):**

$$FE(\%) = \frac{\text{Fluid remaining inside frac}}{\text{Total injected fluid}} \quad \text{(III.6)}$$

$$FE(\%) = \frac{G_C}{2 + G_C} \quad \text{(III.7)}$$

where: $G_c$ is the G-function time at fracture closure.

- **Leak-off Coefficient ($C_L$):**

$$G_L = \frac{\frac{dp}{dG} \cdot 2h}{\pi \sqrt{t_p}} \quad \text{(III.8)}$$

where:

$G_L$ : Total leak-off coefficient in $ft/min^{0.5}$.

dp/dG: Plateau value of first derivative.

$t_p$: Pumping time in mins.

3- G-function analysis can be used to determine the closure pressure.[37]

### III.5.3 Square Root Time Analysis Method

In this technique, the fracture closure pressure is identified by the first peak in the pressure plotted versus the square root of time. **Figure III.14** shows a typical square root time plot. The primary curve in this plot should form a straight line during the fracture closure (similar to G-Function analysis). Unlike the G-Function analysis, where the deviation from the straight line was indicating the fracture closure, in this analysis, the peak of the first derivative of the pressure versus sqrt(*t*) indicated the fracture closure point (pink dashed line in the figure).[38]

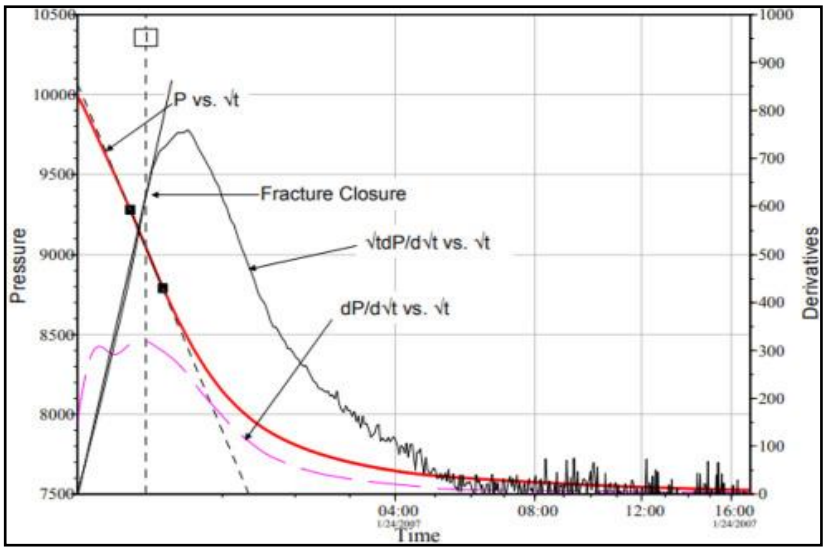


**Figure III.14: A Typical Square Root Time Plot.[38]**

### III.5.4 Nolte & Smith Analysis Method

The basis of this analysis has been the Nolte and Smith (1981) diagnostic net pressure plot. The latter is a plot of the fracture net pressure, or treating pressure above closure stress versus time on a log-log axial system. Analysis of the pressure versus time function was expanded to include derivative analysis. The interpretation of this plot provides significant

insight about dynamic fracture propagation during a treatment, and a useful to corroborate post-fracture geometry (fracture width, and vertical and lateral penetration) investigations. It also provides a perception of fracture width development during a treatment, and can provide insight about edge effects.[39]

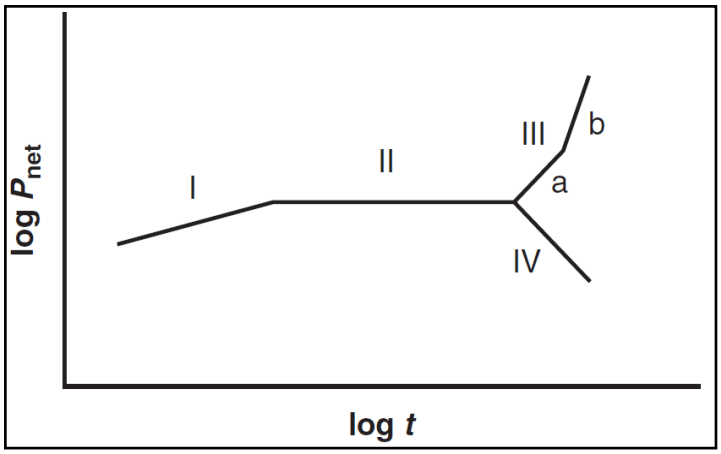


**Figure III.15: Nolte & Smith Analysis Pressure-Response Plot.[39]**

**Table III.2: The Interpretation of Nolte & Smith Analysis.[39]**

| Row index | Approximate Slope | Interpretation |
|---|---|---|
| **I** | **1/8 To 1/4** | The fracture extends in length and slightly in height. So, it spreads according to the PKN model |
| **II** | **0** | The increase is regulated by an increase in height in barriers or by natural fissure openings. So, the fracture spreads radially |
| **$III_A$** | **1** | Extension restriction and width increase (W) |
| **$III_B$** | **2** | Extension restriction (on only one active side) |
| **IV** | **Negative** | Height increase in another low stress area. (screenout). Both models, KGD and Radial can be considered. |

## Conclusion

Hydraulic fracture propagation models and hydraulic fracture analysis are essential tools in the field of hydraulic fracturing. These models provide valuable insights into fracture behavior, fluid flow patterns, and fracture geometry, enabling engineers to optimize fracture designs for maximum productivity. By analyzing factors such as rock properties, in-situ stress, and fluid properties, these models aid in predicting fracture growth and understanding the complex interactions between fractures and the reservoir. Through continuous refinement and improvement of these models, operators can make informed decisions to enhance the effectiveness and efficiency of hydraulic fracturing operations, ultimately leading to increased hydrocarbon recovery.

# Chapter IV:

## Study Cases On Hydraulic Fracture Propagation In Naturally Fractured Reservoirs

# CHAPTER IV: Study Cases On Hydraulic Fracture Propagation In Naturally Fractured Reservoirs

## Introduction

The objective of this study is to evaluate hydraulic fracture propagation in Gassi El Agreb and Hassi R'mel reservoirs which they are considered as naturally fractured reservoirs. Therefore, for this study field data from three wells and post job reports of hydraulic and acid fracturing were used. This study is concerned with the following steps:

- Identifying the behaviors associated with the fracture propagation by analyzing G-Function plots.
- Interpreting of fracture propagation modes utilizing Nolte & Smith analysis.
- Predicting the path of hydraulic fracture propagation by interpreting of temperature log.

## IV.1 EL-GASSI Field

### IV.1.1 Description

The EL-GASSI region is oil-based. It is one of the oldest regions where hydrocarbons discovered in 1959.

Its oil production is connected to the pipeline leading to Haoud EL Hamra by pipes from the production center of El-Gassi. Currently, a redevelopment process is underway for the deposits, which includes the installation of new production facilities, will allow greater injection capacity throughout the deposit and a general modernization of equipment and operations in the field.

In April 2000 and after the drop in crude production, SONATRACH signed a production sharing contract with AMERADA HESS (duration: 20 years, possibility of extension for 5 years). in order to increase the rate of crude recovery by the reinjection of the miscible gas into the deposit and the gas lift into the producing wells as well as the water.

The EL-Gassi region includes three (03) crude producing fields (EL-GASSI, ZOTTI and EL-AGREB) where there are four (04) crude processing centers (West Agreb, AR06, Old Zotti and GS01), water reinjection center (AR02) and gas compression and reinjection center (New Zotti).


**Figure IV.1: El Gassi Field Centers.**

**- El-Gassi:** Area 207 km$^2$, discovered in 1956. In this center we find:

- Separation
- Storage
- Dispatch
- Boosting
- Produced water
- OOS (Oil Optimization System)

**- Zotti:** Area 77 km$^2$, discovered in 1959. This center is consisted of the following units:

- Separation
- Dehydration
- Stabilization
- Boosting
- Gas lift
- Miscible flood
- Water dilution
- Power plant

**- El Agreb:** Area 126 km$^2$, discovered in 1963. It made up of the following units:

- AR2: Water injection & Chemical injection.
- AR6: Separation, water dilution unit, produced water unit and transfer of water.
- WA: Separation, water dilution unit, produced water unit and injection water

### IV.1.2 Geographic Location

The GEA deposits are in the Sahara, about 900 km southeast of the capital and 100 km southwest of the town of Hassi Messaoud.

The geographical coordinates of the region are:

- **East Longitude : 5º 30.**
- **North Longitude : 30º 45.**
- **Altitude : 195 m.**


**Figure IV.2: Geographic Location.**

### IV.1.3 The GEA Field Production:

The El-Gassi region is important because of its share in the country's hydrocarbon production, all the quantities of oil and gas produced are sent to the various storage centers in the region.

With the start of the GCR (Gas Compression & Reinjection) project, production from the GEA field has been maintained at an average of 52,000 barrels per day. The main activities of the region are:

- Oil production (GS1, AR06, West Agreb, Zotti).
- Injection of miscible gas and gas lift (ZOTTI).
- Water injection (AR02).

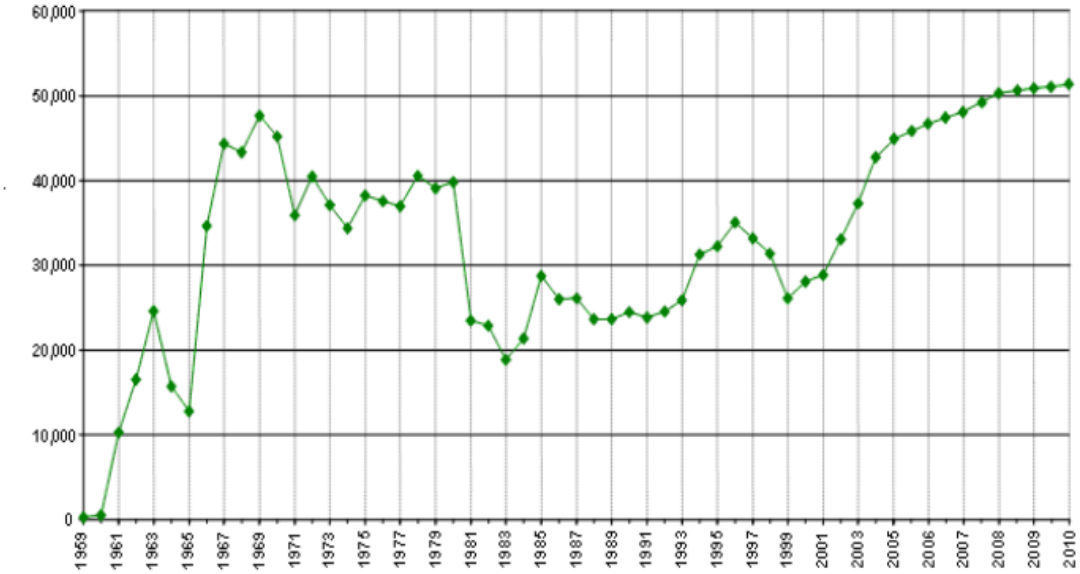


**Figure IV.3: The GEA Production History.**

**Table IV.1: The GEA Field Wells**

| Gisement | El-Gassi | El-Agreb | Zotti | Total |
|---|---|---|---|---|
| Drilled Wells | 53 | 68 | 24 | 145 |
| Oil producing wells in service | 24 | 34 | 05 | 63 |
| Gas Injector Wells | 13 | 00 | 00 | 13 |
| Wells Water Producers | 00 | 11 | 00 | 11 |
| Wells Water Injectors | 00 | 09 | 00 | 09 |
| Closed wells | 16 | 14 | 19 | 49 |

## IV.2 Hassi R'Mel Field

### IV.2.1 Description

The gas giant Hassi R'mel is at the heart of the history of hydrocarbons in Algeria. It is the first gas pole in the country that was discovered in 1956 at a depth of 2200 m, 550 km south of Algiers, on an area of 4800 km$^2$. It is considered as one of the largest gas fields in the world and the largest on the African continent producing mainly gas condensate and oil on its eastern and southern periphery.

### IV.2.2 Geographic Location

The Hassi R'mel field is located in the center of the northern part of the Algerian Saharan basin, about 550 km south of Algiers and about 110 km north of GHARDAIA and 100 km from LAGHOUAT between the meridians 2°55' and 3°50' east and the parallels 33°15' and 33°45' north. The average altitude of the region is of the order of more than 760 m. It is considered as one of the main gas-producing fields in the world.

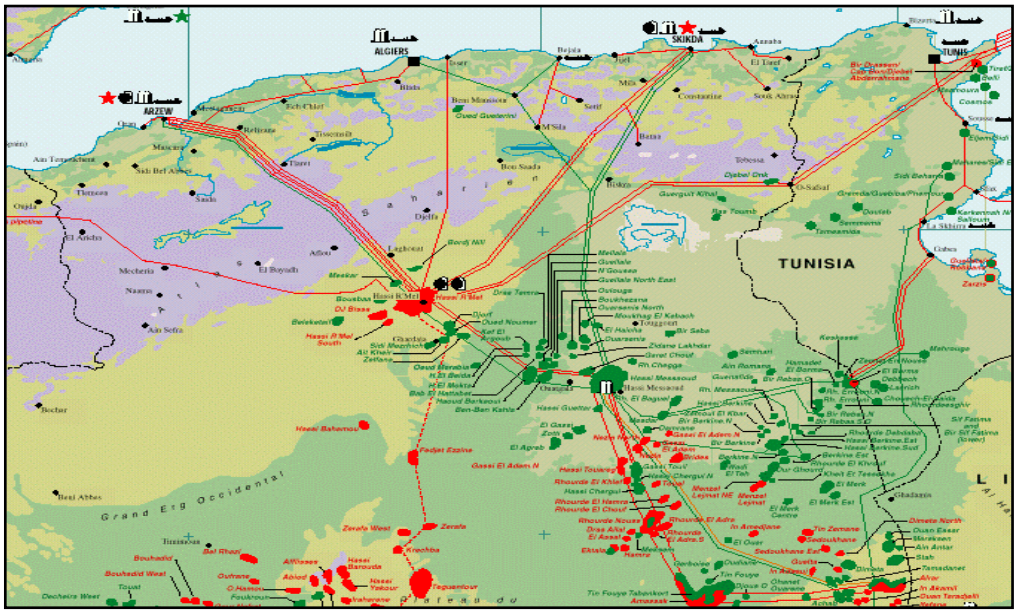


**Figure IV.4: Hassi R'mel Geographic Location.**

### IV.2.3 Geological Location Position

The Hassi R'mel field is located on the Saharan platform in the northwestern part of the Triassic basin on the vault of Tilghemt. It is limited to the North by the chain of the Atlas Saharan, to the east by the structures of Djemaa, Touggourt and the Oued Mya basin, to the west by the Benoud furrow and to the south by the Edjirane M'zab ridge.

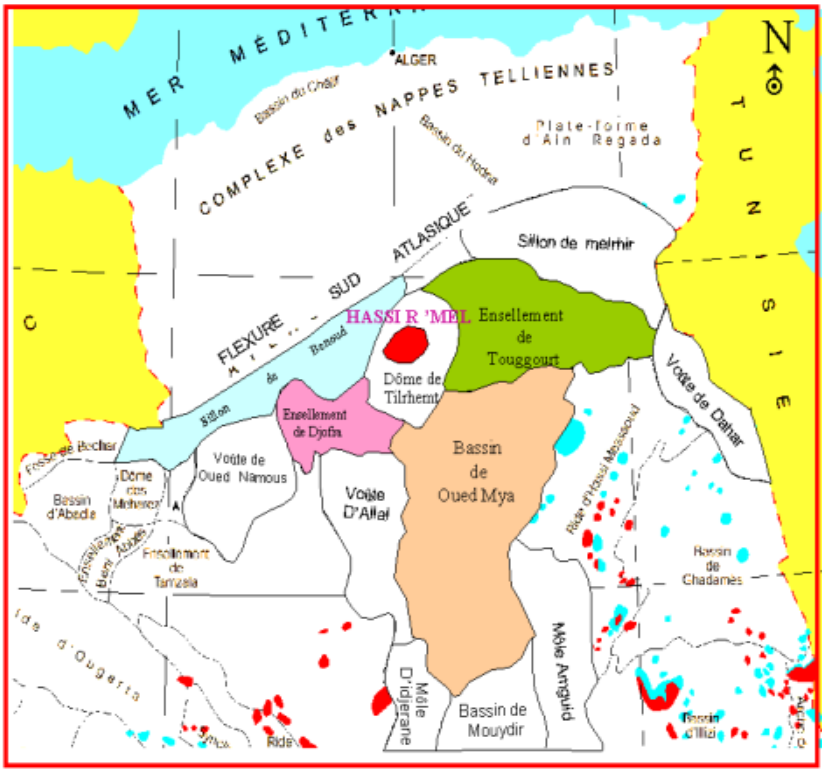


**Figure IV.5: Hassi R'mel Geological Location.**

### IV.2.4 History of Hassi R'mel and Development

The structure of Hassi R'mel was revealed through a seismic reflection campaign conducted in 1951 not far from Bordj Tilghemt, that was discovered the structure field anticline.

HR-1 is the first well implanted in 1956, on the top of an anticline, it showed a significant accumulation of condensate gas in the clay-sandstone Triassic at a depth average of 2200 m.

Ahead of time, by virtue of the drilling of the HR-8 well in 1958, the presence of oil in Hassi R'mel was detected in the southwest sector of the field. A certain number of wells were implanted on the southeast flank of the field to delineate the deposit. Wells HR154, HR166 and HR165 have confirmed the existence of an economically exploitable oil ring.

Since its discovery, the Hassi R'mel field has gone through several phases and development plans main developments:

•1961- 1974: Commissioning of 12 gas treatment units to reach a capacity of 14 MD $m^3$/year.

•1975-1980: Development master plan (drilling of gas wells and construction of processing modules and compressor stations).

•1982 to 1990: exploration of the field deposit limits continued, particularly in south, and the location of the boreholes in the southern part of the field only highlighted the level A and the lower Triassic series.

•1990 to 2000: drilling of new horizontal wells at the level of the oil ring in order to develop their potential.

•2000 to 2008: other wells installed in the southern part and the commissioning of recycling of gas cap. Currently, the field is in full development, and other wells have been drilled especially in the southern part; it has more than 400 gas and oil producing wells with injection wells.

### IV.2.5 Hassi R'mel Field

The overall plan of the gas installations located on the Hassi R'mel field is drawn up in such a way as to have a rational exploitation of the deposit and to be able to recover the maximum of the liquid the installations implemented are represented in the figure.

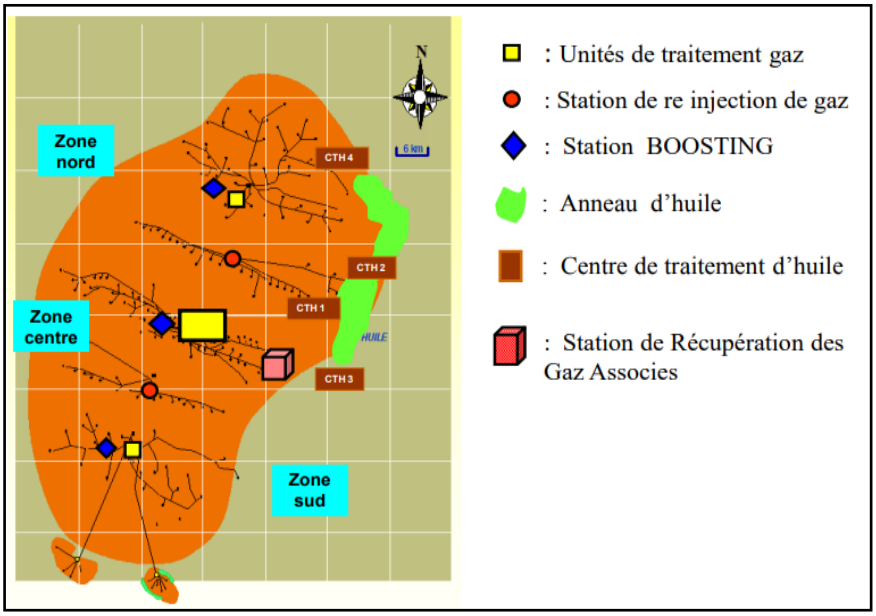


**Figure IV.6: Schematic Representation of Hassi R'mel Field.**

## IV.3 Cases of Study

Field data from three wells and post job reports of hydraulic and acid fracturing were used to complete this study:

### IV.3.1 GS-Well 1

In certain instances, oil wells initially exhibit promising production potential upon drilling, but within a short span of time (months), their output declines earlier than anticipated. It becomes evident that there is significant damage to the formation resulting from completion

operations, necessitating an intervention such as matrix acidizing or hydraulic fracturing to stimulate the damaged zone. An illustration of this scenario is GS-well 1.

### IV.3.1.1 Well History

- The GS-Well 1 is an oil producer well was drilled and completed in April 2022. Targeting the Cambrian reservoir Ri & Ra. It was implanted in the El Gassi field.
- The DST test gave 5.7 $m^3$/h production during the drilling with skin of 27. After completing and perforate the well, negative production was encountered.
- Some water production was observed during the DST. Cement plug was placed at 3,248 m in order limit the water flow.
- A stimulation attempts of Reformat/Xylene clean out and squeeze; kickoff tub clean was conducted on the well but no significant production improvement gained.
- Based on above, a significant NWB damage could be occurred on the well after completion. A Hydraulic fracturing with sufficient prop size may help to bypass the NWB damage and communicate with the frac-field reservoir.[40]

### IV.3.1.2 Reservoir Petrophysics

The petrophysics parameters of units **Ri** and **Ra** shown in the **Table IV.2** are obtained from well logging and DST.

**Table IV.2: The petrophysics of Units Ri & Ra of GS-Well 1.**

| Pay Zone | Gross pay (m) | Net pay (m) | Porosity (%) | Water saturation (%) | Permeability (mD) |
|---|---|---|---|---|---|
| **Ri** | 21.24 | 16.73 | 7.2 | 29.1 | 3.92 |
| **Ra** | 61.99 | 39.2 | 6.8 | 31 | 3.92 |

➢ **Comments:**

1- The average porosity value is 7% below 10%, so the reservoir is classified in low porosity reservoirs.

2- The permeability is 3.92 mD below 10 mD, so the reservoir is classified in low permeability reservoirs.

3- Moderate water saturation < 50%.

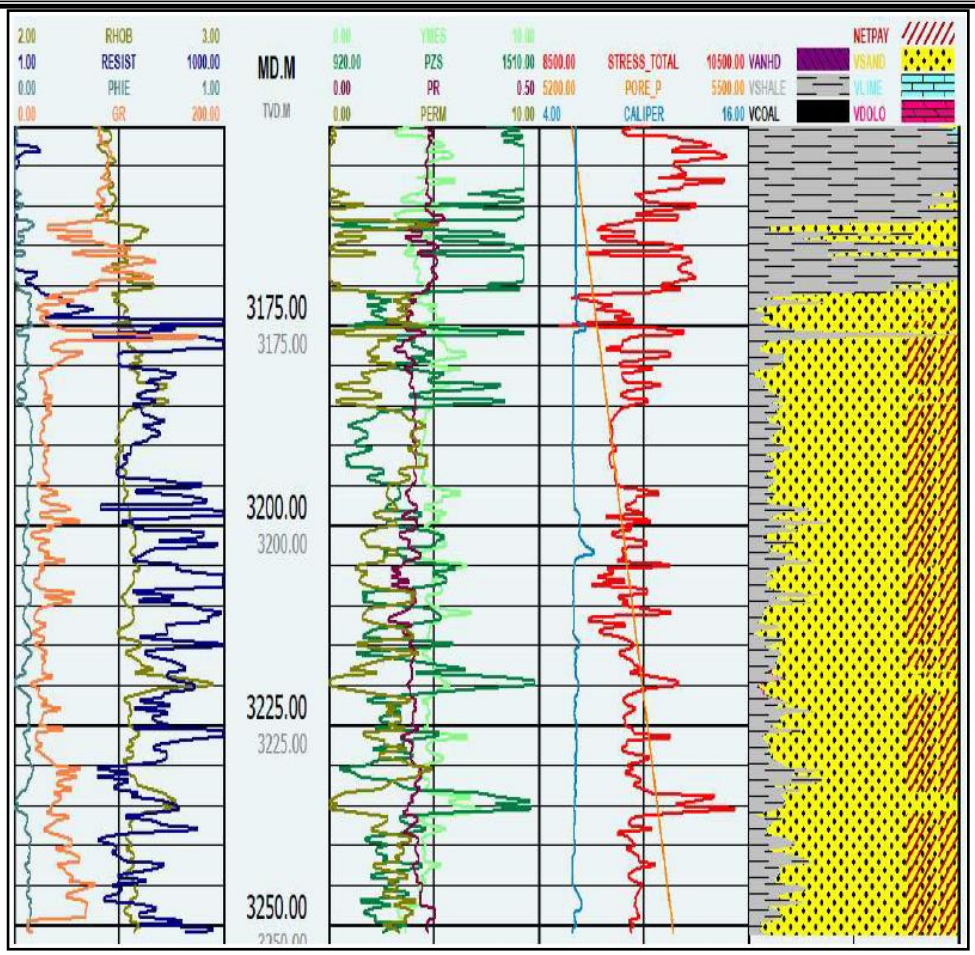


**Figure IV.7: Composite Log (GOHFER).[40]**

### IV.3.1.3 Minifrac Treatment

Prior to the main treatment, a minifracture test was conducted, involving the injection of a total volume of 49772 gallons at a rate of 30 barrels per minute. The data obtained from the minifracture test, including fluid loss properties and closure stress, were utilized to redesign the main treatment with the goal of optimizing the fracture geometry.

#### IV.3.1.3.1 Design of Pumping

**Table IV.3: Designed Pumping Schedule for Minifrac Treatment.[40]**

| Stage Number | Description | Fluid System | Clean Volume (gal) | Slurry Volume (gal) | Rate Stage End (bpm) |
|---|---|---|---|---|---|
| 1 | Breakdown | Treated Water | 8000 | 8000 | 30.0 |
| 2 | Shut-In | | 0 | 0 | 0.0 |
| 3 | Acid 15% HCL | Acid 15% HCL | 4000 | 4000 | 5.0 |
| 4 | Over-displacement | Treated Water | 9200 | 9200 | 30.0 |
| 5 | Shut-In | | 0 | 0 | 0.0 |
| 6 | Pre-Pad | Linear Gel 35# | 1000 | 1004 | 30.0 |
| 7 | Pad | Hybor G 35# | 6000 | 6055 | 30.0 |

| | | | | | |
|---|---|---|---|---|---|
| 8 | 1.5 ppg Prop Slug (30/50) | Hybor G 35# | 2000 | 2122 | 30.0 |
| 9 | Pad | Hybor G 35# | 12000 | 12110 | 30.0 |
| 10 | Flush | Linear Gel 35# | 7280 | 7280 | 30.0 |
| 11 | Shut-In | | 0 | 0 | 30.0 |
| Total | | | 49480 | 49772 | 0.0 |

➢ **Comments:**

1- Acid stimulation treatment before the pre-frac used to clean up the perforation and treat the possible skin damage around wellbore.

2- Based on offset frac experiences the Prop slug used to reduce BH friction and get visibility of formation response before pumping the proppant into the formation.

### IV.3.1.3.2 Minifrac Pressure Curves

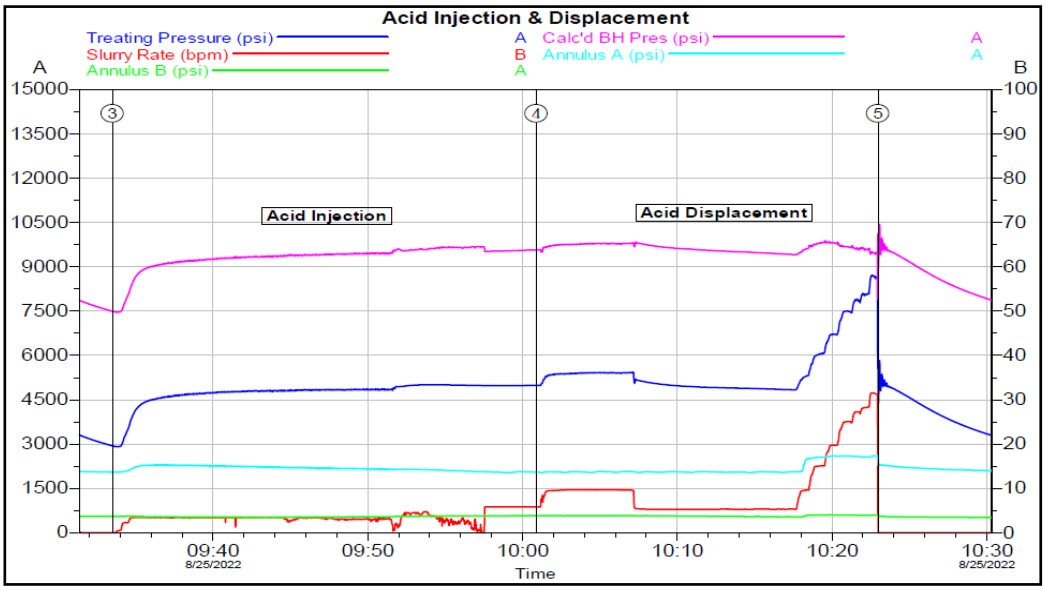


**Figure IV.8: Injection Test Plot.[40]**

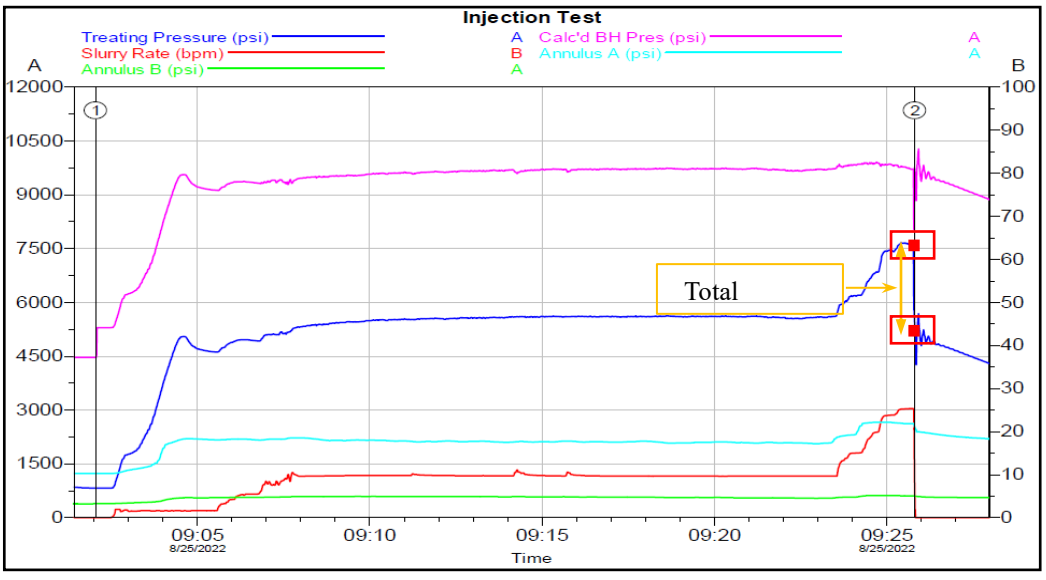


**Figure IV.9: Acid Injection & Displacement Plot.[40]**

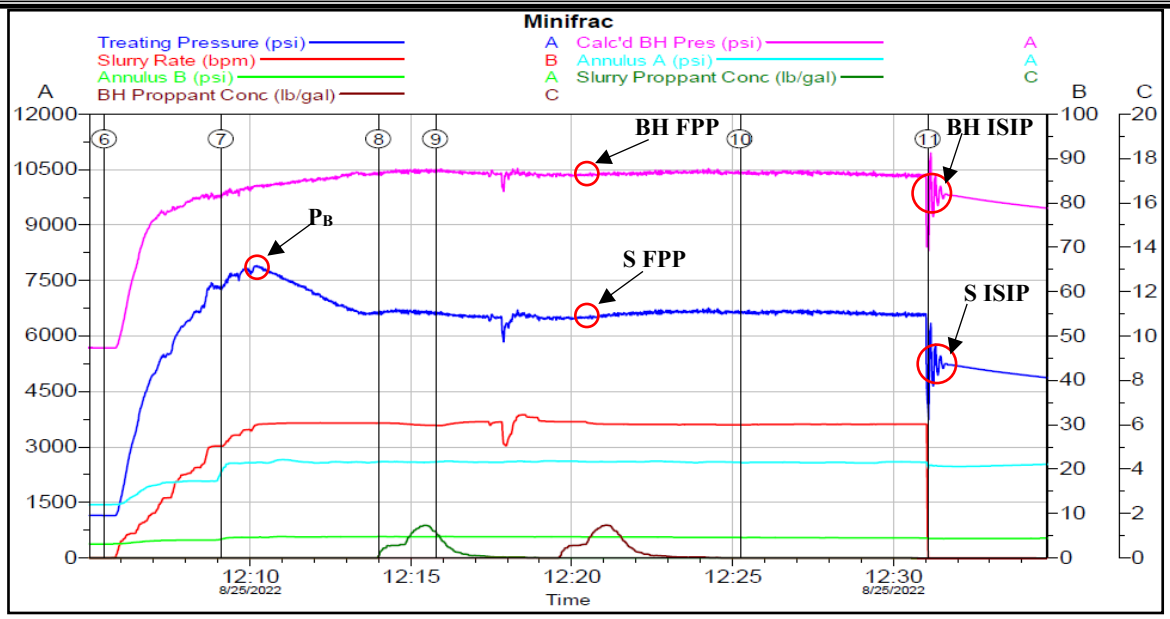


**Figure IV.10: Minifrac Injection Plot.[40]**

➢ **Results and Discussions:**

Based on the data collected from monitoring of pressure response during minifrac treatment, here is the interpretation:

- **Breakdown Pressure ($P_B$) = 7875 psi:**

The breakdown pressure refers to the pressure at which the formation or rock formation being fractured starts to break or fracture. In this case, the breakdown pressure is determined to be 7875 psi.

- **Total Frictions = 3000 psi:**

Total frictions represent the combined effect of all frictional forces acting against the fluid flow during the hydraulic fracturing process. In this case, the total frictional pressure is calculated to be 3000 psi.

- **Bottom Hole:**

- **Formation Propagation Pressure (FPP) = 10500 psi:**

The formation pressure, also known as reservoir pressure, indicates the pressure of the fluid within the reservoir or the rock formation at the bottom of the well. Here, the formation pressure is recorded as 10500 psi.

- **Initial Shut-In Pressure (ISIP) = 9750 psi:**

The initial shut-in pressure refers to the pressure measured at the bottom of the well immediately after the hydraulic fracturing treatment is completed and before any flowback occurs. In this case, the initial shut-in pressure is reported as 9750 psi.

- **Pressure Change (ΔP) = 750 psi:**

The pressure change (ΔP) represents the difference between the formation pressure and the initial shut-in pressure. In this scenario, the pressure change is calculated to be 750 psi.

- **Surface:**

- **Formation Pressure (FPP) = 6750 psi:**

The formation pressure at the surface denotes the pressure of the fluid at the wellhead or the surface of the well. In this case, the surface formation pressure is recorded as 6750 psi.

- **Initial Shut-In Pressure (ISIP) = 5250 psi:**

Similar to the bottom hole ISIP, the surface initial shut-in pressure is the pressure measured at the surface immediately after the hydraulic fracturing treatment, before any flowback occurs. Here, the surface initial shut-in pressure is reported as 5250 psi.

- **Pressure Change (ΔP) = 1500 psi:**

The pressure change (ΔP) at the surface indicates the difference between the surface formation pressure and the surface initial shut-in pressure. In this instance, the pressure change is calculated to be 1500 psi.

### IV.3.1.3.3 Minifrac G-Function Plot

The G- function used to evaluate the fracture propagation behaviors and estimate different parameters such as closure pressure, net pressure and fluid efficiency.

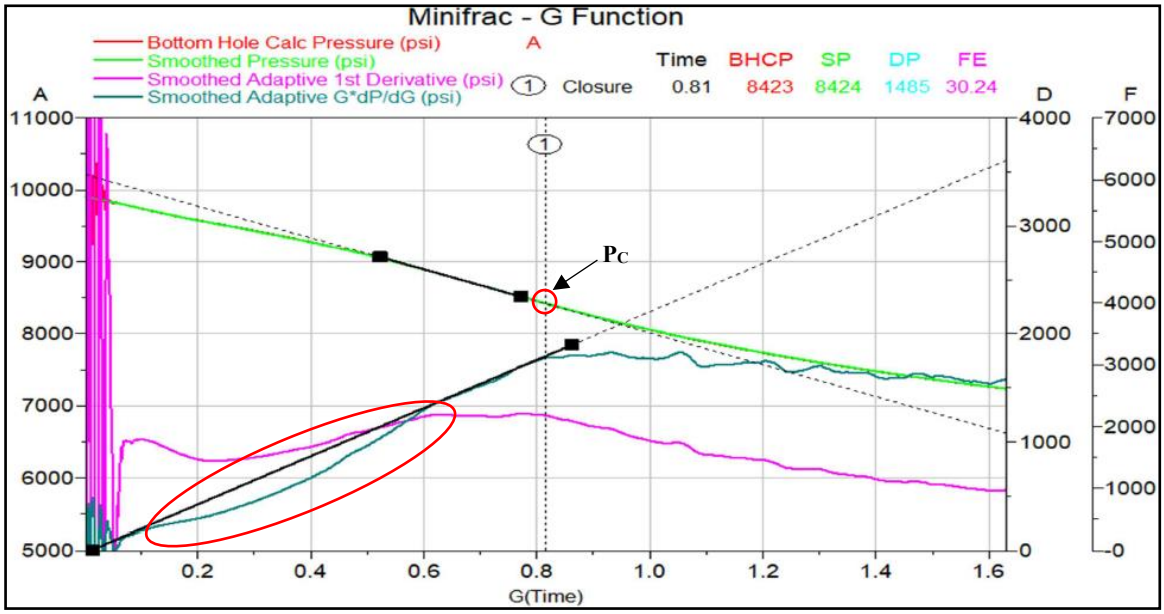


**Figure IV.11: Minifrac G-Function Plot.[40]**

- **Results and Discussions:**

Based on the data obtained from the G-function plot, here is the interpretation:

- **BH Closure Pressure ($P_C$):** The BH Closure Pressure is determined to be 8423 psi. This pressure represents the point at which the fractures in the formation close and the fluid flow is hindered.
- **Closure Gradient:** The Closure Gradient is calculated as 0.80 psi per foot. It indicates the rate of pressure increase with respect to depth in the wellbore when approaching the closure pressure.
- **G-Function Closure Time ($G_C$):** The G-Function Closure Time is measured at 0.81. It represents the time it takes for the fractures to close and the pressure to stabilize.
- **Fluid Efficiency (FE):** The Fluid Efficiency is determined to be 30.24%. This value reflects the effectiveness of the fluid in transmitting the pressure and creating fractures within the formation.
- **Calculated FE:** The Calculated FE is evaluated using the G-Function Closure Time ($G_c$) and is calculated as 28.82%. It provides an alternate way to estimate the fluid efficiency based on the G-Function Closure Time. In this case there is low fluid efficiency.
- **G-Function Net Pressure:** The G-Function Net Pressure is recorded as 1485 psi. This pressure indicates the net effect of fluid pressure on the fractures in the formation.
- **Calculated Net Pressure (Pnet):** The Calculated Net Pressure (Pnet) is obtained by subtracting the BH Closure Pressure ($P_C$) from the BH ISIP and is calculated as 1327 psi. It represents the effective pressure difference at the bottom hole, taking into account the closure pressure.

These values obtained from the G-function plot provide insights into the fracture behavior, closure pressure, and fluid efficiency within the formation. They assist in evaluating the effectiveness of hydraulic fracturing operations and optimizing fracture design.

➢ **Interpretation of minifrac G-Function plot:**

The G-Function plot shows a delayed leak-off behavior. This behavior indicates that the fracturing fluid is leaking slower than what expected, two scenarios: Transverse storage mechanism and height recession mechanism. Based on the trend line of the first derivative, the most appropriate scenario explains this behavior is:

- **Transverse Storage:**

The main fracture intercepts a secondary fracture network. These fractures close faster and provide a pressure support, then charging the main fracture with fluid rather than additional surface area for leak-off, the main fracture become the dominant fracture.

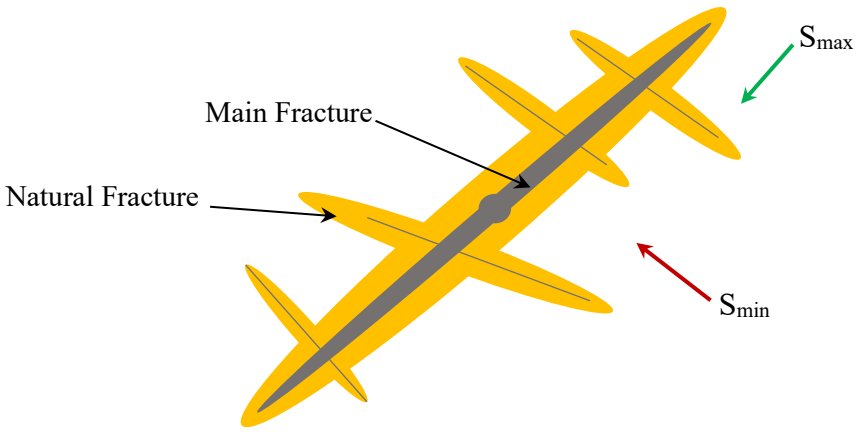


**Figure IV.12: Illustration of Transverse Storage Mechanism.**

### IV.3.1.3.4 Minifrac Net Pressure Plot

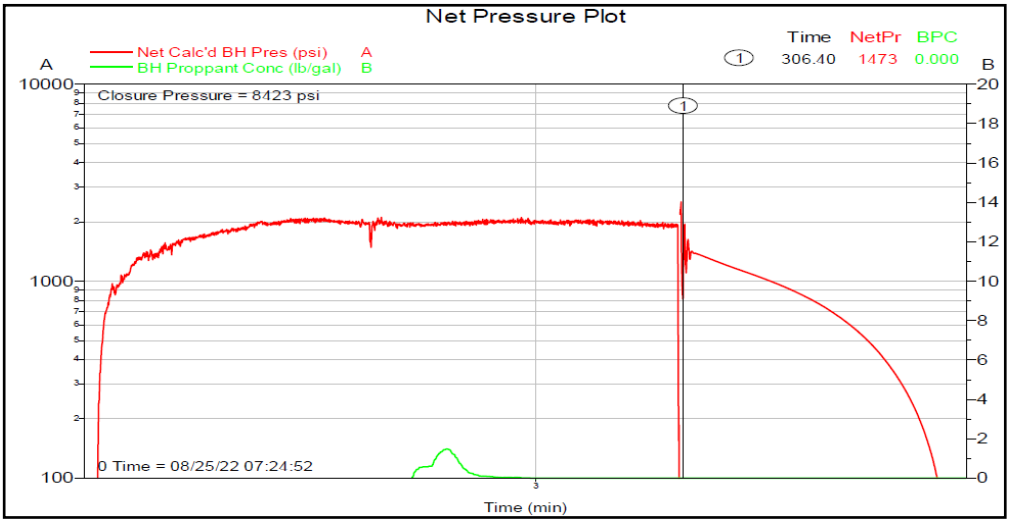


**Figure IV.14: Minifrac Net Pressure Plot.[40]**

➢ **Interpretation of minifrac net pressure plot using Nolte & Smith analysis:**

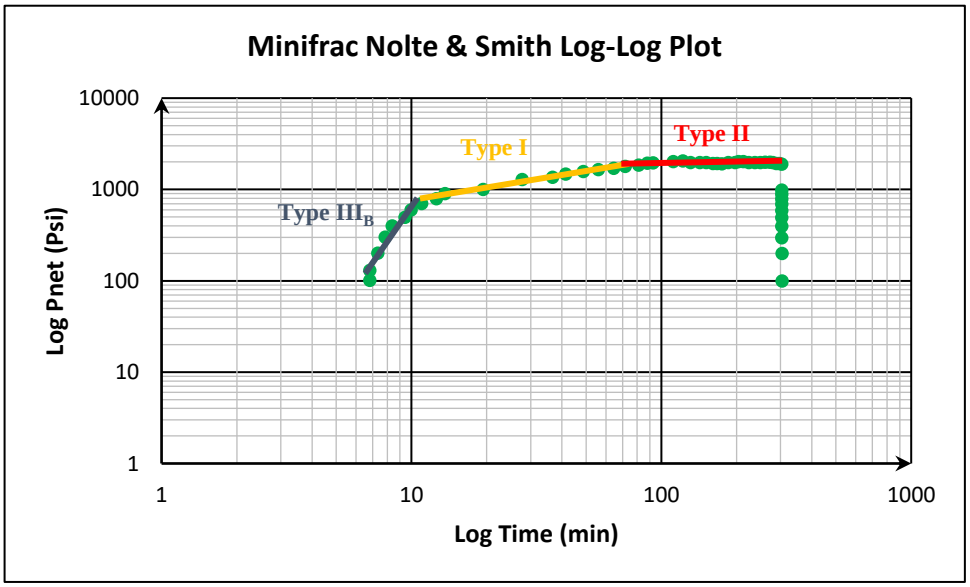


**Figure IV.15: Minifrac Nolte & Smith Analysis Plot.**

The figure IV.15 shows that the evolution of fracture propagation mode goes through 3 stages:

**Mode 1:** corresponds to Type $III_B$ of the Nolte & Smith analysis due to its steep slope. It indicates a restriction of the fracture extension, only one active side and a possible screen-out scenario near the wellbore.

**Mode 2:** corresponds to Type I based on the Nolte & Smith analysis as it exhibits a slight positive slope. It signifies propagation in line with (PKN) model, where the fracture length extends while the height remains nearly constant.

**Mode 3:** corresponds to Type II according to the Nolte & Smith analysis, as it demonstrates a consistent slope. It indicates that the increase in fracture propagation is controlled either by height increase in barriers or by the presence of natural fissure openings, resulting in radial spreading of the fracture.

- **Comparison between Nolte & Smith Analysis and the Fracture Geometry Design:**

The comparison between the designed fracture geometry by **FRACPRO** and the fracture geometry obtained from minifrac treatment by **FRACPRO** shows that there is a difference in dimensions between the estimated fracture and the fracture obtained from minifrac:

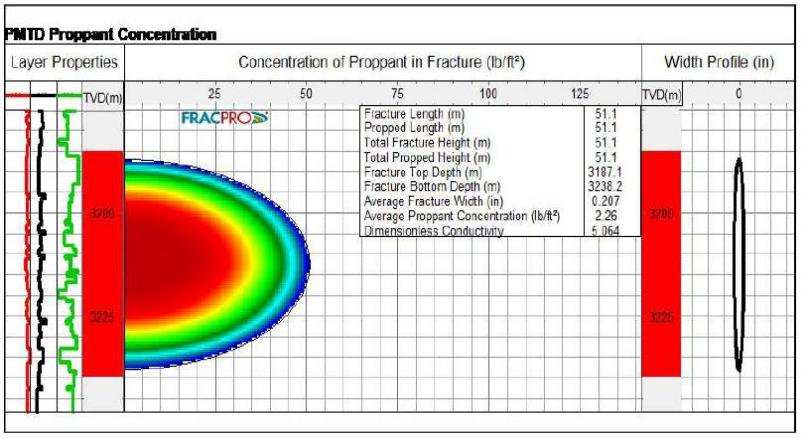


**Figure IV.16: The Designed Fracture Geometry for minifrac.[40]**

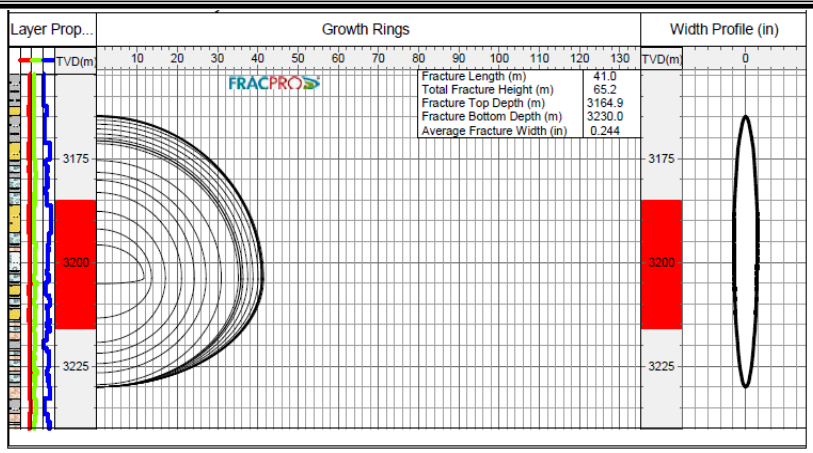


**Figure IV.17: The Fracture Geometry Obtained from Minifrac.[40]**

**Table IV.4: The comparison between the designed fracture and the fracture obtained from minifrac.**

| Dimensions / The fracture geometry | Length (m) | Height (m) | Width (in) |
|---|---|---|---|
| The designed fracture geometry. | 51.1 | 51.1 | 0.207 |
| The fracture geometry obtained from minifrac. | 41.0 | 65.2 | 0.244 |
| The difference | 10.1 | 14.1 | 0.037 |

The results above confirm the propagation mode of the main fracture, length & height growth profile, and the effects of natural fractures on the geometry of the main fracture.

### IV.4.1.3.5 Minifrac Temperature Log

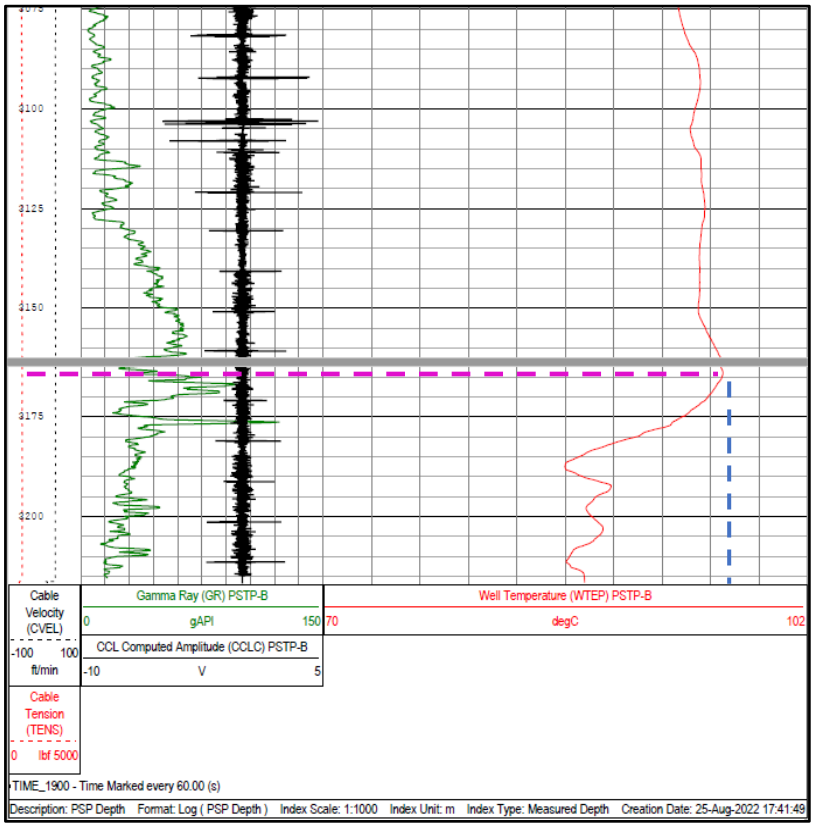


**Figure IV.18: The Temperature Log After Minifrac of GS-Well 1.[40]**

The temperature Log shows that the top of fracture is 3165 mRT and the bottom (downwards the Top of the sand plug). (**See Appendix 1**).

### IV.3.1.4 Evaluation of Minifrac Treatment Effectiveness

After gathered minifrac data, the results described briefly below:

- Low fluid efficiency (FE < 40%).
- High fluid leak-off inside the formation.
- Small fracture geometry.
- Possible screenout scenario.
- The fracture propagated upwards to the 7″ casing shoe (3165 mRT), this may affect the well integrity.
- The fracture propagated downwards to the WOC, this may lead to more water production and low productivity rate.

### IV.3.1.5 Main Treatment

After analyzing the data gathered from the minifrac test, the design of the primary treatment underwent a revision. A total volume of 40,799 gallons of slurry was injected in four stages, at a rate of 25 barrels per minute, with the objective of creating a moderate fracture covers both units **Ri** and **Ra**.

#### IV.3.1.5.1 Design of Pumping

**Table IV.5: Designed Pumping Schedule for Main Treatment.[40]**

| Stage Number | Description | Fluid System | Clean Volume (gal) | Slurry Volume (gal) | Rate Stage End (bpm) | Prop Type |
|---|---|---|---|---|---|---|
| 1 | Pre-Pad | Linear Gel 35# | 1000 | 1004 | 25.0 | |
| 2 | Pad | Hybor G 35# | 14000 | 14140 | 25.0 | |
| 3 | 1 ppg SLF | Hybor G 35# | 3000 | 3127 | 25.0 | 30/50 HSP |
| 4 | 2 ppg SLF | Hybor G 35# | 3000 | 3231 | 25.0 | 30/50 HSP |
| 5 | 3 ppg SLF | Hybor G 35# | 2500 | 2780 | 25.0 | 30/50 HSP |
| 6 | 4 ppg SLF | Hybor G 35# | 2000 | 2284 | 25.0 | 20/40 HSP |
| 7 | 5 ppg SLF | Hybor G 35# | 2000 | 2351 | 25.0 | 20/40 HSP |
| 8 | 6 ppg SLF | Hybor G 35# | 2000 | 2418 | 25.0 | 20/40 HSP |
| 9 | 7 ppg SLF | Hybor G 35# | 2000 | 2485 | 25.0 | 20/40 HSP |
| 10 | Flush | Linear Gel 35# | 6980 | 6980 | 25.0 | |
| 11 | Shut-In | | 0 | 0 | 0.0 | |
| Total | | | 38480 | 40799 | | |

➢ **Comments:**

1- The pumping rate is decreased to 25 bpm to limit the fracture growth upwards to the 7" casing shoe and downwards to the WOC.

2- The designed Pad volume Hybor G 35# helps to mitigate the high leak-off. This would keep more width in the main fracture, as well as to have a better chance to avoid the screen-out. (**See Appendix 2**)

**IV.3.1.5.2 Main Treatment Pressure Curve**

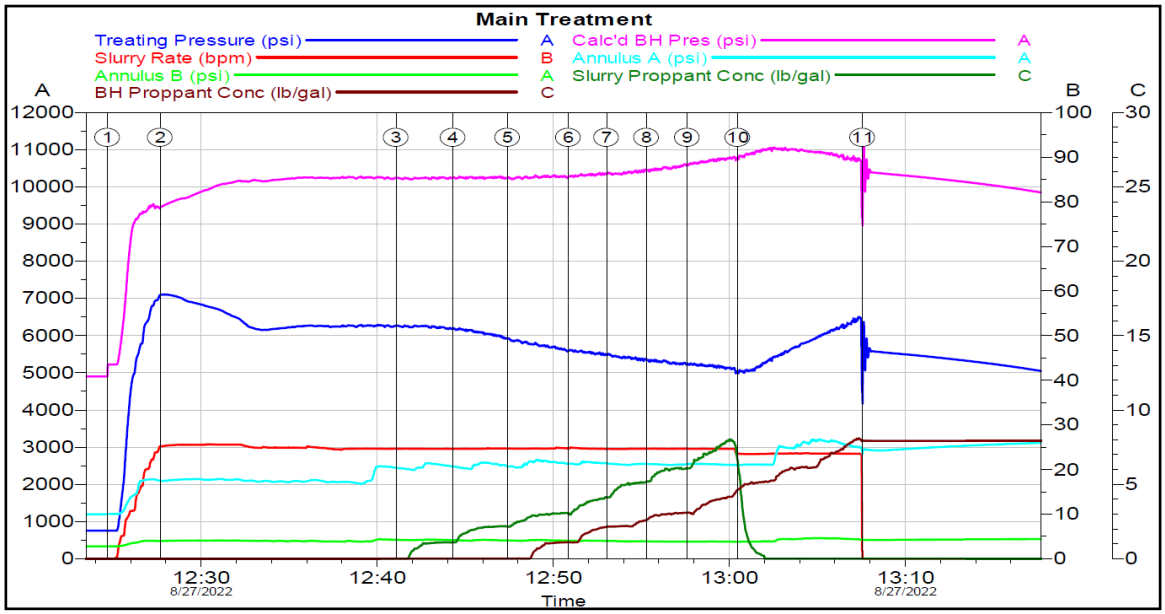


**Figure IV.19: Main Treatment Injection Plot.[40]**

➢ **Results and Discussions:**

Based on the data obtained from the mainfrac treatment, here is the interpretation:

- **Breakdown Pressure ($P_B$):** The breakdown pressure is measured at 7100 psi. This refers to the pressure required to initiate fractures in the formation during the mainfrac treatment.

**- Bottom Hole:**

- **Fracture Propagation Pressure (FPP):** The fracture propagation pressure at the bottom hole is recorded as 10200 psi. It represents the pressure required to propagate and extend the fractures within the formation.
- **Instantaneous Shut-in Pressure (ISIP):** The ISIP is determined to be 10500 psi. It signifies the pressure observed in the wellbore when the fluid flow is temporarily stopped.
- **The difference in pressure (ΔP):** is calculated as 300 psi. It indicates the variation between the fracture propagation pressure and the ISIP.

**-Surface:**

- **Fracture Propagation Pressure:** The fracture propagation pressure at the surface is measured at 6200 psi. It represents the pressure required to propagate and extend the fractures near the wellhead.
- **Instantaneous Shut-in Pressure (ISIP):** The ISIP at the surface is recorded as 5500 psi. It signifies the pressure observed at the wellhead when the fluid flow is temporarily stopped.
- **The difference in pressure (ΔP):** is calculated as 700 psi. It indicates the variation between the fracture propagation pressure and the ISIP.

These values provide important information about the pressure's response in the mainfrac treatment.

### IV.3.1.5.3 Main Treatment Net Pressure Plot

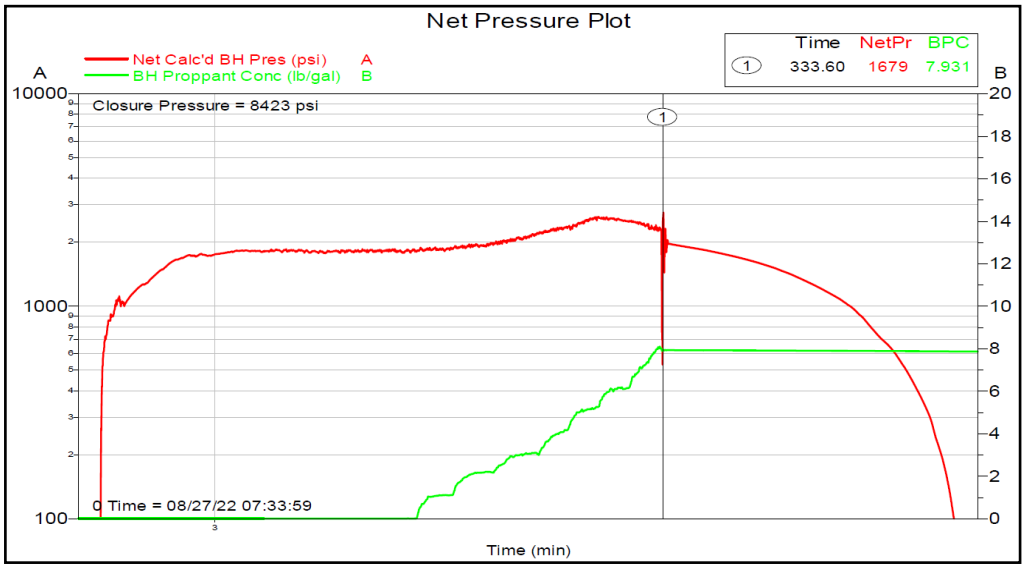


**Figure IV.20: Main Treatment Net Pressure Plot.[40]**

➢ **Interpretation of main treatment net pressure plot using Nolte & Smith analysis:**

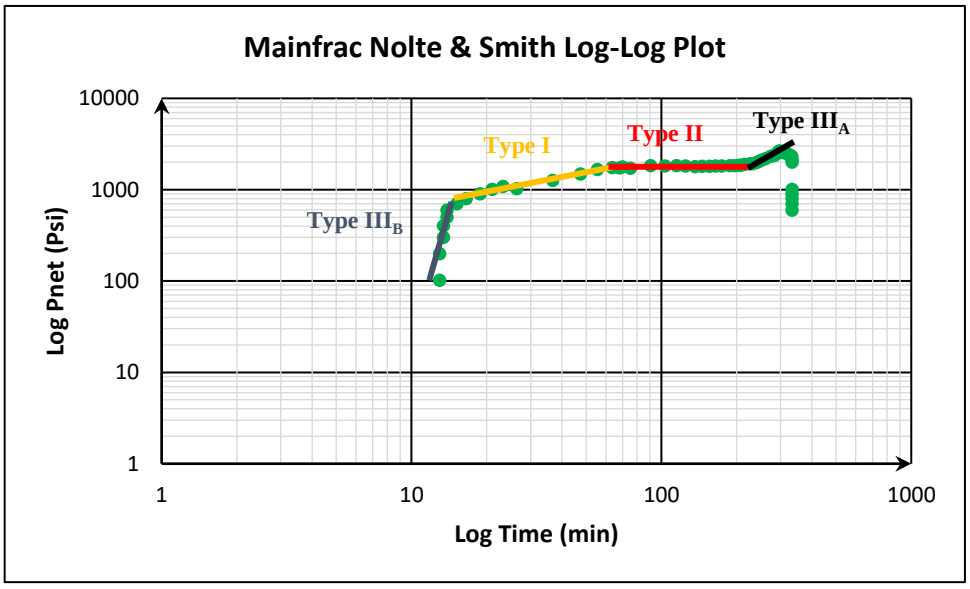


**Figure IV.21: Main Treatment Nolte & Smith Analysis Plot.**

The figure IV.21 shows that the evolution of fracture propagation mode goes through 4 stages:

**Mode 1:** corresponds to Type $III_B$ of the Nolte & Smith analysis due to its steep slope. It indicates a restriction of the fracture extension, only one active side and a possible screen-out scenario near the wellbore.

**Mode 2:** corresponds to Type I based on the Nolte & Smith analysis as it exhibits a slight positive slope. It signifies propagation in line with (PKN) model, where the fracture length extends while the height remains nearly constant.

**Mode 3:** corresponds to Type II according to the Nolte & Smith analysis, as it demonstrates a consistent slope. It indicates that the increase in fracture propagation is controlled either by height increase in barriers or by the presence of natural fissure openings, resulting in radial spreading of the fracture.

**Mode 4:** corresponds to Type $III_A$ in the Nolte & Smith analysis, as it exhibits a unit slope. It signifies a limitation in fracture extension, along with additional width growth resulting from a tip screen-out process.

- **Comparison between the Fracture Geometry Design and the obtained Fracture Geometry from main treatment:**

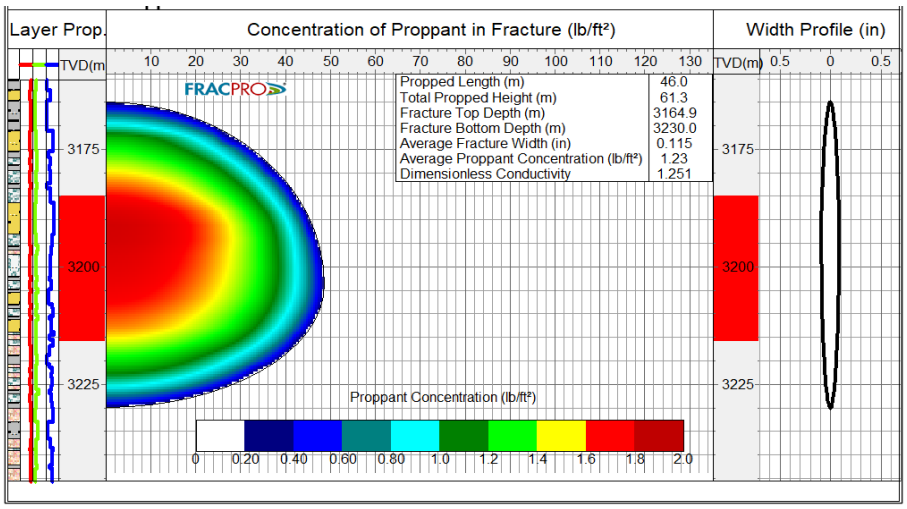


**Figure IV.22: The Designed Fracture Geometry for Main Frac.[40]**

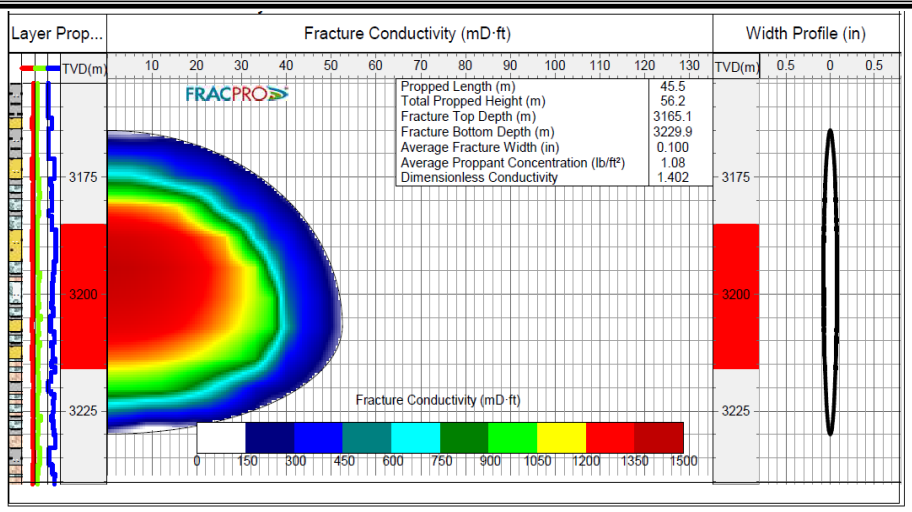


**Figure IV.23: The Fracture Geometry Obtained from Main Frac.[40]**

**Table IV.6: Dimensions of The Designed Fracture and The Fracture Obtained from Main Frac.**

| Dimensions / The fracture geometry | Length (m) | Height (m) | Width (in) |
|---|---|---|---|
| The designed fracture geometry. | 46.0 | 61.3 | 0.115 |
| The fracture geometry obtained from main Frac | 45.5 | 56.2 | 0.100 |
| The difference | 0.5 | 5.1 | 0.015 |

The results confirm the propagation mode of the main fracture, and show the restriction of length & height growth.

### IV.3.1.6 Evaluation of Mainfrac Treatment Effectiveness

Upon analyzing the data gathered from the mainfrac treatment, it becomes evident that the presence of natural fractures significantly impacts the intended geometry of the primary fracture and overall operational efficiency.

**Table IV.7: Fracture Geometry Summary.[40]**

| | | | |
|---|---|---|---|
| Fracture Half-Length (m) | 52 | Propped Half-Length (m) | 45 |
| Total Fracture height (m) | 65 | Total Propped height (m) | 56 |
| Depth to Fracture Top (m) | 3165 | Depth to Propped Fracture Top (m) | 3171 |
| Depth to Fracture Bottom (m) | 3230 | Depth to Propped Fracture Bottom (m) | 3227 |
| Fracture Slurry Efficiency | 0.16 | Max Fracture Width (in) | 0.15 |
| Avg Proppant Concentration ($lb/ft^2$) | 1.08 | Avg Fracture Width (in) | 0.10 |
| Total Proppant Pumped (klbs) | 65.6 | Total Proppant in Fracture (klbs) | 62.3 |

- The decrease of pumping rate to 25 bpm did not limit the fracture growth upwards to the 7″ casing shoe and downwards to the WOC.
- Low slurry efficiency (FE=16% < 40%).

- Small propped fracture geometry.
- The high proppant concentration (1.08 lb/ft$^2$ > 0.5 lb/ft$^2$), and the difference between the total proppant pumped and the total proppant in fracture is 3.3 klbs. these indicators of screen-out mechanism that is generated by natural fractures presence which provide a path for the proppants to flow out of the wellbore.
- After main frac treatment production of water increased in GS-Well 1 which means that the fracture propagation reaches out the WOC. This is clear evidence that the main fracture connects several natural fractures leading to more water production and low productivity rate.

### IV.3.2 GS-Well 2

In some cases, the application of matrix acidizing alone proved ineffective in mitigating wellbore damage and restoring well productivity. As a result, hydraulic fracturing stimulation becomes necessary to bypass the formation damage and establish a clear flow path from the reservoir to the wellbore. GS-well 2 serves as an example illustrating this need for hydraulic fracturing stimulation.

#### IV.3.2.1 Well History

- The GS-well 2 is an oil producer well drilled in June 2021. Targeted the Cambrian reservoir Ri & Ra units. It was implanted in the El Gassi field.
- The DST gave 9.46 m3/h production during the drilling (May 2021) & skin of 52.3, using choke 24/64″.
- Another test was conducted in July 2021 (after CT Naphta/xylene operation) which gave a production of 7.16 m$^3$/h, with choke size 24/64″.
- It was undergone to a frequent stimulation with Reformat/Naphta/Xylene, due to the existing of Asphaltene. Currently the well production is around 6.5 m$^3$/h (1000 stb/d).
- The objective of Hydraulic fracturing is to re-gain the well production obtained in DST, by creating a skin bypass with sufficient conductive fracture.[41]

#### IV.3.2.2 Reservoir Petrophysics

The petrophysics parameters of units **Ri** and **Ra** shown in the **Table IV.8** are obtained from well logging and DST.

**Table IV.8: The petrophysics of Units Ri & Ra of GS-Well 2.**

| Pay Zone | Gross pay (m) | Net pay (m) | Porosity (%) | Water saturation (%) | Permeability (kh) (mD) |
|---|---|---|---|---|---|
| **Ri** | 28.5 | 22.08 | 6.9 | 19.3 | 2660 |
| **Ra** | 55.12 | 45.9 | 6.5 | 21.7 | 2660 |

➢ **Comments:**

1- The average porosity value is 6.7% below 10%, so the reservoir is classified in low porosity reservoirs.

2- The horizontal permeability is 2660 mD, so the reservoir is classified in high permeability reservoirs.

3- Low water saturation < 20%.

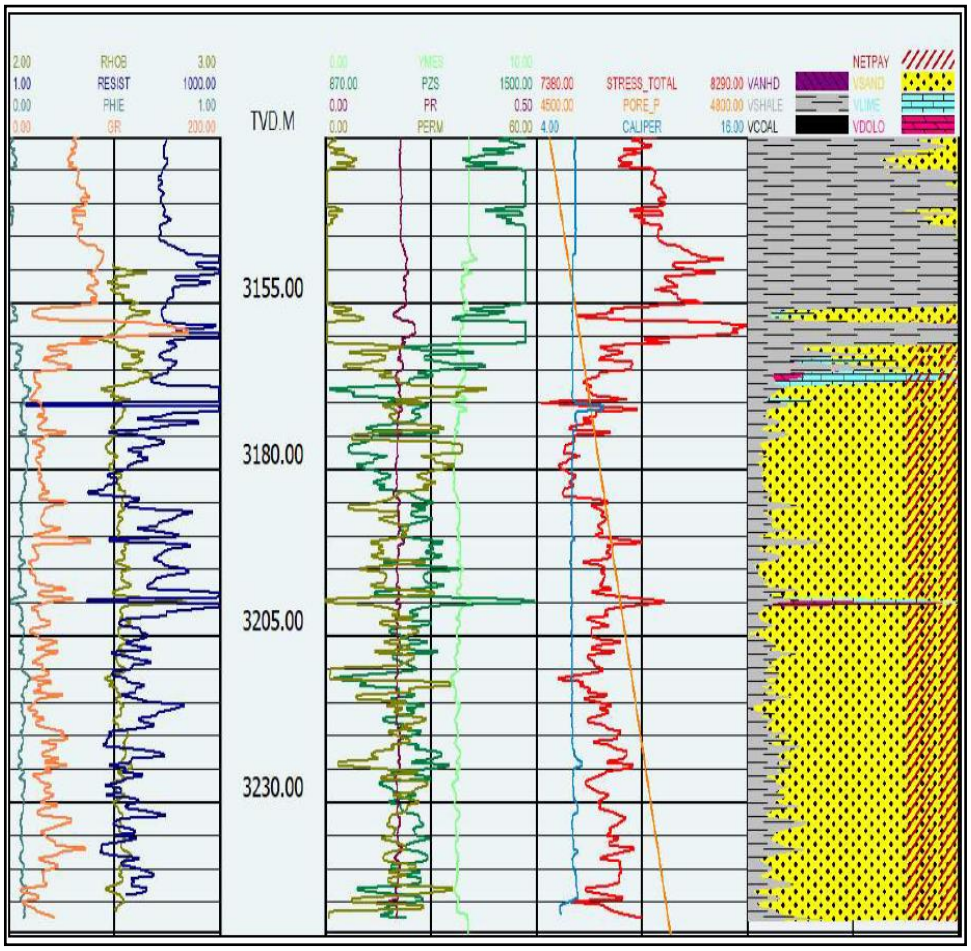


**Figure IV.24: Composite Log (GOHFER).**

### IV.3.2.3 Minifrac Treatment

Prior to the main treatment, a minifracture test was conducted, involving the injection of a total volume of 32602 gallons at a rate of 25 barrels per minute. Based on the high fracture gradient (1.2 psi/ft) from offset well, the minifrac test will confirm the possibility to continue

the main treatment. The data obtained from the minifracture test, including fluid loss properties and closure stress, were utilized to redesign the main treatment with the goal of optimizing the fracture geometry.

### IV.3.2.3.1 Design of Pumping

**Table IV.9: Designed Pumping Schedule for Minifrac Treatment.[41]**

| Stage Number | Description | Clean Volume (gal) | Slurry Volume (gal) | Rate Stage End (bpm) |
|---|---|---|---|---|
| 1 | Breakdown | 8000 | 8000 | 25.0 |
| 2 | Shut-In | 0 | 0 | 0.0 |
| 3 | Pre-Pad | 1000 | 1004 | 25.0 |
| 4 | Pad | 6000 | 6064 | 25.0 |
| 5 | Prop Slug (20/40 HSP) | 2000 | 2089 | 25.0 |
| 6 | Pad | 8000 | 8086 | 25.0 |
| 7 | Flush | 7360 | 7360 | 25.0 |
| 8 | Shut-In | 0 | 0 | 0.0 |
| Total | | 32360 | 32602 | |

➢ **Comments:**

1- The pumping rate kept low because of the high fracture gradient 1.2 psi/ft (offset wells).

2- The Prop slug (20/40) used to reduce BH friction and get visibility of formation response before pumping the proppant into the formation.

### IV.3.2.3.2 Minifrac Pressure Curves

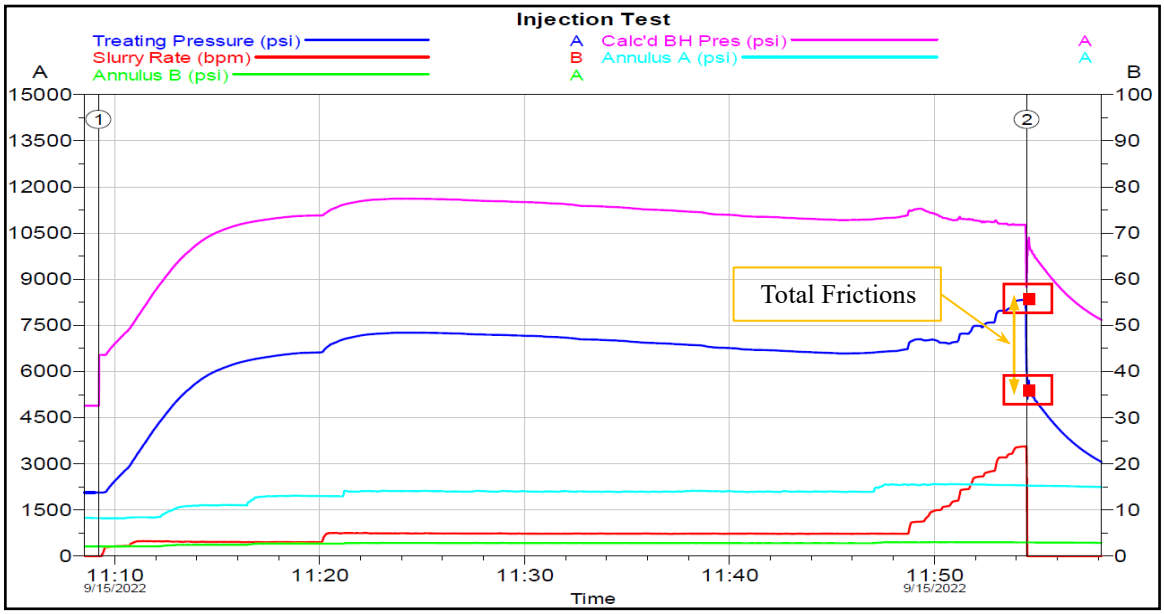


**Figure IV.25: Injection Test Plot.[41]**

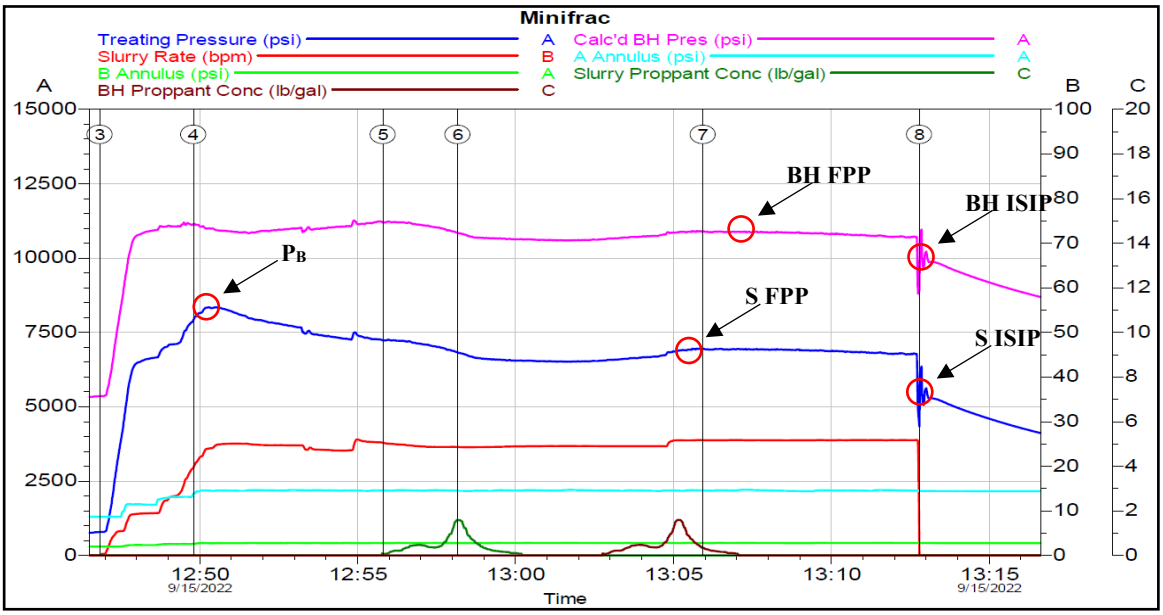


**Figure IV.26: Minifrac Injection Plot.[41]**

➢ **Results and Discussions:**

After analyzing the data obtained from the minifrac test, here is the interpretation:

- **Breakdown Pressure ($P_B$):** The breakdown pressure is measured at 8250 psi. This refers to the pressure required to initiate fractures in the formation during the minifrac test.
- **Total Frictions:** The total frictions are recorded at 3000 psi. This value represents the combined effect of frictional forces encountered during the minifrac test.

**- Bottom Hole:**

- **Fracture Propagation Pressure (FPP):** The fracture propagation pressure at the bottom hole is recorded as 10750 psi. It represents the pressure required to propagate fractures in the formation.
- **Instantaneous Shut-in Pressure (ISIP):** The ISIP is determined to be 10000 psi. It signifies the pressure observed in the wellbore when the fluid flow is temporarily stopped.
- **The difference in pressure (ΔP):** is calculated as 750 psi. It indicates the variation between the fracture propagation pressure and the ISIP.

**- Surface:**

- **Fracture Propagation Pressure (FPP):** The fracture propagation pressure at the surface is measured at 7000 psi. It represents the pressure required to propagate fractures at the wellhead.
- **Instantaneous Shut-in Pressure (ISIP):** The ISIP at the surface is recorded as 5500 psi. It signifies the pressure observed at the wellhead when the fluid flow is temporarily stopped.

- **The difference in pressure (ΔP):** is calculated as 1500 psi. It indicates the variation between the fracture propagation pressure and the ISIP.

#### IV.3.2.3.3 Minifrac G-Function Plot

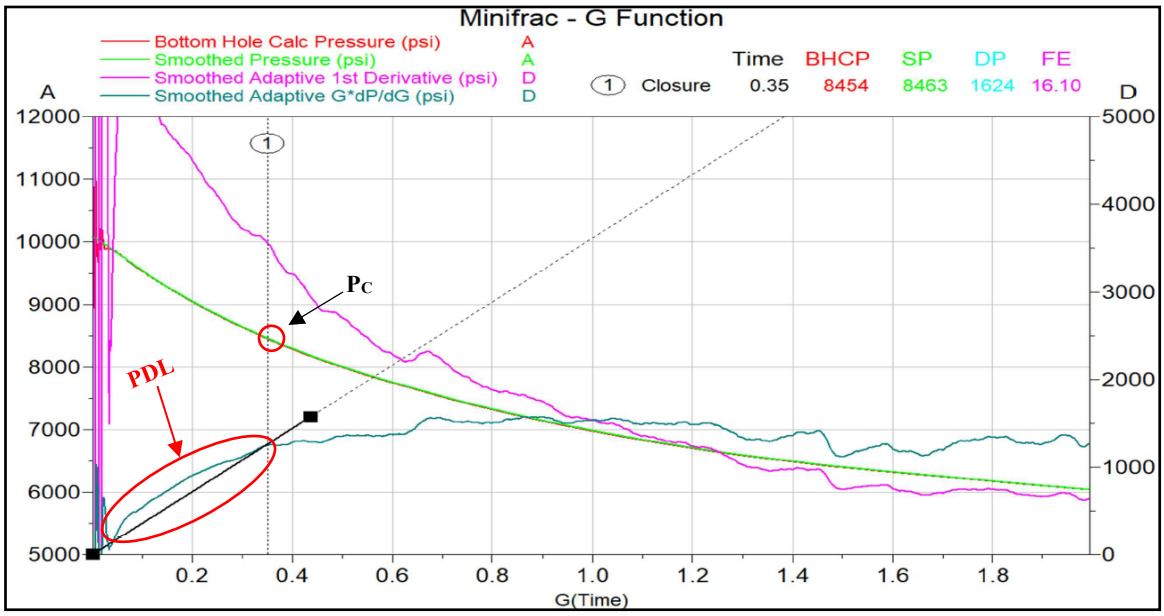


**Figure IV.27: Minifrac G-Function Plot.[41]**

➢ **Interpretation of minifrac G-Function plot:**

The G-Function plot shows a Pressure-Dependent Leak-off (PDL) as it is called accelerated leak-off. This behavior indicates that the fracturing fluid is leaking faster than what expected because of the intersecting of the main fracture by natural fractures. This differs from delayed leak-off in the dominant effect of the secondary fractures, which provide an additional area and allow the fluid leaking through it.

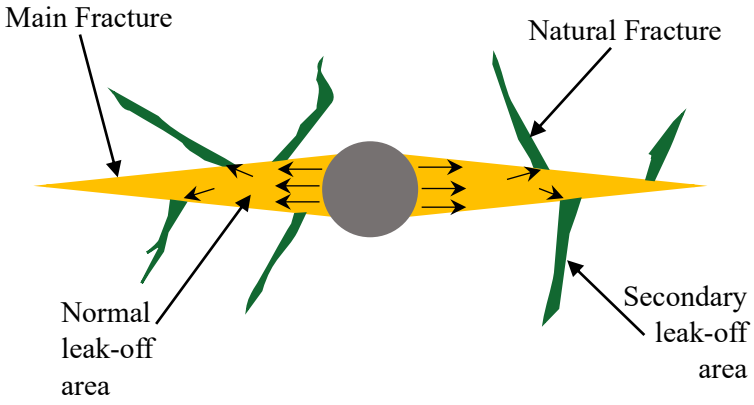


**Figure IV.28: Illustration of Pressure-Dependent Leak-off Mechanism.**

➢ **Results and Discussions:**

Based on the data obtained from the G-function of the minifrac test, here is the interpretation:

- **BH Closure Pressure ($P_C$):** The BH Closure Pressure is determined to be 8454 psi. This pressure represents the point at which the fractures in the formation close and the fluid flow is hindered.
- **Closure Gradient:** The Closure Gradient is calculated as 0.81 psi per foot. It indicates the rate of pressure increase with respect to depth in the wellbore when approaching the closure pressure.
- **G-Function Closure Time ($G_C$):** The G-Function Closure Time is measured at 0.35. It represents the time it takes for the fractures to close and the pressure to stabilize.
- **Fluid Efficiency (FE):** The Fluid Efficiency is determined to be 16.10%. This value reflects the effectiveness of the fluid in transmitting the pressure and creating fractures within the formation.
- **Calculated FE:** The Calculated FE is evaluated using the G-Function Closure Time (GC) and is calculated as 14.89%. It provides an alternate way to estimate the fluid efficiency based on the G-Function Closure Time.
- **G-Function Net Pressure:** The G-Function Net Pressure is recorded as 1624 psi. This pressure indicates the net effect of fluid pressure on the fractures in the formation.
- **Calculated Net Pressure (Pnet):** Pnet is obtained by subtracting the BH Closure Pressure from the BH ISIP and is calculated as 1546 psi. It represents the effective pressure difference at the bottom hole, taking into account the closure pressure.

#### IV.3.2.3.4 Minifrac Net Pressure Plot

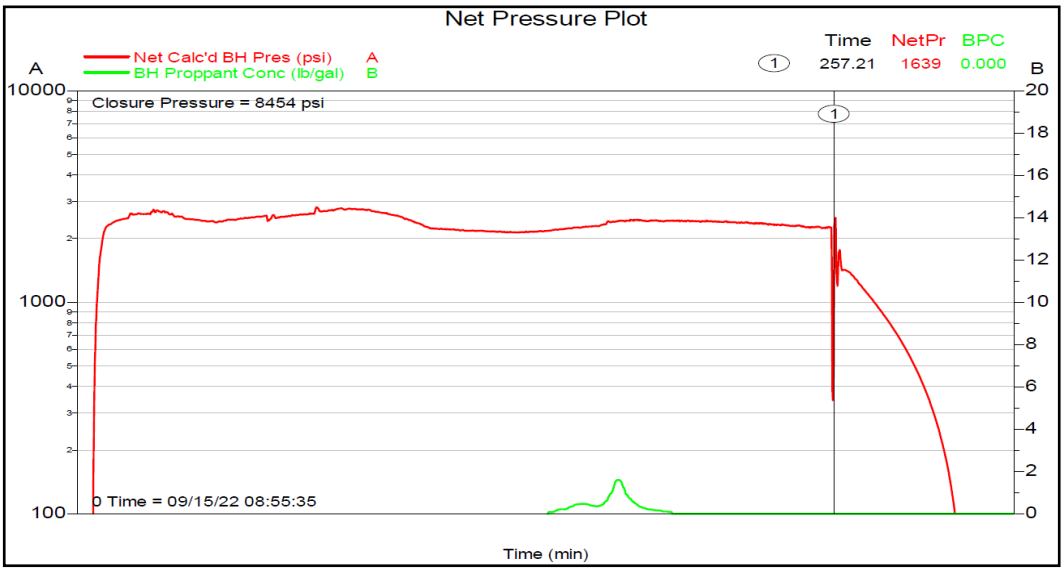


**Figure IV.29: Minifrac Treatment Net Pressure Plot.** [41]

➢ **Interpretation of main treatment net pressure plot using Nolte & Smith analysis:**

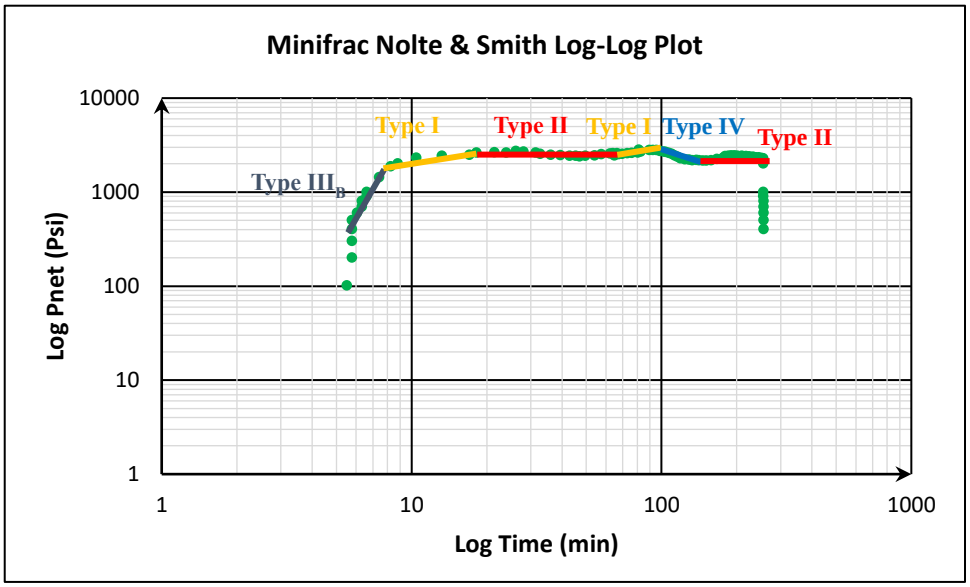


**Figure IV.30: Minifrac Treatment Nolte & Smith Analysis Plot.**

The figure IV.30 shows that the evolution of fracture propagation mode goes through 6 stages:

**Mode 1:** corresponds to Type $III_B$ of the Nolte & Smith analysis due to its steep slope. It indicates a restriction of the fracture extension, only one active side and a possible screen-out scenario near the wellbore.

**Mode 2:** corresponds to Type I based on the Nolte & Smith analysis as it exhibits a slight positive slope. It signifies propagation in line with (PKN) model, where the fracture length extends while the height remains nearly constant.

**Mode 3:** corresponds to Type II according to the Nolte & Smith analysis, as it demonstrates a consistent slope. It indicates that the increase in fracture propagation is controlled either by height increase in barriers or by the presence of natural fissure openings, resulting in radial spreading of the fracture.

**Mode 4:** corresponds to Type I based on the Nolte & Smith analysis as it exhibits a slight positive slope. It signifies propagation in line with (PKN) model, where the fracture length extends while the height remains nearly constant.

**Mode 5**: corresponds to Type IV in the Nolte & Smith analysis, as it demonstrates a negative slope. It indicates a rapid growth in fracture height. Both the and Radial models can be considered applicable in this case.

**Mode 6:** corresponds to Type II according to the Nolte & Smith analysis, as it demonstrates a consistent slope. It indicates that the increase in fracture propagation is controlled either by

height increase in barriers or by the presence of natural fissure openings, resulting in radial spreading of the fracture.

#### IV.3.2.3.5 Comparison between the Fracture Geometry Design and The Temperature Log after Minifrac

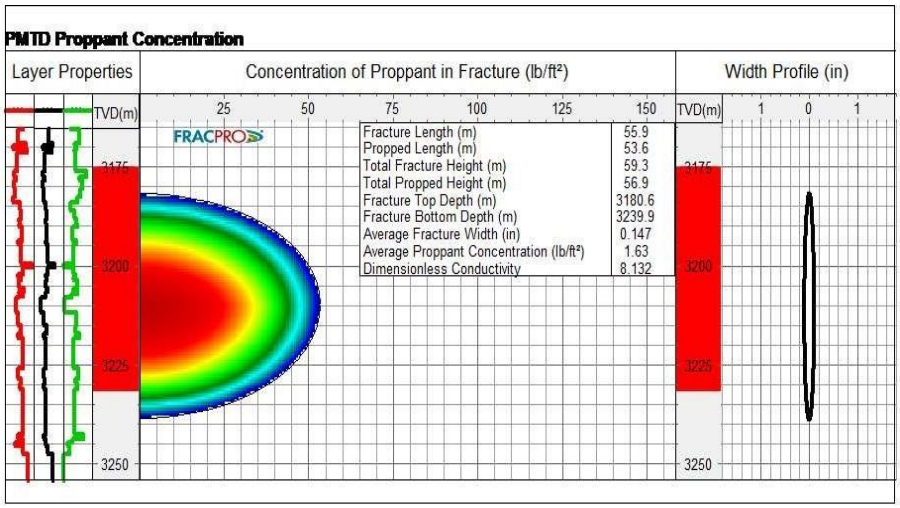


**Figure IV.31: The Designed Fracture Geometry for Minifrac.[41]**

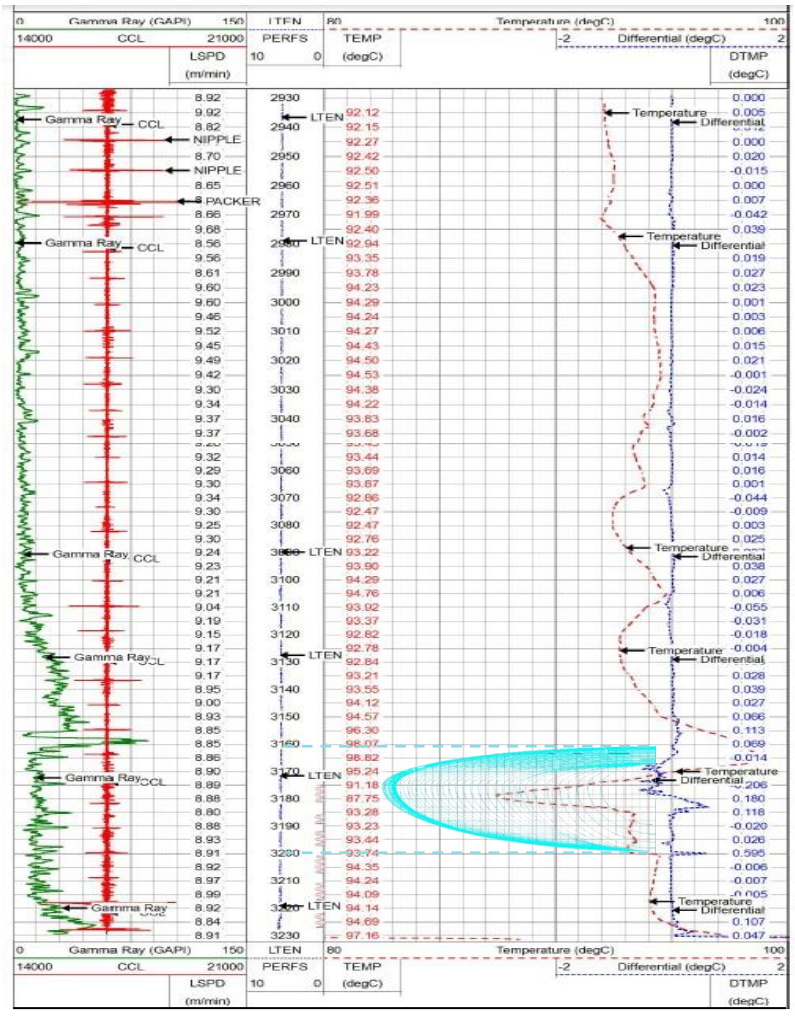


**Figure IV.32: The Temperature Log After Minifrac of GS-Well 2.[41]**

- The temperature log shows an unwanted cooling above the perforation interval behind the 4 1/2″ liner. The main cooling started from 5 m above the 7″ casing shoe (3,165 mRT) and downwards 3,200 mRT. (**See Appendix 3**)
- The top depth of the fracture is 3165 mRT and the bottom depth of the fracture is 3200 mRT, the fracture covered only the unit **Ri**.

**Table IV.10: The comparison between the designed fracture and the fracture obtained from temperature log.**

| Dimensions | Fracture Top Depth (m) | Fracture Bottom Depth (m) | Fracture Height (m) |
|---|---|---|---|
| The designed fracture. | 3180.5 | 3239.9 | 59.4 |
| The fracture after minifrac obtained from temperature log. | 3165 | 3200 | 35 |
| The difference | 20.5 | 39.9 | 24.4 |

### IV.3.2.4 Evaluation of Minifrac Treatment Effectiveness

After analyzing the data from the minifrac treatment, it assisted in determining whether to proceed with the main treatment for this well or not. The analysis of propagation modes revealed that the main fracture extended in height, effectively connecting multiple natural fractures throughout its entire length.

- Low fluid efficiency (FE=14.89 < 40%).
- High fluid leak-off inside the formation.
- Small fracture geometry compared to the designed fracture geometry (a difference of 20 m)
- Possible screenout scenario.
- The fracture propagated above the 7″ casing shoe (3165 mRT) and downwards 3,200 mRT.
- The fracture covered only the unit **Ri**, moreover the temperature log showed that the fracture propagated above the interval of the perforation.
- The fracture propagated out of the target zone was the main reason to cancel the main treatment for GS-Well 2.

### IV.3.3 HR-Well 1

Acid fracturing is a recently developed technique suitable for carbonate reservoirs. It involves injecting acid fluid at a pressure exceeding the fracture breakdown pressure to generate a conductive fracture of significant length (often spanning several hundred feet). This process facilitates enhanced drainage of the reservoir by etching pathways that enhance conductivity.

HR-well 1 exhibited Dolomitic Limestone facies, indicating its suitability as a promising candidate for acid fracturing.

### IV.3.3.1 Well History

- HR-well 1 is a gas well, located in Oued Mya field of Hassi R'mel region. Targeting the Carbonate reservoir.
- The main objective for HR-Well 1 is to stimulate Carbonate LD-2 productive intervals by Acid Frac, to increase flow capacity & transmissibility of reservoir. The treatment performance then will be evaluated by correlating offsets and pre/post well testing technique.
- The Carbonate reservoir pressure is 4399 psi, and temperature is 85°C.
- Perforation interval was selected at 2135 - 2138.5 mMD based on the petrophysical evaluation (**See Appendix 4**).[42]

### IV.3.3.2 Reservoir Petrophysics

The petrophysics parameters of unit **LD-2** shown in the **Table IV.11** are obtained from well logging and DST.

**Table IV.11: The petrophysics of Unit LD-2 of HR-Well 1.**

| Pay Zone | Gross pay (m) | Net pay (m) | Porosity (%) | Water saturation (%) | Permeability (mD) |
|---|---|---|---|---|---|
| **LD-2** | 5 | 3.5 | 7 | 45 | 1 to 10 |

➢ **Comments:**

1- The average porosity value is 7% below 10%, so the reservoir is classified in low porosity reservoirs.

2- The permeability varies from 1 to 10, so the reservoir is classified in moderate permeability reservoirs.

3- Moderate water saturation.

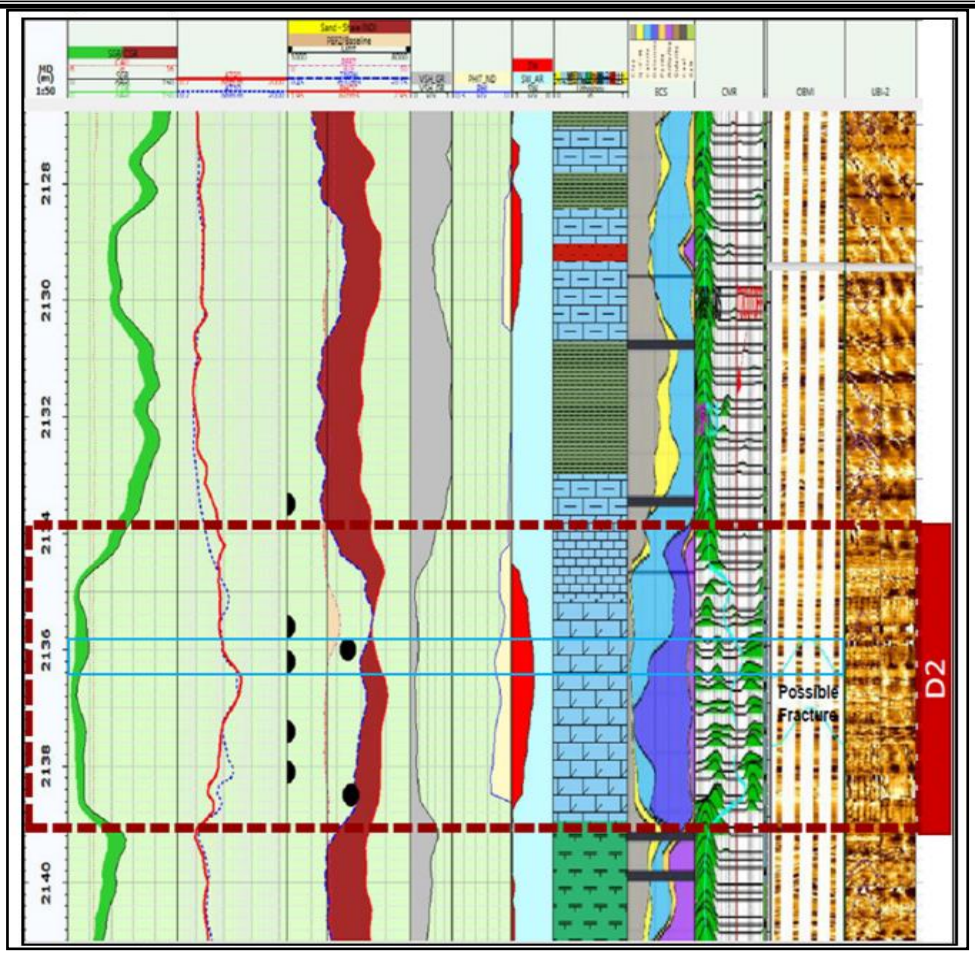


**Figure IV.33: Log Analysis of HR-Well 1.[42]**

### IV.3.3.3 Minifrac Treatment

Before the primary treatment, a minifracture test was performed, which involved injecting a total volume of 19,500 gallons at a rate of 15 barrels per minute. The data acquired from the minifracture test, including information on fluid loss properties and closure stress, were employed to refine the design of the main treatment, aiming to optimize the geometry of the fracture.

#### IV.3.3.3.1 Design of Pumping

**Table IV.12: Designed Pumping Schedule for Minifrac Treatment.[42]**

| Stage Number | Description | Fluid System | Clean Volume (gal) | Slurry Volume (gal) | Rate Stage End (bpm) |
|---|---|---|---|---|---|
| 1 | Load Well | LG 25# | 4700 | 4700 | 15.0 |
| 2 | Injection Test | LG 25# | 10000 | 10000 | 15.0 |
| 3 | Displacement | LG 25# | 4800 | 4800 | 15.0 |
| 4 | Shut-In | | 0 | 0 | 0.0 |
| Total | | | 19500 | 19500 | |

### IV.3.3.3.2 Minifrac Pressure Curves

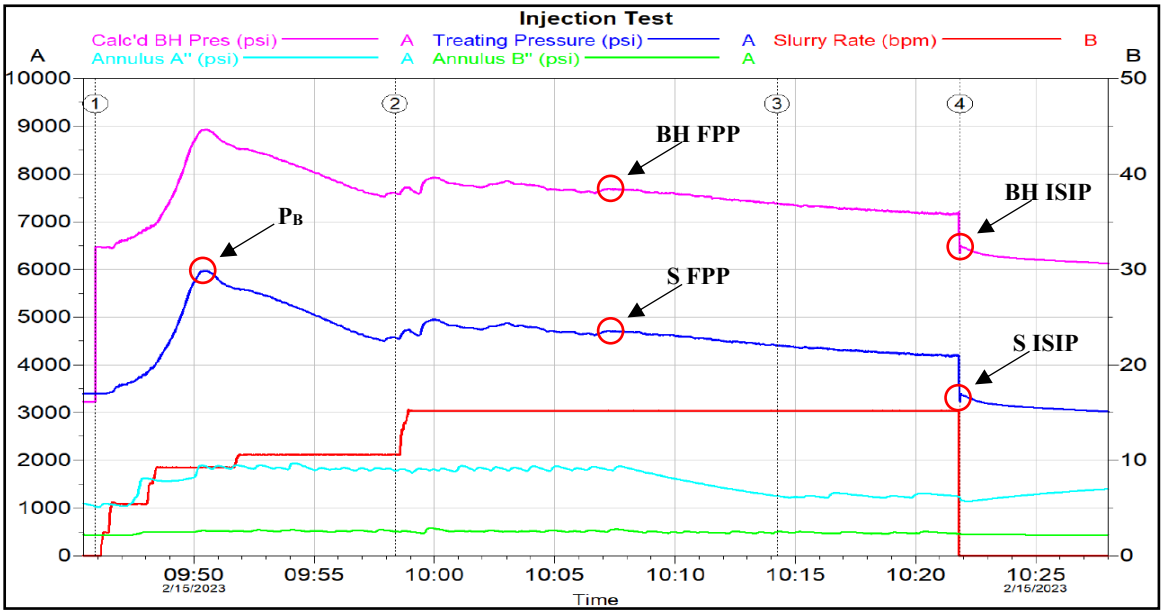


**Figure IV.34: Minifrac Injection Plot.[42]**

➢ **Results and Discussions:**

Based on the data obtained from the pressure curves of the minifract test, here is the interpretation:

- **Breakdown Pressure ($P_B$):** The breakdown pressure is measured at 6000 psi.
- **Total Frictions:** The total frictions are recorded at 800 psi.

**- Bottom Hole:**

- **Fracture Propagation Pressure (FPP):** The fracture propagation pressure at the bottom hole is recorded as 7750 psi.
- **Instantaneous Shut-in Pressure (ISIP):** The ISIP is determined to be 6400 psi.
- **The difference in pressure (ΔP):** is calculated as 1350 psi. It indicates the variation between the fracture propagation pressure and the ISIP.

**-Surface:**

- **Fracture Propagation Pressure (FPP):** The fracture propagation pressure at the surface is measured at 4750 psi.
- **Instantaneous Shut-in Pressure (ISIP):** The ISIP at the surface is recorded as 3300 psi
- **The difference in pressure (ΔP):** is calculated as 1450 psi. It indicates the variation between the fracture propagation pressure and the ISIP.

The ISIP values give insight into the wellbore pressure when the fluid flow is halted, and the pressure differentials (ΔP) indicate the variations between different pressure points.

This data assists in evaluating the characteristics of the formation and the effectiveness of the fracturing treatment during the minifract test.

### IV.3.3.3.3 Minifrac G-Function Plot

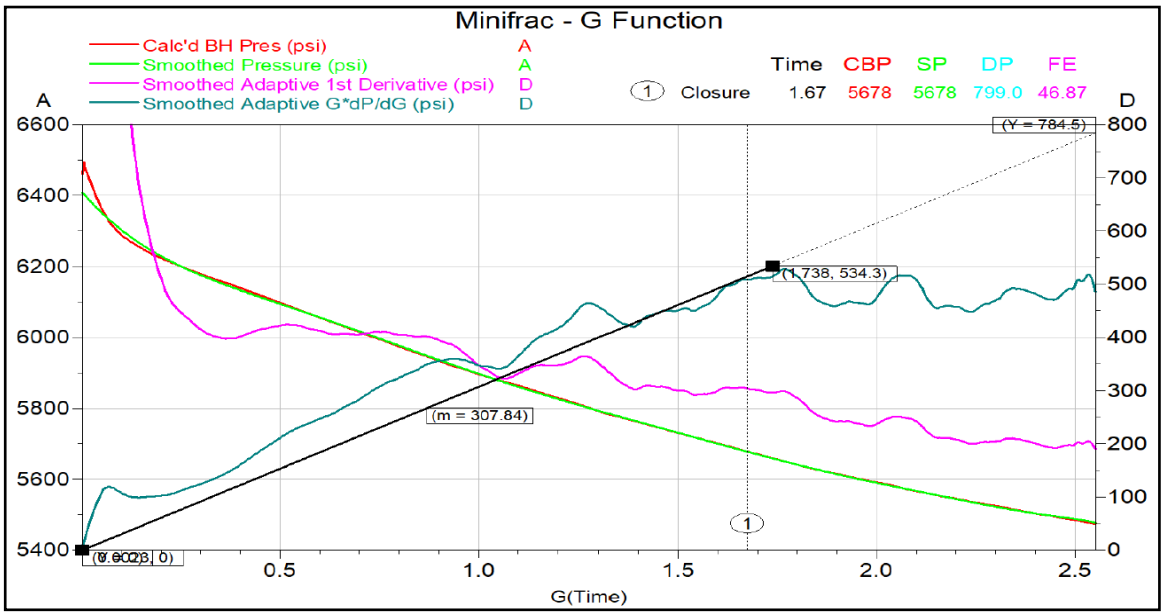


**Figure IV.35: Minifrac G-Function Plot.[42]**

➢ **Interpretation of minifrac G-Function plot:**

The G-Function plot shows fracture tip extension behavior. This mechanism occurs when a fracture continues to grow even after injection is stopped and the well is shut-in. It is a phenomenon that occurs in very low permeability reservoirs, as the energy which normally would be released through leakoff is transferred to the ends of the fracture resulting in fracture tip extension.

➢ **Results and Discussions:**

After analyzing data obtained from the minifrac test, here is the interpretation:

- **BH Closure Pressure ($P_C$):** The BH Closure Pressure is determined to be 5678 psi.
- **Closure Gradient:** The Closure Gradient is calculated as 0.812 psi per foot.
- **G-Function Closure Time ($G_C$):** The G-Function Closure Time is measured at 1.67.
- **Fluid Efficiency (FE):** The Fluid Efficiency is determined to be 46.87%. This value reflects indicates high fluid efficiency.
- **Calculated FE:** The Calculated FE is evaluated using the G-Function Closure Time ($G_C$) and is calculated as 45.50%. It provides an alternate way to estimate the fluid efficiency based on the G-Function Closure Time.
- **G-Function Net Pressure:** The G-Function Net Pressure is recorded as 799 psi.

- **Calculated Net Pressure (Pnet):** The Calculated Net Pressure is obtained by subtracting the BH Closure Pressure from the BH ISIP and is calculated as 722 psi. It represents the effective pressure difference at the bottom hole, taking into account the closure pressure.

### IV.3.3.3.4 Minifrac Net Pressure Plot

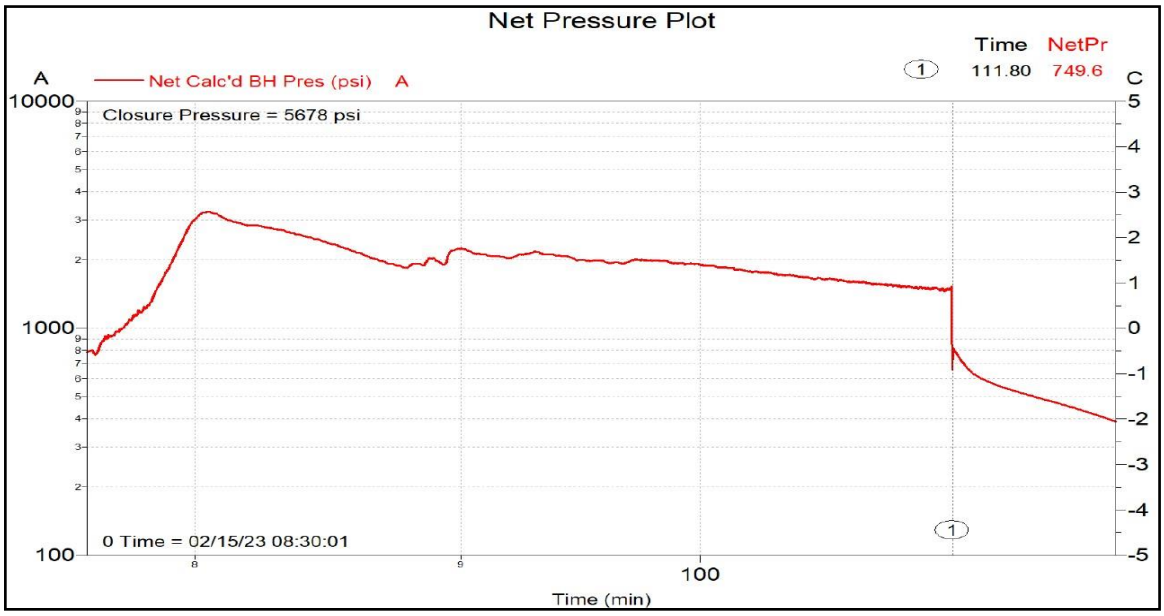


**Figure IV.36: Minifrac Treatment Net Pressure Plot.[42]**

➢ **Interpretation of minifrac net pressure plot using Nolte & Smith analysis:**

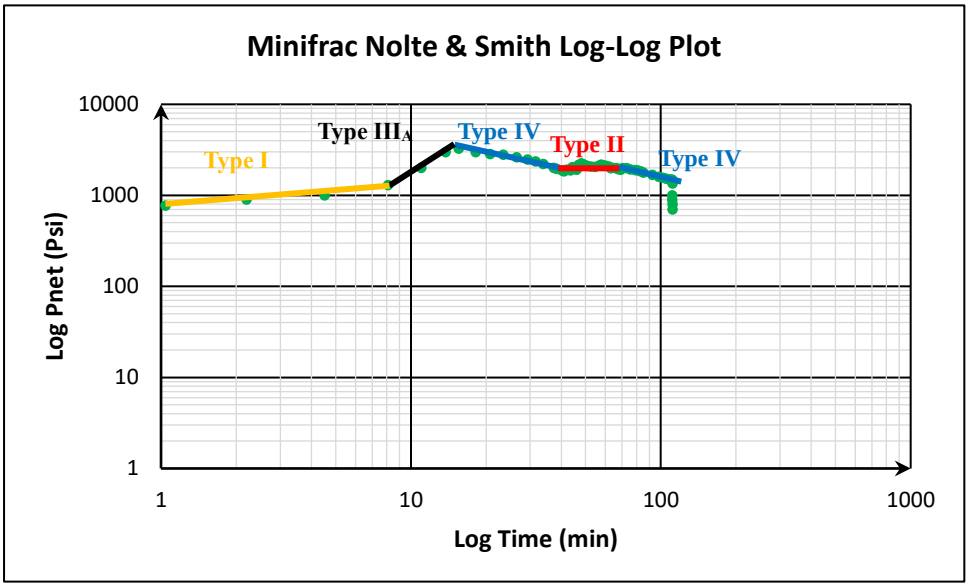


**Figure IV.37: Minifrac Treatment Nolte & Smith Analysis Plot.**

The figure IV.37 shows that the evolution of fracture propagation mode goes through 5 stages:

**Mode 1:** corresponds to Type I based on the Nolte & Smith analysis as it exhibits a slight positive slope. It signifies propagation in line with (PKN) model, where the fracture length extends while the height remains nearly constant.

**Mode 2:** corresponds to Type $III_A$ in the Nolte & Smith analysis, as it exhibits a unit slope. It signifies a limitation in fracture extension, along with additional width growth.

**Mode 3**: corresponds to Type IV in the Nolte & Smith analysis, as it demonstrates a negative slope. It indicates a rapid growth in fracture height. Both the and Radial models can be considered applicable in this case.

**Mode 4:** corresponds to Type II according to the Nolte & Smith analysis, as it demonstrates a consistent slope. It indicates that the increase in fracture propagation is controlled either by height increase in barriers or by the presence of natural fissure openings, resulting in radial spreading of the fracture.

**Mode 5**: corresponds to Type IV in the Nolte & Smith analysis, as it demonstrates a negative slope. It indicates a rapid growth in fracture height. Both the and Radial models can be considered applicable in this case.

#### IV.3.3.3.5 Comparison between the Fracture Geometry Design and The Temperature Log after Minifrac:

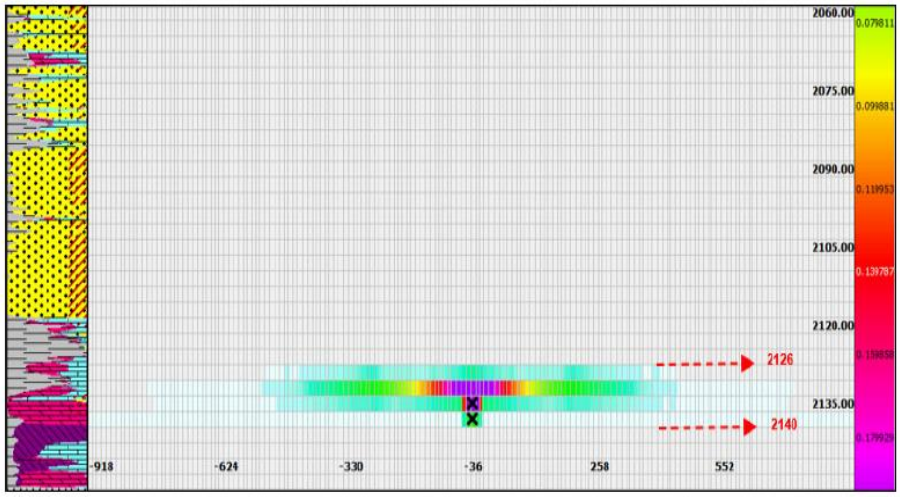


**Figure IV.38: The Designed Fracture Geometry for Mainfrac.[42]**

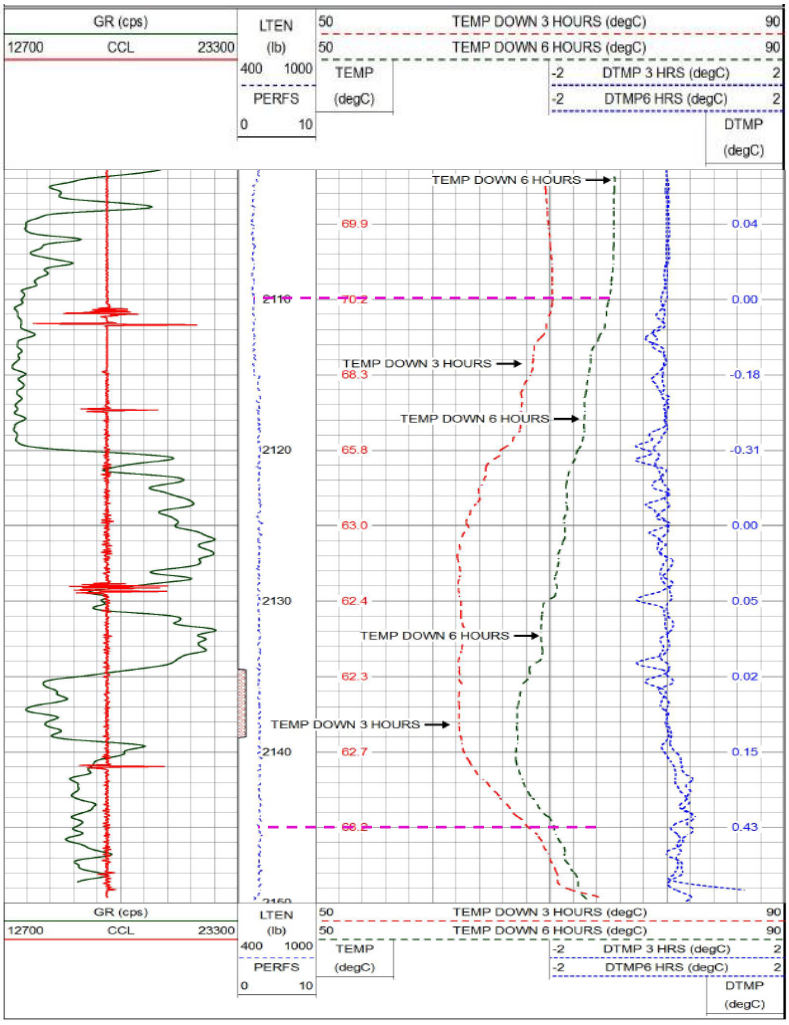


**Figure IV.39: The Temperature Log After Minifrac of HR-Well 1.[42]**

The temperature log shows a cooling started from 2110 mRT and downwards 2145 mRT.

**Table IV.13: The comparison between the designed fracture and the fracture obtained from temperature log.**

| Dimensions | Fracture Length (m) | Fracture Width (in) | Fracture Height (m) | Fracture Top Depth (m) | Fracture Bottom Depth (m) |
|---|---|---|---|---|---|
| The designed fracture. | 20 | 0.194 | 14 | 2126 | 2140 |
| The fracture after minifrac obtained from temperature log. | / | / | 35 | 2110 | 2145 |
| The difference | / | / | 21 | 16 | 5 |

➢ **Comment:**

1- There is a difference of 21 m between the designed fracture and the fracture obtained from minifrac.

### IV.3.3.4 Evaluation of Minifrac Treatment Effectiveness

After analyzing the data from the minifrac treatment. The analysis of propagation modes revealed that the main fracture extended in height and spreads up and down the perforation interval.

- High fluid efficiency (FE=46.87 % < 40%).
- Tip extension behavior occurred refers to the phenomenon where fractures grow beyond their initial length or height, extending further into the reservoir. This behavior could be explained by the presence of natural fractures or stress variations. (See appendix).
- The designed fracture height is small compared to the height obtained from minifrac.
- The fracture propagated 1 m downwards the 7″ casing shoe (2146.7 mVD).
- The fracture covered LD-2 Unit, moreover the temperature log showed that the fracture propagated up and down the target zone.

### IV.3.3.5 Main Treatment

Upon analyzing the data obtained from the minifrac test, modifications were made to the design of the primary treatment. The treatment involved injecting a total volume of 43,538 gallons of slurry in two phases, followed by Closed Fracture Acidizing (CFA), at a rate of 15 barrels per minute. The primary goal of this treatment was to create an etching fracture that covers the LD-2 unit.

#### IV.3.3.5.1 Design of Pumping

**Table IV.14: Designed Pumping Schedule for Mainfrac Treatment.[42]**

| Stage Number | Description | Fluid System | Clean Volume (gal) | Slurry Volume (gal) | Rate Stage End (bpm) |
|---|---|---|---|---|---|
| 1 | Pre-Pad | 25# Linear Gel | 3000 | 3002 | 15.0 |
| 2 | PAD | Hybor H 25# | 4000 | 4018 | 15.0 |
| 3 | Acid 15% HCL | Acid HCL 15% 180F | 4000 | 4000 | 15.0 |
| 4 | CSA | CSA 15% 180F | 4000 | 4000 | 15.0 |
| 5 | Pad | Hybor H 25# | 4000 | 4018 | 15.0 |
| 6 | Acid 15% HCL | Acid HCL 15% 180F | 4000 | 4000 | 15.0 |
| 7 | CSA | CSA 15% 180F | 4000 | 4000 | 15.0 |
| 8 | Displacement | 25# Linear | 5500 | 5500 | 15.0 |
| 9 | Shut In | Shut-In for closure time | 0 | 0 | 0.0 |
| 10 | CFA | X-Tend 28% 180F | 3000 | 3000 | 15.0 |
| 11 | Flush | 25# Linear | 8000 | 8000 | 15.0 |
| 12 | Shut-In | | 0 | 0 | 0.0 |
| Total | | | 43500 | 43538 | |

➢ **Comments:**

1- The cross-linked gel used in the main treatment is a delayed cross-linked Borate gel Hybor H 25# with ClaWeb. It provides higher viscosity from less gel loading. The high viscosity and lower gel loading are obviously an advantage and offers better fluid loss control and width development with less damage than other fluid systems with the same fluid viscosity. (**See Appendix 5**)

2- The frac acid design consists of pumping in two sequences Pad, Acid 15% HCL & CSA (Carbonate Stimulation Acid), then shut-in to resume after that with pumping CFA (Closed Fracture Acidizing).

### IV.3.3.5.2 Main Treatment Pressure Curves

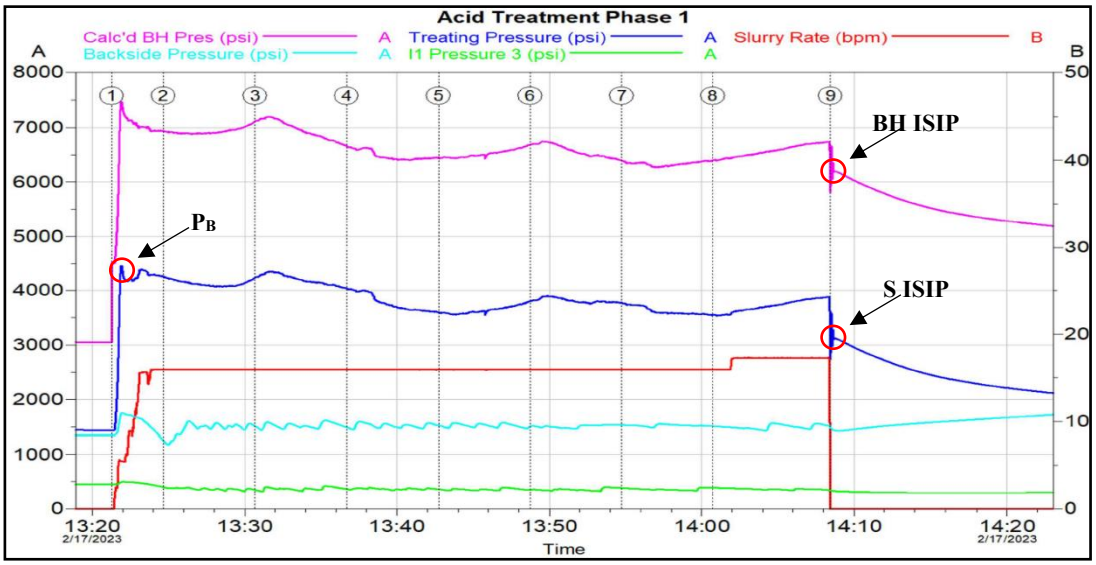


**Figure IV.40: Acid Treatment Phase 1 Injection Plot.[42]**

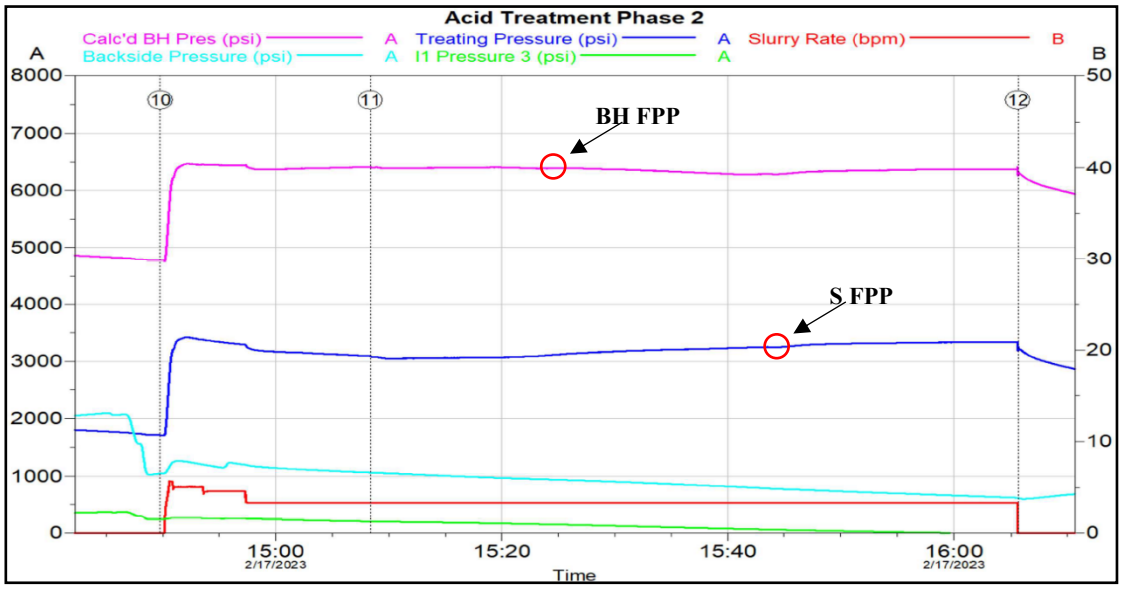


**Figure IV.41: Acid Treatment Phase 2 Injection Plot.[42]**

➢ **Results and Discussions:**

Based on the data obtained from the mainfrac treatment, here is the interpretation:

- **Breakdown Pressure ($P_B$):** The breakdown pressure is measured at 4500 psi.
- **Total Frictions:** The total frictions are recorded at 1100 psi.

**- Bottom Hole:**

- **Fracture Propagation Pressure (FPP):** The fracture propagation pressure at the bottom hole is recorded as 6300 psi.
- **Instantaneous Shut-in Pressure (ISIP):** The ISIP is determined to be 6200 psi.
- **The difference in pressure (ΔP):** is calculated as 100 psi. It indicates the variation between the fracture propagation pressure and the ISIP.

**- Surface:**

- **Fracture Propagation Pressure (FPP):** The fracture propagation pressure at the surface is measured at 3200 psi.
- **Instantaneous Shut-in Pressure (ISIP):** The ISIP at the surface is recorded as 3100 psi.
- **The difference in pressure (ΔP):** is calculated as 100 psi. It indicates the variation between the fracture propagation pressure and the ISIP.

### IV.3.3.5.3 Mainfrac G-Function Plot

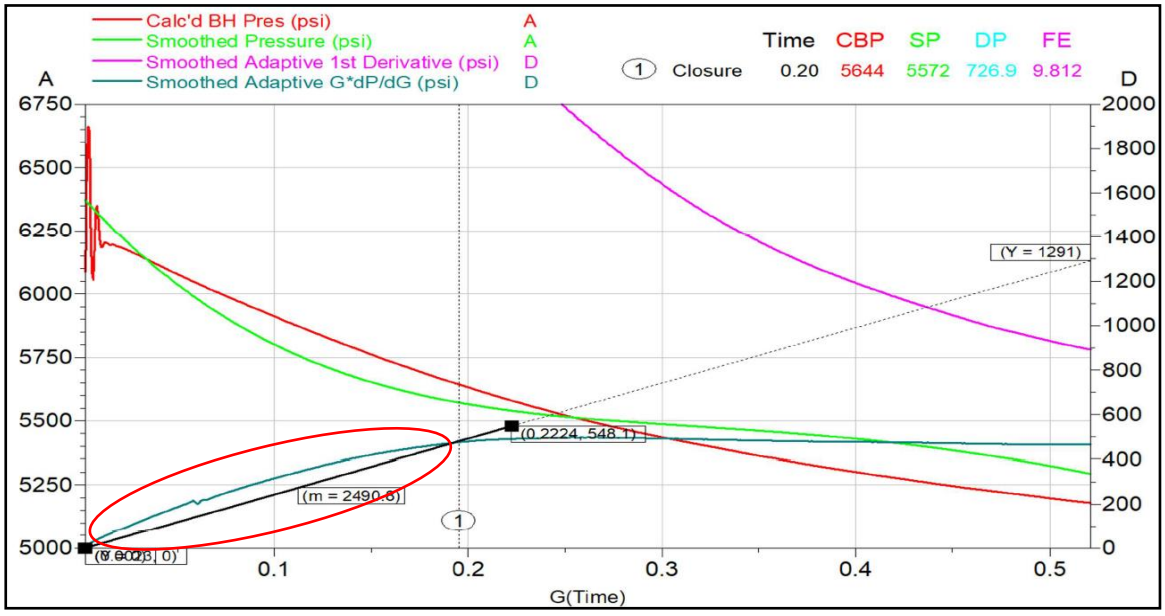


**Figure IV.42: Mainfrac G-Function Plot.[42]**

➢ **Interpretation of mainfrac G-Function plot:**

The G-Function plot shows a Pressure-Dependent Leak-off (PDL). This behavior indicates that the fracturing fluid is leaking faster than what expected because of the intersecting

of the main fracture by natural fractures, which provide an additional area and allow the fluid leaking through it.

➢ **Results and Discussions:**

Based on the data obtained from the main treatment, here is the interpretation:

- BH Closure Pressure ($P_C$): The BH Closure Pressure is determined to be 5644 psi.
- Closure Gradient: The Closure Gradient is calculated as 0.807 psi per foot.
- G-Function Closure Time ($G_C$): The G-Function Closure Time is measured at 0.20.
- Fluid Efficiency (FE): The Fluid Efficiency is determined to be 9.812%. This value indicates low fluid efficiency.
- Calculated FE: The Calculated FE is evaluated using the G-Function Closure Time ($G_C$) and is calculated as 9.09%.
- G-Function Net Pressure: The G-Function Net Pressure is recorded as 726.9 psi.
- Calculated Net Pressure (Pnet): The Calculated Net Pressure is obtained by subtracting the BH Closure Pressure from the BH ISIP and is calculated as 606 psi.

### IV.3.3.5.4 Mainfrac Net Pressure Plot

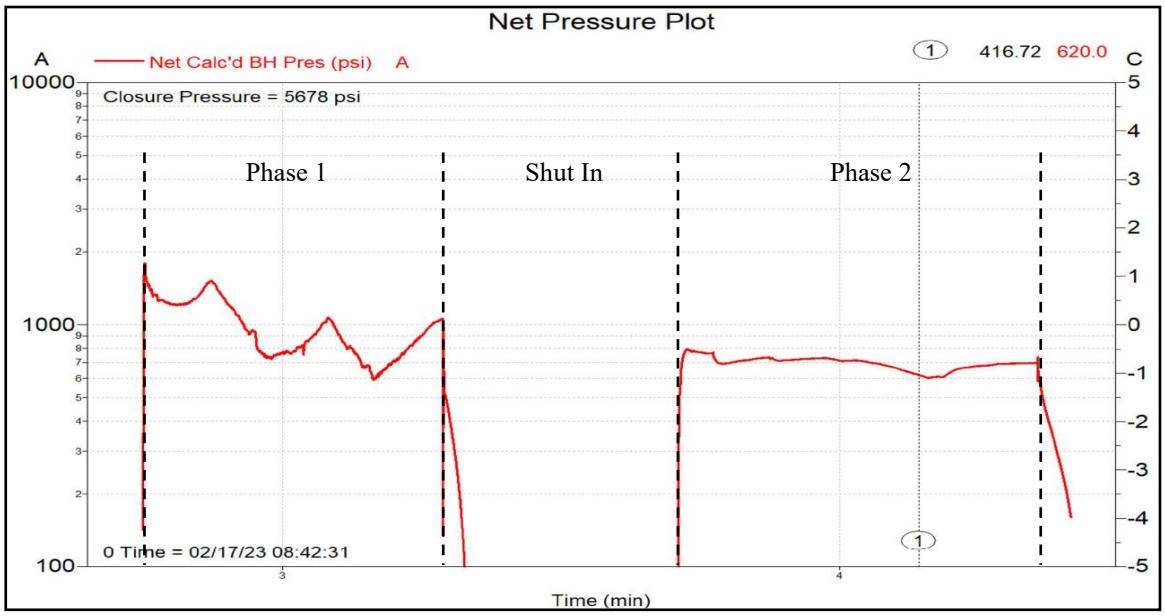


**Figure IV.43: Mainfrac Treatment Net Pressure Plot.[42]**

➢ **Interpretation of mainfrac net pressure plot using Nolte & Smith analysis:**

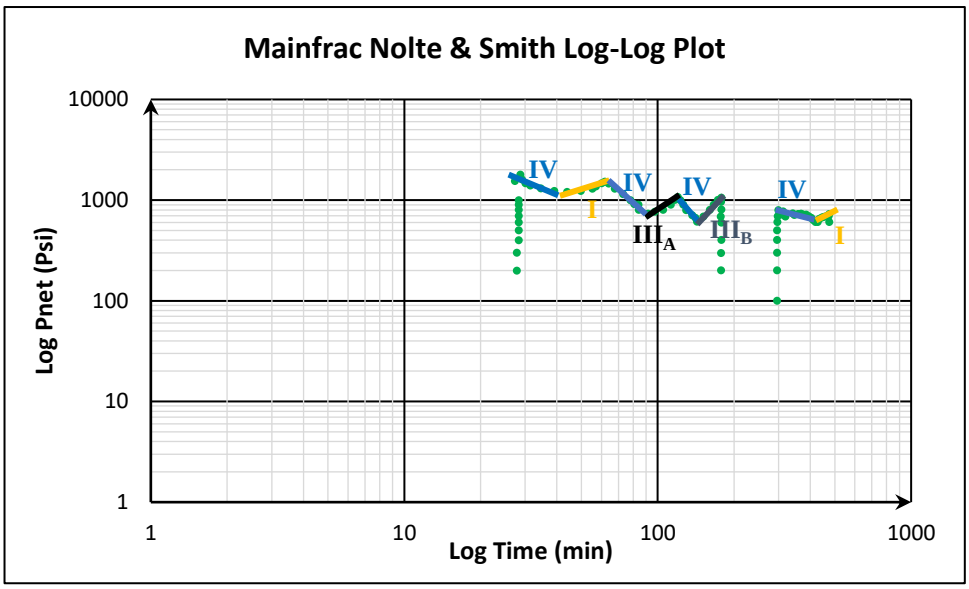


**Figure IV.44: Mainfrac Treatment Nolte & Smith Analysis Plot.**

The figure IV.44 shows that the evolution of fracture propagation mode goes through 8 stages:

**Mode 1**: corresponds to Type IV in the Nolte & Smith analysis, as it demonstrates a negative slope. It indicates a rapid growth in fracture height. Both the and Radial models can be considered applicable in this case.

**Mode 2:** corresponds to Type I based on the Nolte & Smith analysis as it exhibits a slight positive slope. It signifies propagation in line with (PKN) model, where the fracture length extends while the height remains nearly constant.

**Mode 3**: corresponds to Type IV in the Nolte & Smith analysis, as it demonstrates a negative slope. It indicates a rapid growth in fracture height. Both the and Radial models can be considered applicable in this case.

**Mode 4:** corresponds to Type $III_A$ in the Nolte & Smith analysis, as it exhibits a unit slope. It signifies a limitation in fracture extension, along with additional width growth.

**Mode 5**: corresponds to Type IV in the Nolte & Smith analysis, as it demonstrates a negative slope. It indicates a rapid growth in fracture height. Both the and Radial models can be considered applicable in this case.

**Mode 6:** corresponds to Type $III_B$ of the Nolte & Smith analysis due to its steep slope. It indicates a restriction of the fracture extension, only one active side and a possible screen-out scenario near the wellbore.

**Mode 7**: corresponds to Type IV in the Nolte & Smith analysis, as it demonstrates a negative slope. It indicates a rapid growth in fracture height. Both the and Radial models can be considered applicable in this case.

**Mode 8:** corresponds to Type I based on the Nolte & Smith analysis as it exhibits a slight positive slope. It signifies propagation in line with (PKN) model, where the fracture length extends while the height remains nearly constant.

#### IV.3.3.6 Evaluation of Minifrac Treatment Effectiveness

After examining the data collected from the acid frac treatment, it is clear that the existence of natural fractures has a substantial influence on the intended geometry of the primary fracture.

- Low Fluid efficiency (FE=9.81% < 40%).
- The cross-linked gel used Hybor H 25# did not mitigate the high leak-off rate.
- The fluid efficiency value of minifrac and mainfrac indicates that the obtained fracture geometry from a mainfrac is small compared to which obtained from minifrac.
- The natural fractures add an additional area which allow the fracturing fluid to leak-off and effect fracture geometry.

## Conclusion

The following conclusions summarize the results obtained from analyzing and interpreting the data of three wells:

- The common observation in naturally fractured reservoirs is a high leak-off rate and low fluid efficiency during hydraulic fracturing.
- Non ideal behaviors (Pressure-Dependent Leak-off, Delayed Leak-off and Tip extension) associated with hydraulic fracture propagation in naturally fractured reservoirs.
- The propagation mode varies from mode to another and goes through several stages.
- Small fracture geometry compared to the designed fracture geometry.
- The temperature log of GS-well 1 shows unwanted cooling downwards the WOC, this is a clear evidence that the main fracture connects several natural fractures leading to the WOC.
- The temperature log of GS-well 2 shows unwanted cooling above the 7″ casing shoe, because of that the mainfrac cancelled for the well integrity.
- Acid fracturing is a valuable technique for stimulating carbonate reservoirs. However, in naturally fractured reservoirs (NFRs), there is a risk of acid leakage into pre-existing natural fractures. This can result in acid loss outside the intended target zone, thereby reducing the

effectiveness of the treatment and potentially causing damage to the formation near the wellbore.

# Conclusions and Recommendations

# Conclusions and Recommendations

## Conclusions

Based on this study it is evident that hydraulic fracture propagation in naturally fractured reservoirs exhibits complex behavior due to interactions between hydraulic fractures and pre-existing fractures. The presence of natural fractures can enhance or hinder fracture growth, affecting fracture geometry and connectivity.

Field data analysis plays a crucial role in the evaluation of hydraulic fracture propagation. It involves monitoring fracture geometry, pressure responses, and production performance during and after the stimulation process. This real-time data helps calibrate and validate the analytical and numerical models, improving their accuracy and reliability.

After evaluating the hydraulic fracture propagation in naturally fractured reservoirs using field data from three wells, the following conclusions have been drawn:

- Common observations during hydraulic fracturing in naturally fractured reservoirs include high leak-off rate, low fluid efficiency, small fracture geometry, and unintended propagation beyond the target zone, even after stress calculations and data calibration.
- Non-ideal behaviors such as Pressure-Dependent Leak-off, Delayed Leak-off, and Tip extension are associated with the propagation, indicating the intersection of hydraulic fractures with the natural fracture network.
- The main fracture exhibits multiple propagation modes, and its geometry undergoes changes from one mode to another, impacting the accurate estimation of its dimensions.
- The presence of natural fractures diverts the hydraulic fracture away from the target zone, resulting in reduced production and economic losses. It is worth noting that the estimated cost of a minifrac test is $150,000, while the cost of the main treatment is half a million dollars.

In conclusion, the evaluation of hydraulic fracture propagation in naturally fractured reservoirs is a complex task that requires an integrated approach involving analytical models, numerical simulations, and field data analysis. By considering the geological complexities, fracture network interactions, and real-time data, a more accurate understanding of fracture behavior can be achieved, leading to optimized production and improved recovery in these challenging reservoirs.

## Recommendations

Naturally fractured reservoirs pose unique challenges in the evaluation of hydraulic fracture propagation due to the presence of pre-existing fractures and complex fracture networks. Understanding the behavior of hydraulic fractures in these reservoirs is crucial for optimizing production and recovery.

Various techniques and models have been developed to assess the behavior of hydraulic fractures in naturally fractured reservoirs. These include analytical models, numerical simulations, and field data analysis. Each approach has its advantages and limitations, requiring a comprehensive evaluation methodology.

Analytical models provide quick insights into fracture propagation behavior, but they often make simplifying assumptions that may not capture the complex interactions between hydraulic fractures and natural fractures. Numerical simulations offer a more detailed understanding of fracture behavior by considering the geological complexities, but they require significant computational resources and accurate input parameters.

The evaluation of hydraulic fracture propagation in naturally fractured reservoirs requires an integrated approach that combines analytical models, numerical simulations, and field data analysis. By incorporating the geological and geomechanical characteristics of the reservoir, along with fracture data and production performance, a more accurate understanding of fracture behavior can be achieved.

An integrated approach called a discrete fracture network approach was developed for evaluation of hydraulic fracture stimulation of naturally fractured reservoirs. This approach is limited by the ability to estimate in-situ stress, uncertainty in the local natural fracture network geometry and hydraulic proprieties.

XSite is a powerful three-dimensional hydraulic fracturing numerical simulation program introduced in 2015 based on the Lattice and Synthetic Rock Mass (SRM) methods.

The evaluation process should also consider the heterogeneity and anisotropy of the reservoir, as well as the stress field and fluid flow characteristics. These factors significantly influence fracture propagation behavior and the ultimate success of the hydraulic fracturing operation.

## References


[1] Tarek Ahmed, '' Reservoir engineering handbook- 4th Edition'', Gulf Professional Publishing, 2010.

[2] R.A. Nelson, '' Geologic Analysis of Naturally Fractured Reservoirs- 2nd Edition'', Gulf Professional Publishing, 2001.

[3] Djebbar Tiab, Erle C. Donaldson, ''Petrophysics: Theory and Practice of Measuring Reservoir Rock and Fluid Transport Properties- 3rd Edition'', Gulf Professional Publishing, 2012.

[4] Nibir Mandal, Atin Kumar Mitra, Santanu Misra, Chandan Chakraborty, ''Is the outcrop topology of dolerite dikes of the Precambrian Singhbhum Craton fractal?'', Journal of Earth System Science. December 2006.

[5] T.D. Van Golf-Racht, ''fundamentals of fractured reservoir engineering'',

[6] Reda Abdel Azim, Sara Faiz, Shaik Rahman, Ahmed Elbagir and Nour Al Obaidi, ''Numerical Study of Low Salinity Water Flooding in Naturally Fractured Oil Reservoirs'', Published in InTech, 2018.

[7] John C Vardakis, Liwei Guo, Dean Chou, '' A multiple-network poroelastic model for biological systems and application to subject-specific modelling of cerebral fluid transport'', International Journal of Engineering Science, December 2019.

[8] Muhammad Nur Ali Akbar, '' Naturally Fractured Basement Reservoir Characterization in a Mature Field'', Conference: SPE Annual Technical Conference and Exhibition, September 2021.

[9] Mark Tingay, J. Reinecker, Birgit Müller, '' Borehole breakout and drilling-induced fracture analysis from image logs'', January 2008.

[10] https://petrowiki.spe.org/Fluid_flow_in_naturally_fractured_reservoirs

[11] https://petrowiki.spe.org/Hydraulic_fracturing

[12] James G. Speight, "Handbook of hydraulic fracturing", Published by John Wiley & Sons, Inc., Hoboken, New Jersey, 2016.

[13] SHELL TECHNOLOGY EP, RIJSWIJK EP 2000-5540, "Stimulation Field Guidelines Part II (Revision) Hydraulic Fracturing", November 2000.

[14] Basins G. Nitters, B. Pittens, N. Buik, "Well Stimulation Techniques for Geothermal Projects in Sedimentary".

[15] https://petrowiki.spe.org/Fracturing_fluids_and_additives

[16] Erle C. Donaldson, Waqi Alam, Nasrin Begum, "Hydraulic Fracturing Explained Evaluation, Implementation and Challenges''.

[17] https://www.dmp.wa.gov.au/Petroleum/Hydraulic-fracture-stimulation-20018.

[18] https://neftegazru.com/tech-library/recovery/proppant.

[19] https://petrowiki.spe.org/Fracture_treatment_design

[20] https://www.scielo.br/Hydraulic-Fracturing-Proppants

[21] Hobart M. King, "What is Frac Sand?'', published in Geoscience News and Informations, available: https://geology.com/articles/frac-sand/

[22] https://informationtips.wordpress.com/2012/08/12/hydraulic-fracturing-the-process/

[23] Sri Rahayu, "Basic way to understanding the hydraulic fracturing", 2020.

[25] https://petrowiki.spe.org/Fracture_mechanics

[26] Jabbari Hadi, "Hydraulic fracturing design for horizontal wells in the Bakken formation, Williston Basin", Theses and Dissertations, University of North Dakota, 2013.

[27 ]https://www.birmingham.ac.uk/teachers/study-resources/stem/physics/youngs-modulus.

[28] https://byjus.com/physics

[29] https://www.britannica.com/science/bulk-modulus

[30] Dezhi Qiu, "Hydraulic Fracture Propagation and Its Geometry Evolvement In Transversely Isotropic Formations", PhD Thesis, University of North Dakota, 2021.

[31] Youngho Jang, Gayoung Park, Seoyoon Kwon, and Baehyun Min, "Analysis of Hydraulic Fracture Propagation Using a Mixed Mode and a Uniaxial Strain Model considering Geomechanical Properties in a Naturally Fractured Shale Reservoir", Research Article, Published 23 December 2020.

[32] McLellan, P.J, "Designing Stimulation Treatments to Account for Natural Fracture." Presented at the petroleum of CIM Calgary Section Monthly Technical Meeting, March 1993.

[33] Zoback, M. D, "Hydraulic Fracturing in Unconventional Reservoirs", Annual Review of Earth and Planetary Sciences, 2007.

[34] I.A. Garagasha, A.A. Osiptsov, “Effects of nonuniform initial stress state on apparent fracture toughness”, ResearchGate, December 2019.

[35] Jing Xiang, “A PKN Hydraulic Fracture Model Study And Formation Permeability Determination”, Thesis of Master, Texas A&M University, 2011.

[36] https://petrowiki.spe.org/Fracture_propagation_models

[37]https://www.ihsenergy.ca/support/documentation/analysis_types/minifrac_test_analyses/minifrac-pre-closure_analysis

[38] https://www.sciencedirect.com/topics/engineering/fracture-closure

[39] Ralph W. Veatch, “Fundamentals of hydraulic fracturing: vertical and horizontal wellbores”, by PennWell Corporation, 2017.

[40] Halliburton Design of Service and Post Frac Job Reports of GS-well 1.

[41] Halliburton Design of Service and Post Frac Job Reports of GS-well 2.

[42] Halliburton Design of Service and Post Frac Job Reports of HR-well 1.

# Appendices

## Appendix 1: Well Completion Schematic of GS-Well 1.

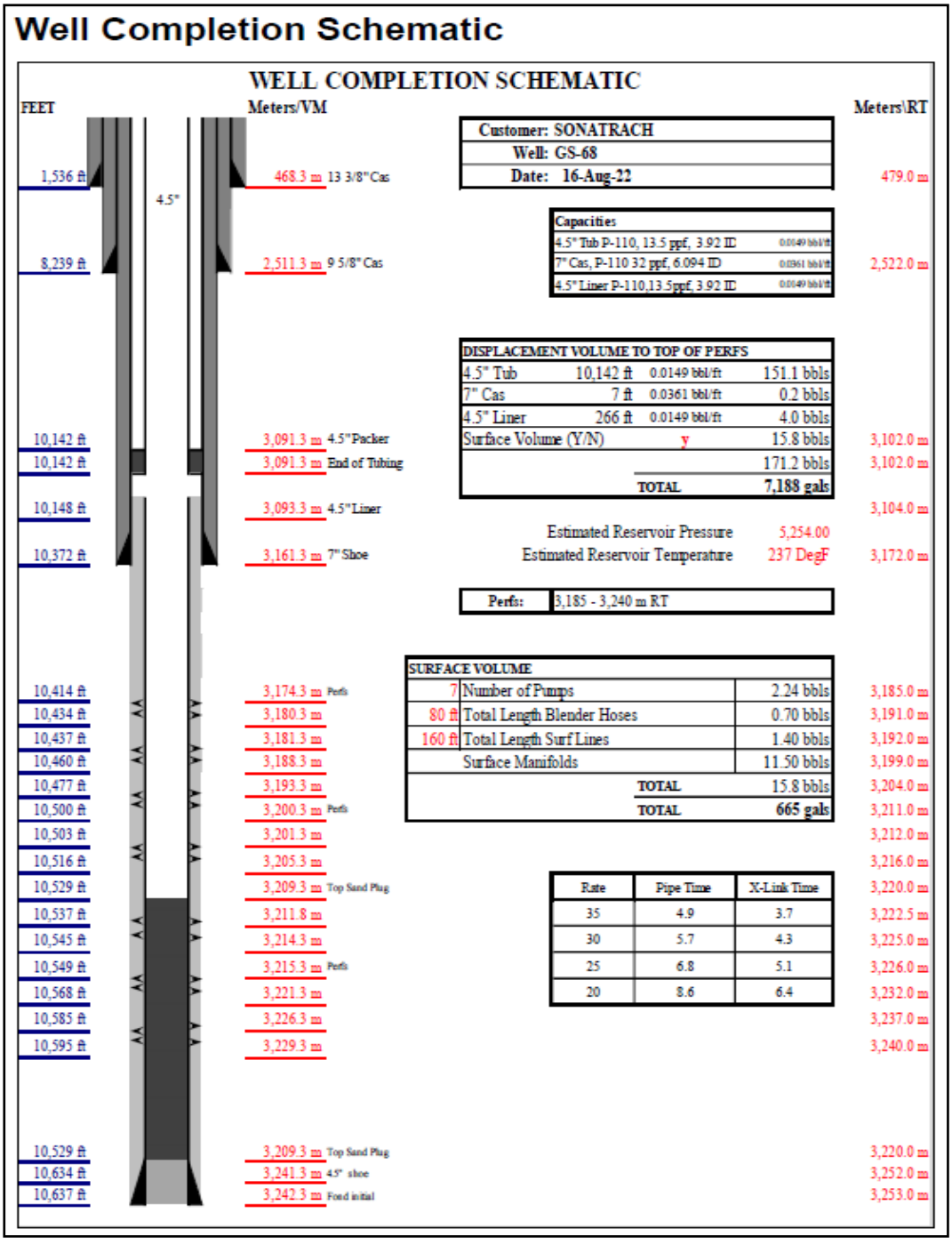

## Appendix 2: Hybor-G 35# Chemical Compositions.

### Hybor-G 35# Cross-Linked Gel Additives

| Description | Additive Name | Concentration |
|---|---|---|
| Gelling Agent | WG-36 | 35 lb/Mgal |
| Cross-linker | CL-28M | 1.2 gal/Mgal |
| Cross-Linker | K-38 | 3.0 gal/Mgal |
| Clay Control | CLAWEB | 0.7 gal /Mgal |
| Clean up Additive | LOSURF-300/DCA-32014 | 1.0 gal/Mgal |
| Biocide | BE-3S | 0.15 lb/Mgal |
| High pH Buffer | MO-67 | 1.0-2.2 gal/Mgal |
| Gel Stabilizer | Gel Sta L | 2.4 gal/Mgal |
| Low pH Buffer | BA-20 | 0.3 gal/Mgal |
| Breaker | Optiflo III | 0.5 – 3.0 lb/Mgal |
| Breaker | Vicon-NF | 0.6 – 3.0 gal/Mgal |
| Breaker | SP Breaker | 1.0 gal/Mgal |

### Chemical Descriptions

| | | |
|---|---|---|
| WG-36 | : | Gelling Agent (Hydroxyl propyl Guar). |
| CL-28M | : | Borate source delayed cross-linker. |
| K-38 | : | Instantaneous cross-linker. |
| Cla-Web | : | Clay control agent. |
| LOSURF-300 | : | Non-Ionic Emulsion surfactant. |
| DCA-32014 | : | Microemulsion surfactant additive |
| BE-3S | : | Biocide specifically tested for use in water-based. |
| MO-67 | : | High pH Buffer. |
| Gel Sta L | : | Gel Stabilizer. |
| BA-20 | : | Low pH Buffer. |
| OPTIFLO-III | : | Solid delayed-release breaker. |
| VICON NF | : | Liquid oxidizing breaker. |
| SP BREAKER | : | Solid oxidizing breaker for temperatures above 120 °F. |

**Appendix 3: Well Completion Schematic of GS-Well 2.**

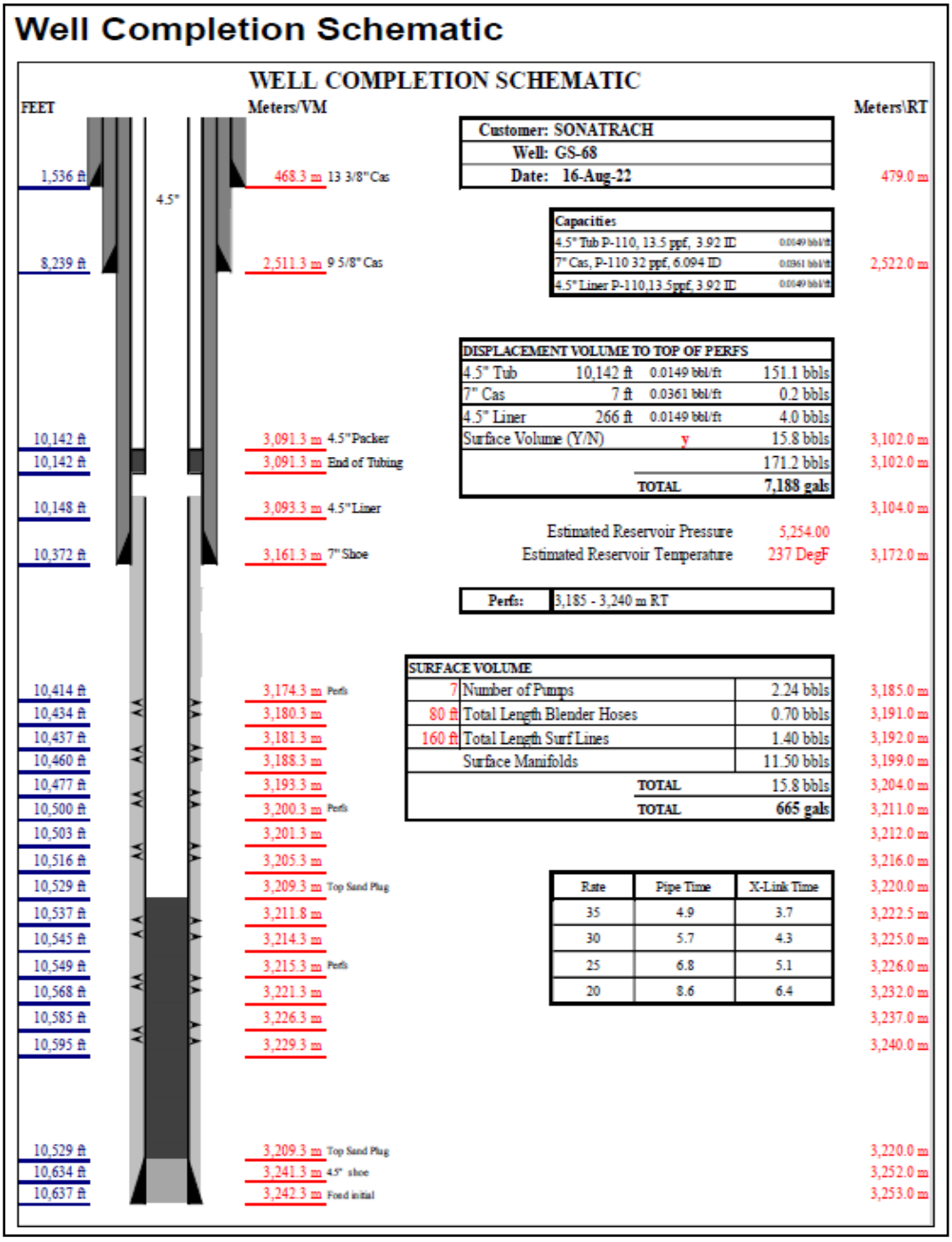

**Appendix 4: Well Completion Schematic of HR-Well 1.**

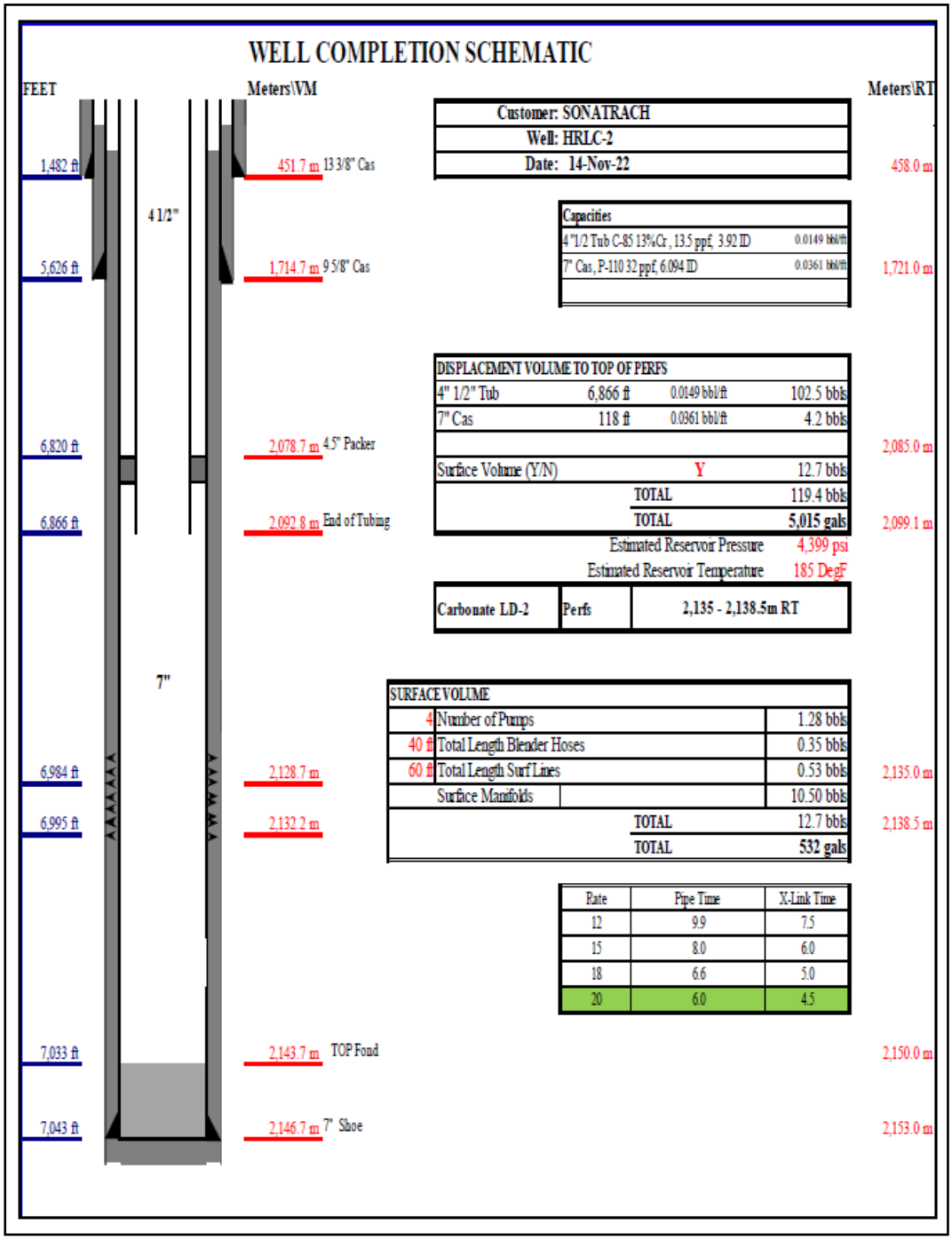

## Appendix 5: Hybor-H 25# Chemical Compositions.

### Hybor-H 25# Cross-Linked Gel Additives

| Description | Additive Name | Concentration |
|---|---|---|
| Gelling Agent | WG-11 | 25 lb/Mgal |
| Cross-linker | CL-28M | 2.2 gal/Mgal |
| Cross-Linker | CL-31 | 1.0 gal/Mgal |
| Clay Control | CLAWEB | 0.7 gal /Mgal |
| Clean up Additive | LOSURF 300 | 1.0 gal/Mgal |
| Biocide | BE-3S | 0.15 lb/Mgal |
| High pH Buffer | MO-67 | 1.5 gal/Mgal |
| Gel Stabilizer | Gel Sta L | 0.0 gal/Mgal |
| Low pH Buffer | BA-20 | 0.2 gal/Mgal |
| Breaker | Vicon-NF | 0.0 gal/Mgal |
| Breaker | SP Breaker | 1.0 gal/Mgal |
| Breaker | Diluted SP Breaker | 0.5-1.0 gal/Mgal |

(1) SP Breaker is only added in the displacement fluid.
(2) Biocide BE-3S is added to the Frac Tanks on Location

### Hybor-H Chemical Descriptions

WG-11 : Gelling Agent (Guar).
CL-28M : Borate source delayed cross-linker.
CL-31 : Instantaneous cross-linker.
Cla-Web : Clay control agent.
LOSURF-300 : Non-Ionic Emulsion surfactant.
BE-3S : Biocide specifically tested for use in water-based.
MO-67 : High pH Buffer.
Gel Sta L : Gel Stabilizer.
BA-20 : Low pH Buffer.
OPTIFLO-III : Solid delayed-release breaker.
VICON NF : Liquid oxidizing breaker.
SP BREAKER : Solid oxidizing breaker for temperatures above 120 °F.
Diluted SP Breaker: Liquid oxidizing breaker for temperatures above 120°F.